CRCLEME
Cooperative Research Centre for
Landscape Evolution & Mineral Exploration

CSIRO
EXPLORATION AND MINING

AMIRA
Australian Mineral Industries Research Association Limited ACN 004 448 266

OPEN FILE REPORT SERIES

REGOLITH/LANDFORM RELATIONSHIPS AND THE PETROLOGICAL, MINERALOGICAL AND GEOCHEMICAL CHARACTERISTICS OF LAGS, LAWLERS DISTRICT, WESTERN AUSTRALIA

R.R. Anand, H.M. Churchward and R.E. Smith

CRC LEME OPEN FILE REPORT 74

February 1999

(CSIRO Division of Exploration Geoscience Report 106R, 1990.
Second impression 1999)

AMIRA
Australian Mineral Industries Research Association Limited ACN 004 448 266

CRCLEME
Cooperative Research Centre for Landscape Evolution & Mineral Exploration

CSIRO
EXPLORATION AND MINING

REGOLITH/LANDFORM RELATIONSHIPS AND THE PETROLOGICAL, MINERALOGICAL AND GEOCHEMICAL CHARACTERISTICS OF LAGS, LAWLERS DISTRICT, WESTERN AUSTRALIA

R.R. Anand, H.M. Churchward and R.E. Smith

CRC LEME OPEN FILE REPORT 74

February 1999

(CSIRO Division of Exploration Geoscience Report 106R, 1990.
Second impression 1999)

CRC LEME is an unincorporated joint venture between The Australian National University, University of Canberra, Australian Geological Survey Organisation and CSIRO Exploration and Mining
Headquarters: CRC LEME c/o CSIRO Exploration and Mining, Private Bag, PO Wembley, Western Australia, 6014

RESEARCH ARISING FROM CSIRO/AMIRA REGOLITH GEOCHEMISTRY PROJECTS 1987-1993

In 1987, CSIRO commenced a series of multi-client research projects in regolith geology and geochemistry which were sponsored by companies in the Australian mining industry, through the Australian Mineral Industries Research Association Limited (AMIRA). The initial research program, "Exploration for concealed gold deposits, Yilgarn Block, Western Australia" (1987-1993) had the aim of developing improved geological, geochemical and geophysical methods for mineral exploration that would facilitate the location of blind, buried or deeply weathered gold deposits. The program included the following projects:

P240: Laterite geochemistry for detecting concealed mineral deposits (1987-1991). Leader: Dr R.E. Smith.
Its scope was development of methods for sampling and interpretation of multi-element laterite geochemistry data and application of multi-element techniques to gold and polymetallic mineral exploration in weathered terrain. The project emphasised viewing laterite geochemical dispersion patterns in their regolith-landform context at local and district scales. It was supported by 30 companies.

P241: Gold and associated elements in the regolith - dispersion processes and implications for exploration (1987-1991). Leader: Dr C.R.M. Butt.
The project investigated the distribution of ore and indicator elements in the regolith. It included studies of the mineralogical and geochemical characteristics of weathered ore deposits and wall rocks, and the chemical controls on element dispersion and concentration during regolith evolution. This was to increase the effectiveness of geochemical exploration in weathered terrain through improved understanding of weathering processes. It was supported by 26 companies.

These projects represented "an opportunity for the mineral industry to participate in a multi-disciplinary program of geoscience research aimed at developing new geological, geochemical and geophysical methods for exploration in deeply weathered Archaean terrains". This initiative recognised the unique opportunities, created by exploration and open-cut mining, to conduct detailed studies of the weathered zone, with particular emphasis on the near-surface expression of gold mineralisation. The skills of existing and specially recruited research staff from the Floreat Park and North Ryde laboratories (of the then Divisions of Minerals and Geochemistry, and Mineral Physics and Mineralogy, subsequently Exploration Geoscience and later Exploration and Mining) were integrated to form a task force with expertise in geology, mineralogy, geochemistry and geophysics. Several staff participated in more than one project. Following completion of the original projects, two continuation projects were developed.

P240A: Geochemical exploration in complex lateritic environments of the Yilgarn Craton, Western Australia (1991-1993). Leaders: Drs R.E. Smith and R.R. Anand.
The approach of viewing geochemical dispersion within a well-controlled and well-understood regolith-landform and bedrock framework at detailed and district scales continued. In this extension, focus was particularly on areas of transported cover and on more complex lateritic environments typified by the Kalgoorlie regional study. This was supported by 17 companies.

P241A: Gold and associated elements in the regolith - dispersion processes and implications for exploration. Leader: Dr. C.R.M. Butt.
The significance of gold mobilisation under present-day conditions, particularly the important relationship with pedogenic carbonate, was investigated further. In addition, attention was focussed on the recognition of primary lithologies from their weathered equivalents. This project was supported by 14 companies.

Although the confidentiality periods of the research reports have expired, the last in December 1994, they have not been made public until now. Publishing the reports through the CRC LEME Report Series is seen as an appropriate means of doing this. By making available the results of the research and the authors' interpretations, it is hoped that the reports will provide source data for future research and be useful for teaching. CRC LEME acknowledges the Australian Mineral Industries Research Association and CSIRO Division of Exploration and Mining for authorisation to publish these reports. It is intended that publication of the reports will be a substantial additional factor in transferring technology to aid the Australian mineral industry.

This report (CRC LEME Open File Report 74) is a Second impression (second printing) of CSIRO, Division of Exploration Geoscience Restricted Report 106R, first issued in 1990, which formed part of the Forsyth Mining Ltd and Geochemex Australia.

Copies of this publication can be obtained from:
The Publication Officer, c/- CRC LEME, CSIRO Exploration and Mining, PMB, Wembley, WA 6014, Australia. Information on other publications in this series may be obtained from the above or from http://leme.anu.edu.au/

Cataloguing-in-Publication:
Anand, R.R.
Regolith/landform relationships and the petrological, mineralogical and geochemical characteristics of lags, Lawlers District, Western Australia
ISBN 0 643 06469 9
1. Regolith 2. Geochemical prospecting 3. Mineralogy - Western Australia 4. Soils
I. Churchward, H.M. II. Smith, Raymond Ernest III. Title
CRC LEME Open File Report 74.
ISSN 1329-4768

ABSTRACT

This study of the regolith in the Lawlers district is focussed upon the Meatoa, Brilliant, and Agnew-McCaffery areas. The regolith units were mapped using 1:25,000 colour air photographs and three times enlargements (1:8333) of selected air photographs as the base. The regolith stratigraphy has been established for each of these areas and some selected surface units characterized petrologically, mineralogically and geochemically. The regolith patterns observed in these areas are explained in terms of the distribution of (a) regimes of erosion of the laterite profile to the level of saprolite/bedrock resulting in terrain characterized by low hills, (b) regimes where the essentially complete laterite profile is preserved, commonly forming gentle ridge crests and backslopes, and (c) regimes characterized by depositional accumulations of detritus derived by the erosion of the laterite profile, burying the partly truncated, and in places complete laterite profile in the lower slopes of colluvial/alluvial outwash plains. Idealized regolith/landform models for these areas have been established for the purpose of predicting regolith relationships in comparable terrain elsewhere.

The soils occurring within those truncational regimes which have mafic or ultramafic bedrock lithologies are predominantly red-coloured light clays and red sandy clay loams. They are often acidic and commonly are underlain by a red-brown hardpan. The red clays often contain pseudomorphic grains after amphiboles, further evidence of their mafic origin. The occurrence of pedogenic calcrete at shallow depths in the erosional regimes generally relates to a mafic lithology. Soils on felsic lithologies are acidic, yellowish brown, sandy loams. Residual regimes are dominated by acidic, brown gravelly sandy loams and sandy clay loams and generally red-brown hardpan is not developed. The soils within the depositional regimes are developed in colluvium/alluvium and are acidic, gravelly sandy clay loams and light clays.

The distribution and characteristics of lag gravels have been placed within the regolith/landform framework established during this study. At Meatoa, four classes of lag have been recognized: black, coarse cobbles after ferruginized saprolite, yellow to reddish-brown lateritic lithic fragments, lateritic lag, and fine lag of mixed origin. The fine lag of mixed origin, which is widespread in the Meatoa area, comprises a variety of clasts derived from the breakdown of large lateritic lithic fragments and lateritic duricrust, both of which occur in the local uplands. These four lag types differ in their morphological, chemical, and mineralogical characteristics and include systematic variations in the Al substitution within the Fe-oxides. Some lateritic lithic fragments preserve the original rock fabric. Lateritic lithic lag is relatively richer in kaolinite while lags of ferruginized saprolite and lateritic lag are poorer in kaolinite. Petrographic examination of the lag gravels has shown that kaolinite is progressively replaced by hematite/goethite. Goethites of ferruginized saprolite contain lowest Al substitution (<5 mole %), whereas those of lateritic lag contain highest Al substitution (19-26 mole %). The low Al substitution in goethites of ferruginized saprolite suggests that these have formed by absolute accumulation of Fe in an environment almost free of available Al. The data on Al substitution of various regolith materials from this study have shown that the degree of Al substitution in goethite can be used to predict the weathering status of regolith materials and the environments within which they have formed.

The lags of lateritic lithic fragments and lateritic lag show relatively high levels of As, Pb, and Ga. Tin, W, and Bi occur in low concentrations and did not show any variations between the lag types. The lags of ferruginized saprolite have significantly higher levels of Mn, Zn, and Co than the other lag types. The differences in the geochemistry of various types of lags are related to the nature of bedrock, degree of weathering, and mechanism of accumulation of weathering products. The concentrations of Cr and Ni were found to be useful in discriminating the origin (mafic vs ultramafic) of lag gravels. The levels of Au are low in the range of 0 to 0.034 ppm.

Investigation suggests that the Fe-rich duricrusts are probably formed by absolute accumulation of Fe. One possible explanation is that Fe originally impregnated the soils/sediments in local valleys which now occur as ridge crests in the present landscape because of inversion of relief.

Gold in lateritic nodules from the North Pit location occurs in two forms (i) grains up to 15 μm in diameter, occurring in cracks, and (ii) large dendritic Au grains which reach 70 μm in diameter and are attached to the surface of goethite. Both occurrences of Au appear to be secondary and are almost free from Ag (<1% Ag). In the lateritic nodules, As and Mn are strongly associated with Fe oxides, while Cu is associated with kaolinite.

---o0o---

CONTENTS

1.0 PROJECT LEADER'S PREFACE

R E Smith 23 March 1990

Research at Lawlers being carried out by the CSIRO Laterite Geochemistry Group is focussed upon the topics listed below. These resulted from revision of the original objectives (in Anand *et al.*, 1989) following an on-site meeting, coupled with field discussions, between Forsayth and CSIRO scientists in June, 1989.

1. District-scale regolith/landform relationships.

2. Methods of reliable identification of laterite types from drill spoil.

3. Execution of a concise laterite orientation study on the North Pit Au deposit.

4. Characterize and establish the origin of various massive ironstones, pods and iron segregations that occur in the upper saprolite/mottle zone, and the coarse ironstone lag from partly truncated landform situations.

5. Investigate the subsurface regolith relationships at Meatoa, in order to clarify the exploration cross sections.

6. Establish the relationships of lag type to regolith situation at Meatoa.

7. Carry out pilot investigation into the siting and bonding of Au and chalcophile elements on samples from the Turret and North Pit laterite anomalies.

8. Establish relationships between bedrock composition and laterite - for anomaly recognition parameters, and prediction of bedrock type.

9. Trial applications of multivariate interpretational procedures on laterite data.

This report addresses topics 4, 5, 6, and 7, whereas the first report, 20R (Anand *et al.*, April 1989) had addressed topics 1, 2, and 3.

Revision of the objectives in June reflected Forsayth's aim to gain a better understanding of lag type and the use of lag as an exploration sampling medium. Topics 8 and 9 have thus been displaced with the intent that they will be covered in a future report.

2.0 INTRODUCTION

The Lawlers district lies some 300 km north of Kalgoorlie and spans the north-central part of the Leonora 1:250,000 map sheet (SH-51-01) and the southern part of the Sir Samuel sheet (SG-51-13). Research being carried out by the CSIRO Laterite Geochemistry Group concerns Forsayth tenements in the Lawlers district. The research extends the Geochemex regolith study reported by Butler *et al.* (1989) and is directed at recognizing, defining and delineating the regolith units, establishing the regolith stratigraphy, mapping the surface and sub-surface distribution of regolith units in selected areas, and compiling a synthesis of regolith facies relationships. These activities have been carried out collaboratively with, and are an integral part of, ongoing exploration by Forsayth (overall exploration and integration) and Geochemex (geochemical exploration and regolith applications for Forsayth). The overall aim of the research is to clarify the use of exploration geochemistry in the district by providing an understanding of selected regolith units and of the prolonged regolith history. This includes generating knowledge of the original lateritic weathering regime, the subsequent partial dismantling and the accompanying sedimentation which resulted in burial of lateritic weathering profiles, and the authigenic alteration and cementation. Since the research commenced in November 1988, the accrued knowledge has formed part of the framework within which exploration geochemical relationships have been interpreted.

This report presents the regolith/landform relationships at the Meatoa, Agnew-McCaffery, and Brilliant areas. It follows the report of Anand *et al.* (April, 1989) which focussed upon regolith relationship in the McCaffery-North Pit area and provided an overview of the district-scale regolith relationships. Emphasis in the present report is also placed on the lag gravels and soil characteristics of the different regolith units. Initial results on the siting and bonding of ore-related elements including Au are also discussed.

3.0 REGOLITH RELATIONSHIPS IN THE MEATOA AREA

3.1 Physical and Geolgical Settings

The area has a hot arid climate with a 250-mm average annual rainfall, most of which falls during the summer and autumn months. A large part of the summer rainfall comes from erratic thunderstorms.

The vegetation of the area is dominated by *Acacia aneura* (mulga) - *Eremophila leucophylla* communities. Locally these may occur as low open woodlands, but more often they are shrublands. This plant cover has, however, been considerably degenerated by a long history of grazing by sheep and many of the more edible species are no longer present.

The Great Plateau of Western Australia, on which the Lawlers study area is situated, presents a gently undulating surface. The generally low relief is broken by occasional belts of rounded hills, usually associated with greenstone lithologies, emergent above the general plateau surface.

The extensive deep mantle of weathering that characterizes the Great Plateau has been stripped to varying degrees, resulting in local variation in the otherwise smooth skyline of the plateau. Lateritic crests cap erosional scarps (breakaways), the more prominent features being associated with the stripping. One such erosion feature is the Agnew breakaway near the western limit of the general study area. Colluvium from the gently sloping laterite capped residuals, as well as detritus from these pockets of erosion are transported to the gently sloping lower slopes and flanking broad alluvial plains. These trends are evident at both the Meatoa and Brilliant areas. At Meatoa, the northward-oriented belt of hills shows stripping along the eastern flanks while its western flanks are characterized by long gentle slopes extending from Fe-rich duricrust forming the upper crests to alluvial plains. The belt of hills at Brilliant, by contrast, is most strikingly modified by erosion along its central axis. Detritus from this central area finds its way to the east or west through gaps in lines of laterite capped summits that appear to be residuals of a once more continuous broad ridge crest zone. In addition, colluvium derived from the lateritic crest has moved down the long gentle westward and eastward slopes of the residuals to join detritus from the centrally placed erosional zone.

Except for the pedimented area of granitoids forming the east third of the Meatoa area, Fig. 1A, outcrop or subcrop of bedrock is generally poor, with some isolated areas having float of saprolitic lithologies amongst abundant ironstone rubble. Typically, the ground surface is soil-covered and is strewn with lag, described systematically in Section 4.0, which is derived from various surficial regolith units.

Apparently to date, no geological map, either showing surface mapping or interpreted bedrock lithologies and relationships, has yet been generated for the Meatoa area.

Bedrock control is important in understanding regolith characeristics and relationships, particularly for those weathering products that are essentially *in situ* or have undergone only limited transport. In order to provide a start towards such control the interpreted geological map (Fig. 1A) has been produced based upon the logging, by Forsayth, of bottom-of-hole lithologies from reverse circulation (RC), air core (AC) and rotary air blast (RAB) drilling, as at 7 July 1989. Limitations of this map result from the problems of interpretation between holes. It seems likely that careful mapping of subcrop tied in with bottom-of-hole lithologies, together with interpretation of detailed air-magnetics would result in a much improved map. We expect that such work, which is outside the scope of this research, would be a proper outcome of the on-going exploration programme.

The Meatoa area spans the hinge zone of the Lawlers synform where the regional stike of the mafic and ultramafic supracrustal sequences, which have an outcrop width of 5 to 8 km, changes through some 320 . Axial plane faulting and/or shearing seems likely because of this structural complexity. In addition some stoping of supracrustal lithologies against granitoids appears to have taken place.

At this stage the stratigraphy of the supracrustal sequence is not clear. Fine-grained mafic and ultramafic rocks, including dolerite, metabasalt and komatiite, are interspersed with coarse-grained mafic and ultramafic rocks such as gabbro and pyroxenite and, in the SW sector, silicified ultramafics with characteristic 3 mm grain-size cumulate features of peridotites and dunites.

The most notable feature in the Meatoa area, and central to the exploration interest to date, appears to be an association of dolerite and gabbro over a 3 by 1 km area. Whether the dolerite/gabbro forms a shape as depicted in Fig. 1A would need to be confirmed. It should be noted that traverse 6891600N crosses the strike of the interpreted bedrock lithologies, as well as crossing the regolith units shown in Fig. 1B.

Previous studies (such as Davy, 1979) have pointed out relationships between the chemical composition of bedrock and that of the corresponding residual laterite. From the published works and from the geochemical data base of the Laterite Geochemistry Group it is clear that where bedrock composition becomes more basic or ultrabasic, corresponding residual laterite compositions have generally higher levels of Fe, Mn, Cr, V, Cu, Zn, Ni, and Co, in comparison with laterites on granitoids and related migmatites.

Although some of the general trends of chemical variation are recognised, systematic information on bedrock and corresponding residual laterite compositions are scarce. Furthermore, the common variations of Cr, Ni, Cu, and Co in mafic and ultramafic rocks are likely to strongly influence the chemical compositions of laterite.

Thus even though control of bedrock type in the Meatoa area is presently limited, as is systematic knowledge of relationships between bedrock composition and corresponding laterite, both issues are relevant to the interpretation of geochemical results.

3.2 The Surface Distribution of Regolith Units

Figure 1B shows the surface distribution of regolith units for the Meatoa area. Their boundaries are based upon interpretation of the 1:25,000 colour air photography carried out in January 1989 by Kevron Aerial Services Pty Ltd for Forsayth. Detailed field observations were carried out between 6891600N to 6892000N and provide the basis for mapping the adjacent areas (see the report on field activities, Anand and Churchward, August, 1989).

The dominant regolith features in the Meatoa area relate to the occurrence of lateritic residuum (Unit 1), to partial truncation of the deep weathering profile and exposure of saprolite (Units 2a, 2b and 11b) to the east, together with colluvial (6a) and alluvial deposition (7a, 7b) in the western part of the area. To the east gentle slopes are mantled by depositional Unit 6b consisting of mafic detritus which overlies felsic bedrocks. Sandy to sandy clay loam soils dominate Unit 1, the soils progressively changing downslope to sandy light clays on Unit 6a. Soils of Units 2a and 2b are predominantly sandy light clays. Patches of pedogenic calcrete related to mafic rocks occur on Unit 2a. Regolith/landform relationships will be discussed below (Section 3.5) after the regolith stratigraphy has been presented and the units described. The mapped regolith units are shown in the legend to Fig.1B and in Table 1. These are based upon the units proposed by Butler *et al.* (1988) and Anand *et al.* (1989).

3.3 Regolith Stratigraphy

Regolith stratigraphy for the Meatoa area (Table 1) was established for this study by the logging of spoil from many of the exploration drill holes along lines 6891600N, 6891800N, and 6892000N. These lines formed a swath, suggested by M. Parker and A. Ewers within the context of the Geochemex regolith/landform mapping and subsurface synthesis, which typified the main Meatoa area. From these

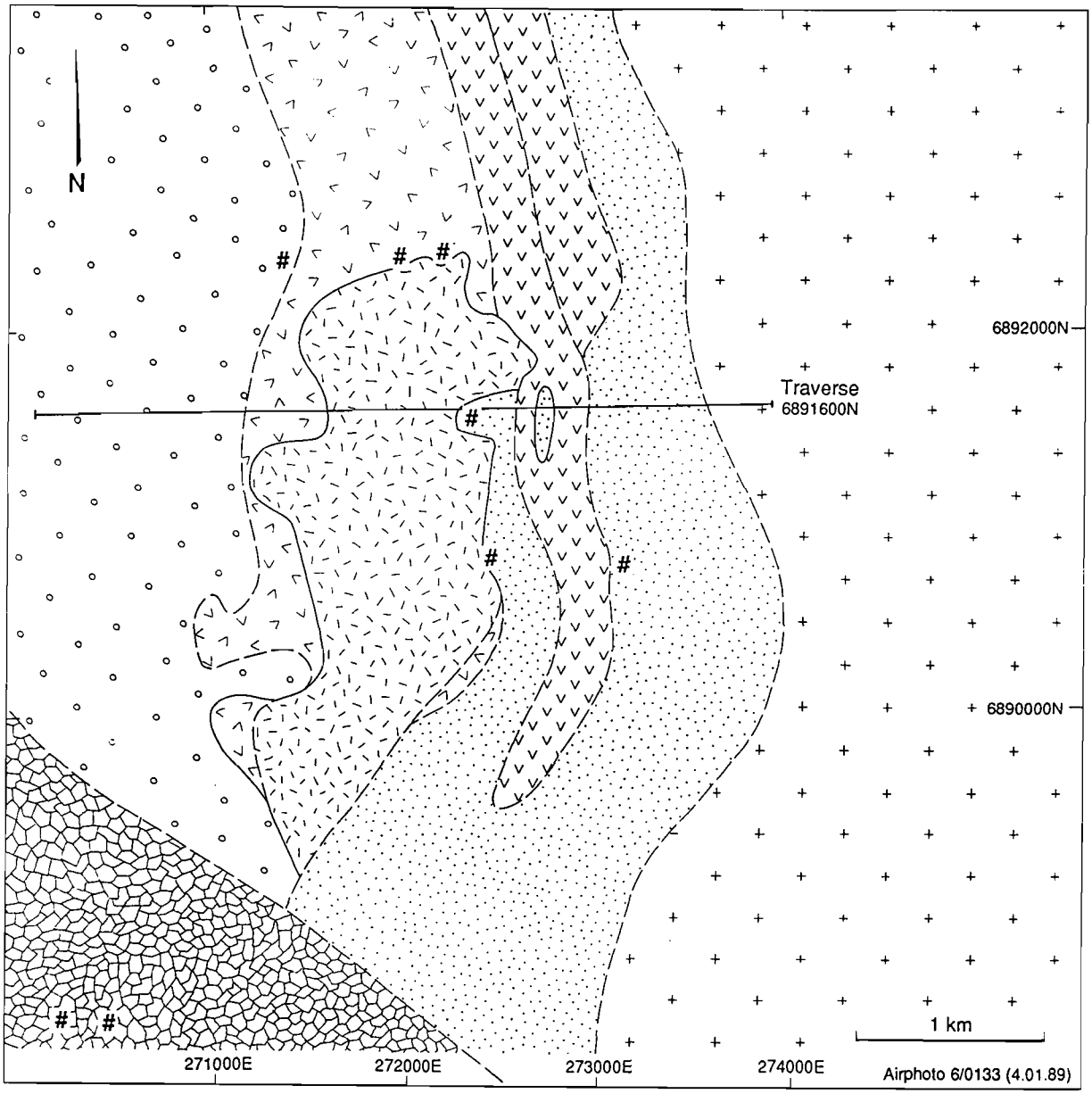

Pyroxenite occurrence

Ultramafics, including pyroxenite, peridotite, dunite

Ultramafics, undistinguished

Metabasalt and ultramafics

Gabbro, dolerite, metabasalt

Metabasalt

Ultramafics, including komatiites

Granitoids

Fig. 1A. Interpreted geological bedrock map for the Meatoa area based upon Forsayth bottom of hole lithologies, airphoto interpretation, and logging of bedrock in isolated holes during this study.

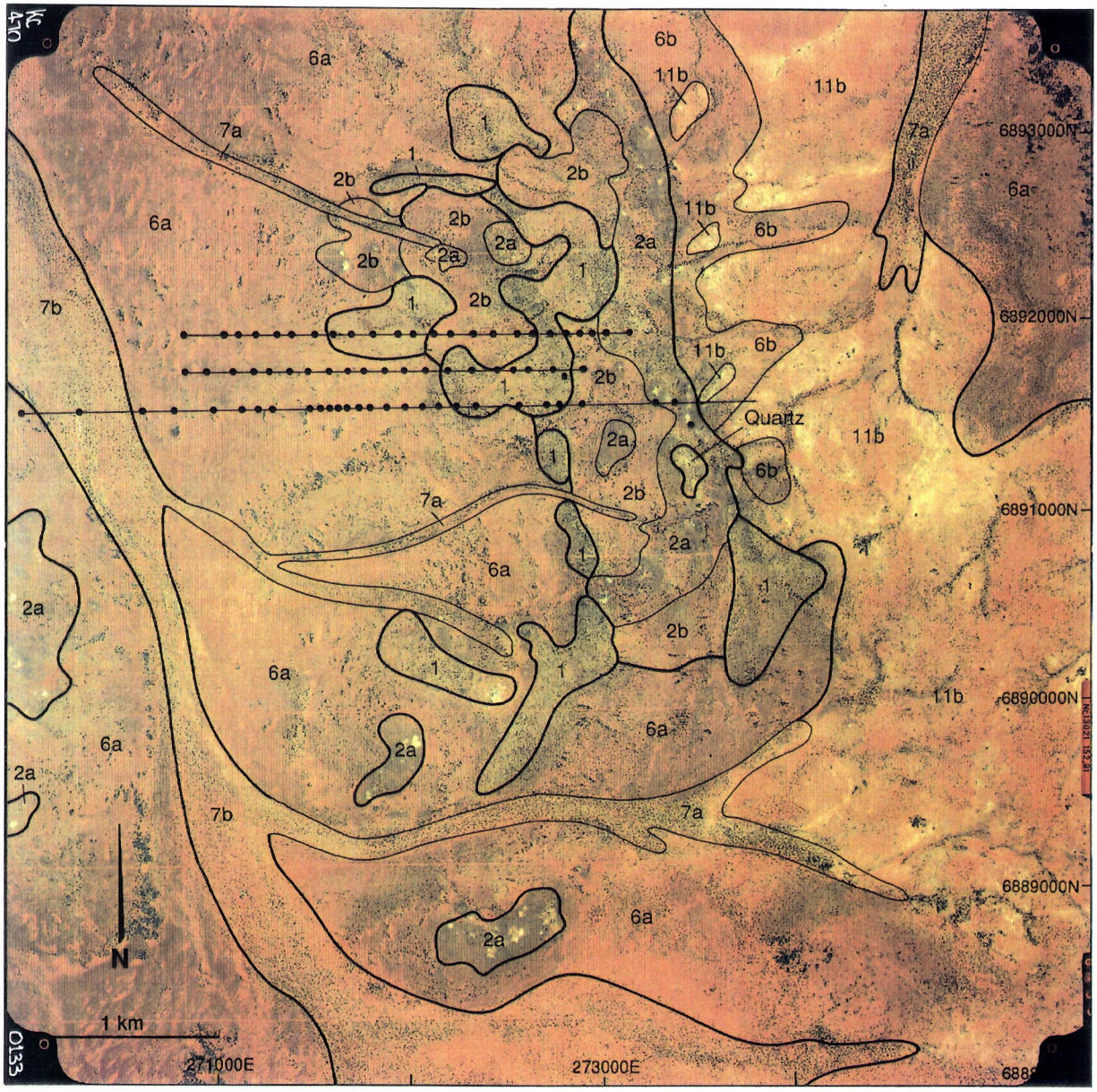

EROSIONAL REGIMES

Saprolite

- 2a — Sandy light clay soil, coarse black lag on saprolite, pedogenic calcrete
- 2b — Sandy clay loam soil, coarse lag on saprolite
- 11b — Granitic, felsic lithologies

RESIDUAL REGIME

Lateritic residuum

- 1 — Sandy light clay loam soil, lateritic lag, lateritic residuum

DEPOSITIONAL REGIMES

Colluvium

- 6a — Sandy clay loam soil, fine mixed lag, colluvium sheet wash
- 6b — Sandy loam soil, on felsic saprolite

Alluvium

- 7a — Light clay soil, alluvium in minor tributaries
- 7b — Sandy clay loam soil, alluvium in major tributaries

- • — Observations and/or sample sites

Fig. 1B. Map showing the surface distribution of regolith units and vegetation for the Meatoa area as an overlay to the colour air photograph (Kevron Aerial Surveys Run 6/0133, 4.1.89) published with permission of Homestake Gold of Australia Limited.

Table 1. Characteristics of Regolith Units: Meatoa Area, Lawlers

TYPE OF REGIME	EROSIONAL REGIMES			RESIDUAL REGIME	DEPOSITIONAL REGIMES			
REGOLITH UNIT AT SURFACE	2a	2b	11b	1	6a	6b	7a	7b
LANDFORM	Low hills, local valleys	Pediments, breakaway scarps (amphitheatres)	Pediplain	Undulating upland (crests, with backslopes)	Long very gentle slopes	Long very gentle slopes	Floors of minor tributaries	Broad wash features of major tributaries
VEGETATION	Mulga shrubs	Mulga shrubs	-	Mulga shrubs	Eremophila shrubs Geranium herbs	Mulga shrubs	-	Eremophila shrubs
LAG	Coarse lag of ferruginized saprolite, vein quartz	Lag of lateritic lithic fragments, ferruginized saprolite	Quartz	Fragments of Fe-rich duricrust, pisoliths and nodules, lateritic lithic fragments	Fine lag of mixed origin (ferruginous granules, lateritic nodules, lateritic lithic fragments)	Lag of ferruginized saprolite, lithic fragments and vein quartz from mafic terrain	Lag not common	Lag not common
SOILS	Red sandy light clays	Red sandy clay loams	Loamy sand	Brown fine sandy loam to fine sandy light clays	Red fine sandy clay loam to fine sandy light clays	Reddish brown sandy loams	Red light clays	Reddish brown sandy clay loams to light clays
ALLUVIUM	-	-	-	-	Some at depth	-	Thickness not known	2 - 3 m
COLLUVIUM	-	1-2m	-	-	Sands, white/grey clays (2-14 m)	1 - 2 m	-	-
HARDPAN (developed in colluvium/alluvium)	-	Minor	-	-	Hardpan can be present at 0.5-6 m	-	?	0.5 - 1.5 m
CALCRETE	Pedogenic calcrete	Pedogenic calcrete (minor)	-	-	-	-	?	-
LATERITIC RESIDUUM	-	-	-	Loose lateritic pisoliths/nodules, nodular duricrust (1-4 m) Duricrust can be Fe-rich	May be present beneath colluvium at 2-8 m. Thickness 0.5-3.5 m	-	?	1 - 2 m
MOTTLED ZONE	-	Minor	-	Minor	-	-	-	-
SAPROLITE	Multicoloured clay-rich/ferruginized saprolite		Granitic/felsic saprolite	Multicoloured clay-rich/ferruginized saprolite, occasionally mottled saprolite, variable thickness		Clay-rich felsic saprolite	Clay-rich/ferruginized saprolite, variable thickness	
BEDROCK	Basalt, Gabbro, Dolerite, Ultramafics, etc.		Granitic/felsic rocks	Basalt, Gabbro, Dolerite, Ultramafics, etc.		Granite	Basalt, Gabbro, Ultramafics, etc.	

data, an eastwest cross section (Fig. 2) was constructed for line 6891600N, showing the regolith stratigraphy and regolith/landform relationships (Fig.2). The eastern end of the cross-section is characterized by red sandy light clay and/or sandy clay loam soils overlying saprolite with sporadic outcrops of pedogenic calcrete. It is interpreted that lateritic residuum once covered this part of the section and has been removed by erosion to the level of saprolite. This eastern part of the area is thus designated an erosional regime. Erosional (2a, 2b) and depositional (6a, 7) regimes are separated by the residual regime (1). The dominant soils of Unit 1 vary from friable brown gravelly fine sandy loams to fine sandy clay loams with lateritic residuum at shallow (1 m) depth which in turn overlies clay rich and/or ferruginized saprolite. Lateritic residuum reaches four metres in thickness in the area and consists of both lateritic duricrust and a unit comprised of loose lateritic nodules and pisoliths.

Extensive red gravelly sandy clay loam to fine sandy light clay soils dominate the depositional areas. These gravelly soils fine downwards and merge at depth with colluvium comprising sandy/silty clay/loam interstratified with more gravel rich intervals. The colluvium reaches a thickness of 13 m in the Meatoa area. The colour of the matrix of the colluvium is generally red at the top, but becomes paler with depth. The lateritic residuum beneath the colluvium forms an almost continuous blanket for a distance of 1.5 km westwards from the broad crest at 272800E reaching a maximum thickness of 3.5 m. However, local truncation has been observed and regolith relationships can be complex. Transported lateritic material occurs as sporadic lenses of loose nodules/pisoliths within the colluvial unit. Hardpanization is widespread in much of the colluvial/alluvial unit, its development decreases westwards. Typically underlying the colluvium or residual laterite horizon is a multicoloured saprolite derived from mafic and ultramafic rocks. The saprolite extends to a depth of around 40 m passing into fresh mafic/ultramafic rock. A mottled zone is generally missing or is only very weakly developed.

3.4 Description of Regolith Units

3.4.1 Definitions

The terms used in the description of regolith materials are as follows:

Ferruginized saprolite refers to black, relatively homogeneous, weathered rock, which is very rich in Fe and may or may not have any relict textures. *Lateritic lithic fragments* are fragments of weathered rock which are yellowish brown to reddish brown, low in Fe relative to ferruginized saprolite, may or may not have any relict textures and can have diffuse mottling and incipient nodular structures. The lateritic lithic fragments are derived from the breakdown of the upper part of the saprolite and/or mottled zone. Lateritic lithic fragments have not yet been categorized in the classification scheme of Anand *et al.* (August, 1989). In this report, the code LG 221 is used as an interim measure. Other terms used are taken from the *Terminology, Classification and Atlas* of Anand *et al.* (August, 1989).

3.4.2 Erosional Regimes

Unit 2

This unit represents areas of mafic and ultramafic bedrock from which lateritic duricrust or any laterally equivalent regolith cap rock has essentially been removed by erosion. Unit 2 is widely distributed throughout the Lawlers district and, in the Meatoa area as at Brilliant, it can be subdivided as is now described.

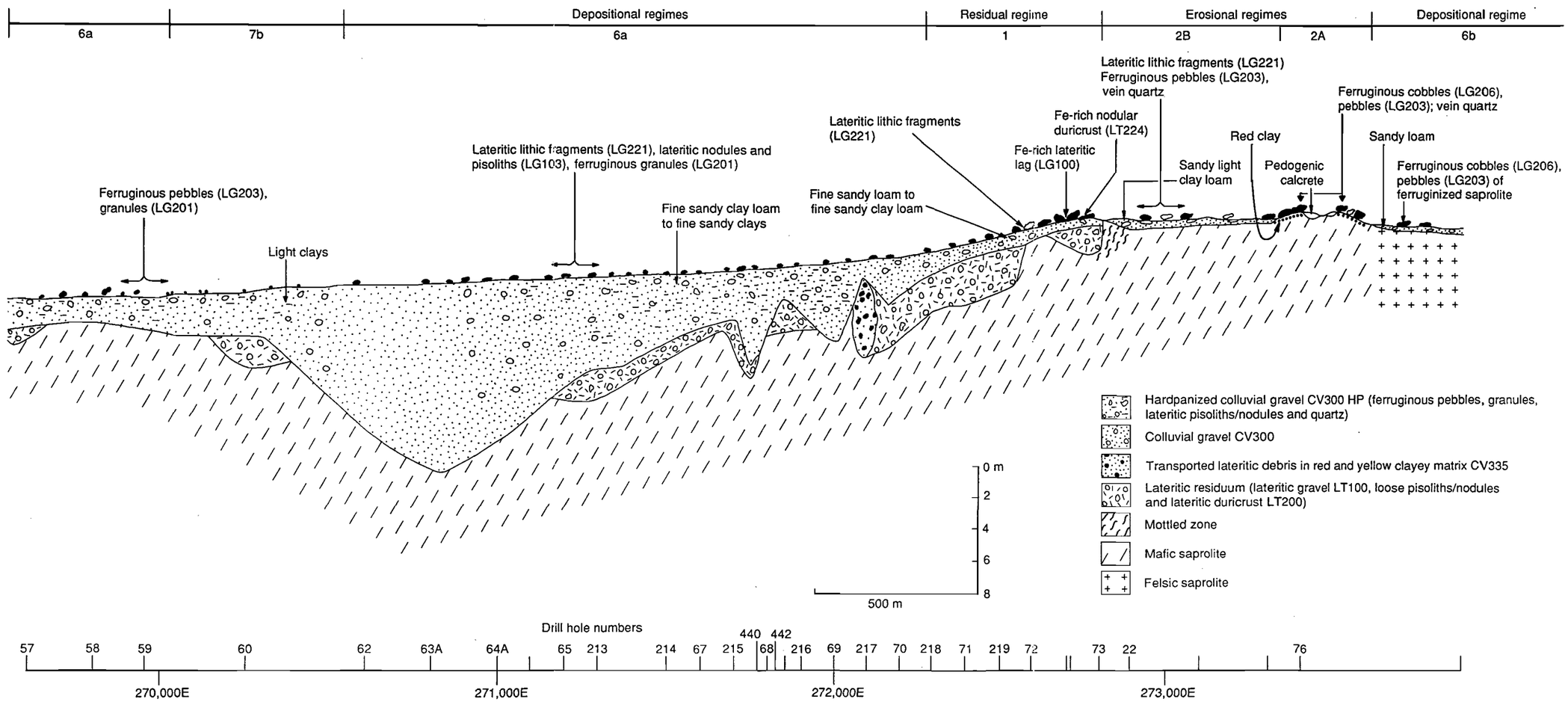

Fig. 2. Diagrammatic cross-section along line 6891600N in the Meatoa study area showing relationships for the regolith.

Unit 2a

Unit 2a at surface shows a consistently heterogenous and almost ubiquitous association of black ferruginous cobbles and pebbles, cobble sized fragments of vein quartz, associated red friable sandy light clay soils and randomly distributed isolated patches of pedogenic calcrete typically from 1 m to 5 m or more across which are commonly sites for goanna activity. The ground appearance of this unit is shown in Figs 3A, B.

The *black lag* consists dominantly of rounded to subrounded fragments of ferruginized saprolite with a goethite-hematite mineralogy (Fig. 3C). The cobbles/pebbles of ferruginized saprolite do not show identifiable relict textures. Cobbles exceeding 10 cm in diameter are common. The calcrete is pinkish, massive and contains inclusions of ferruginized saprolite.

The *soils* are red (10 R 4/6, 2.5 YR 4/6, moist) gravelly sandy light clays reaching 0.4 m in thickness and are acid except in the vicinity of the areas of pedogenic calcrete. Hardpan is generally absent. Several soil samples were separated into their gravel (>2 mm), sand (0.05 to 2 mm) and clay ($<2\mu$m) sized fractions.

The *gravel-sized fraction*, which represents 20-30% of the soil volume, largely consists of black ferruginous pebbles and ferruginous granules. The ferruginous pebbles are similar to the ferruginized saprolite cobbles and pebbles which form the lag. Subordinate amongst the pebble-sized material are subangular to angular yellowish brown (10 YR 5/8 to 10 YR 6/6, dry) lateritic lithic fragments which are goethite- and kaolinite-rich. Some lateritic lithic fragments show recognizable relict textures. Ferruginous granules range in morphology from hard, dense, shiny, magnetic, black (2.5 YR 3/0, dry) granules that contrast strongly with the soft soil matrix, through to red (10R 4/6, dry) mottled, earthy materials that are poorly separated from the soil matrix, being only weakly indurated and slightly Fe impregnated. Hematite, goethite, and kaolinite are the dominant minerals of the red granules. The black granules also contain hematite and goethite but in addition contain maghemite in low to moderate amounts. These magnetic black granules contain only small amounts of kaolinite in comparison with the associated non-magnetic red granules. These observations are in accordance with those of Taylor and Schwertmann (1974a) and are explained by the inhibiting effects of Al on the formation of *r*-phase Fe oxides such as maghemite and lepidocrocite (Taylor and Schwertmann, 1978). The ferruginous granules may have been derived from the breakdown of ferruginized saprolite; however, their mineralogy and fabric do not support this. Another possibility is that the granules have formed *in situ* within the soils. More work, however, is needed to confirm this.

The *sand-sized fraction* consists of ooliths, lateritic lithic fragments, grains of goethite pseudomorphs after primary minerals, earthy siliceous white fragments, and quartz grains. Grains from these five types were handpicked under a binocular microscope. The mineralogical nature of each type was then determined by X-ray diffraction and some representative grains were selected for scanning electron microscopy (SEM).

The *ooliths* are brownish yellow, (10 YR 6/8, dry) rounded, 0.5 - 2 mm in diameter, and are hard to vary hard. They generally have a porous yellowish brown (10 YR 5/8, dry) core with a very thin brownish yellow cutan. Ooliths largely consist of highly crystalline Al-goethite and kaolinite with very small amounts of quartz. Hematite and maghemite were not detected by X-ray diffraction. Additional sub-samples of these ooliths were gently crushed to expose internal surfaces and then analysed by SEM with an energy dispersive system (EDAX). Interior surfaces of ooliths show them to consist of fine crystalline aggregates of kaolinite and goethite (Figs 4A, B) which was confirmed by EDAX. Qualitative chemical analysis of such crystals only shows the presence of Fe, Al and Si. These ooliths are different from lateritic ooliths/pisoliths described in Section 3.4.3 in their morphology and mineralogy. It appears that these ooliths are pedogenic in origin and have formed during post-lateritic weathering.

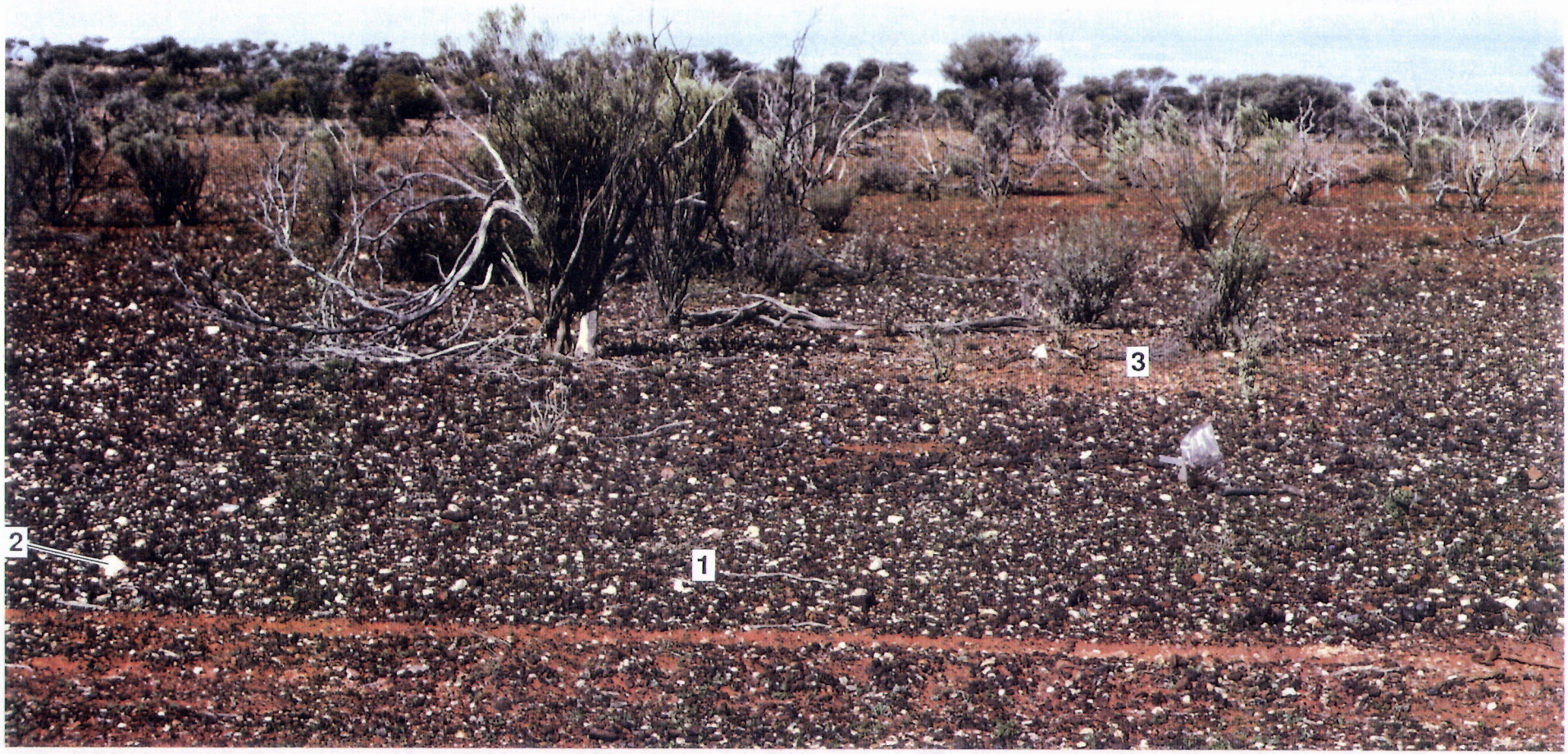

Fig. 3A. Regolith Unit 2a: Abundant lag of cobbles and pebbles after ferruginized saprolite (1), vein quartz (2) and pockets of calcrete (3) over sandy light clay soil, with degraded mulga shrubs, location 6891600N, 273350E.

Fig. 3B. Close up of ferruginous cobbles and vein quartz of Fig. 3A.

Fig. 3C. Hand specimen of cobbles and pebbles after ferruginized saprolite. Sample 07-1310.

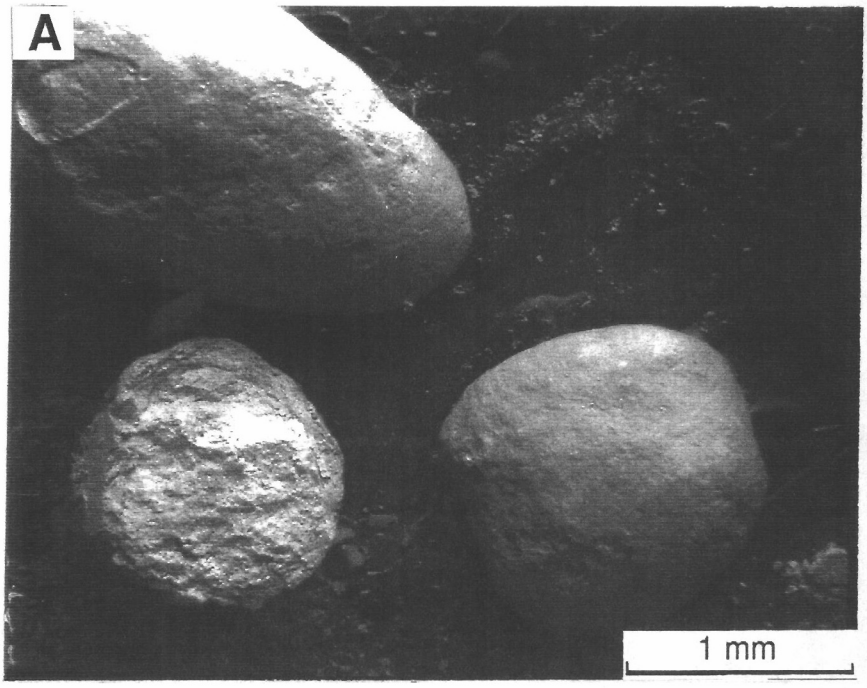

Fig. 4A. Low magnification scanning electron photomicrograph of separated ooliths from soils of regolith Unit 2a, location 6891600N, 273350E.

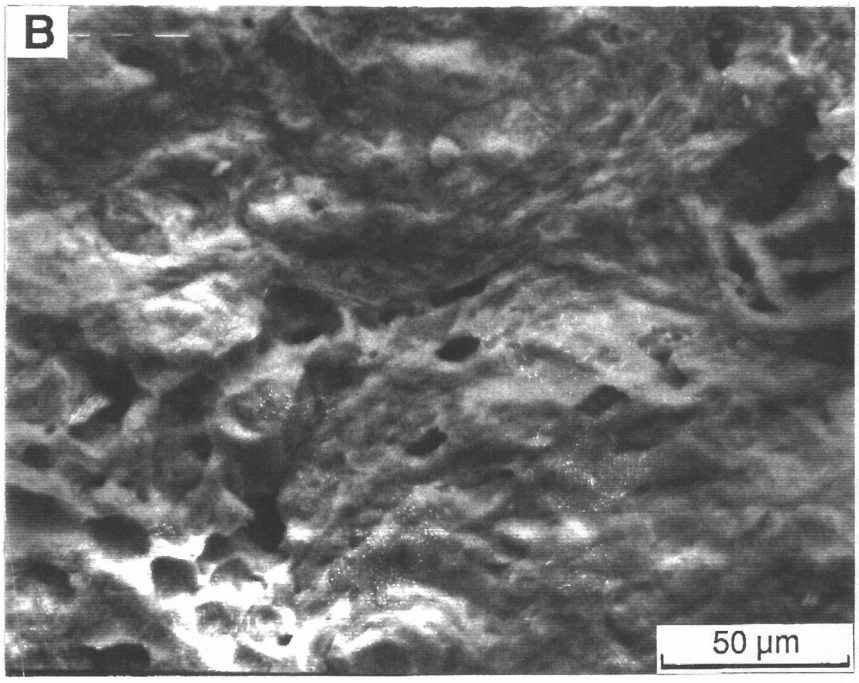

Fig. 4B. High magnification scanning electron photomicrograph of a broken surface of the lower left oolith of Fig. 4A, showing aggregates of goethite/ hematite and kaolinite. Energy dispersive X-ray (EDX) spectra indicated the presence of much Fe with smaller amounts of Al and Si.

The *lateritic lithic fragments* are brownish yellow (10 YR 6/8, dry) to yellowish brown (10 YR 5/8, dry), subangular to angular, 0.5 - 2 mm in diameter, hard and are goethite and kaolinite rich. Some lateritic lithic fragments show recognizable relict textures of mafic lithologies. Morphological and mineralogical characteristics of these lateritic lithic fragments appear to be very similar to those observed in large lateritic lithic fragments in the gravel fraction. This suggests that the sand-sized lateritic lithic fragments have been derived from the breakdown of large lateritic lithic fragments. These lateritic lithic fragments differ from the ooliths described above in shape, retention of relic textures and origin. The lateritic lithic fragments are probably derived from upper parts of the saprolite/mottled zone.

Goethitic pseudomorphs after amphibole form black (7.5R 2.5/0, dry) millimetric grains. Surfaces of the pseudomorphs are heavily pitted which result in the formation of fragile shells or ghosts (Fig. 5) and largely consist of blade-shaped crystals of goethite. The semi-quantitative chemical anlaysis of such crystals shows them to consist of Fe with small amounts of Al, Ca, Ti, K, Si, and Cu. The traces of Ca probably represent the unweathered parts of amphiboles, whereas Ti, Si, Al, and Cu can substitute for Fe^{3+} in goethite, but the presence of K is not explained.

The *clay fractions* of Unit 2a are dominated by kaolinite. Other minerals present are illite, chlorite, smectite and mixed-layer minerals as well as goethite and hematite. The clay minerals are the result of weathering of amphiboles and plagioclase feldspars. The presence of illite cannot be explained by the weathering of primary mineral grains of the bedrock, because mica is generally absent in mafic and ultramafic rocks as is K-feldspar. The formation of illite, however may be explained by the concentration of K in the surface horizons through biocycling giving rise to an ionic environment in which mica would form (Swindale and Uehara, 1966). Alternatively, the illite could be aeolian in origin, travelling distances of 1 to 2 km from the adjacent granitic terrain.

Unit 2b

Unit 2b is characterized by an association of the following regolith components: a coarse lag of lateritic lithic fragments, ferruginized saprolite and vein quartz, a surface red (10 R 4/6, moist) sandy clay loam soil, and locally-derived colluvium of sandy clay loam and sandy light clays. The colluvium may reach 1 m in thickness. The field appearance of this unit is shown by Fig. 6A. Regolith Unit 2b represents areas of Unit 2 where the locally-derived colluvium has accumulated, supressing topographic variations. Authigenic hardpanization affects much of this colluvium. The hardpan matrix is characteristically porous, red to red brown (2.5 R 4/6, 5/6, moist), and films of Mn oxides are present on surfaces. The lag is relatively finer (up to 50 mm) and less abundant on this unit in comparison with Unit 2a and mainly consists of yellowish brown (10 YR 5/8, dry) kaolinite- and goethite-rich lateritic lithic fragments, black (2.5 YR 3/8, dry) hematite-goethite rich ferruginous pebbles of ferruginized saprolite, and a few scattered pisoliths (Fig. 6B). The goanna mounds marking the presence of calcrete in Unit 2a are characteristically absent from Unit 2b.

Unit 11b

This unit represents areas of outcrops of granitic/felsic lithologies with a thin sandy soil cover. Quartz lag is common.

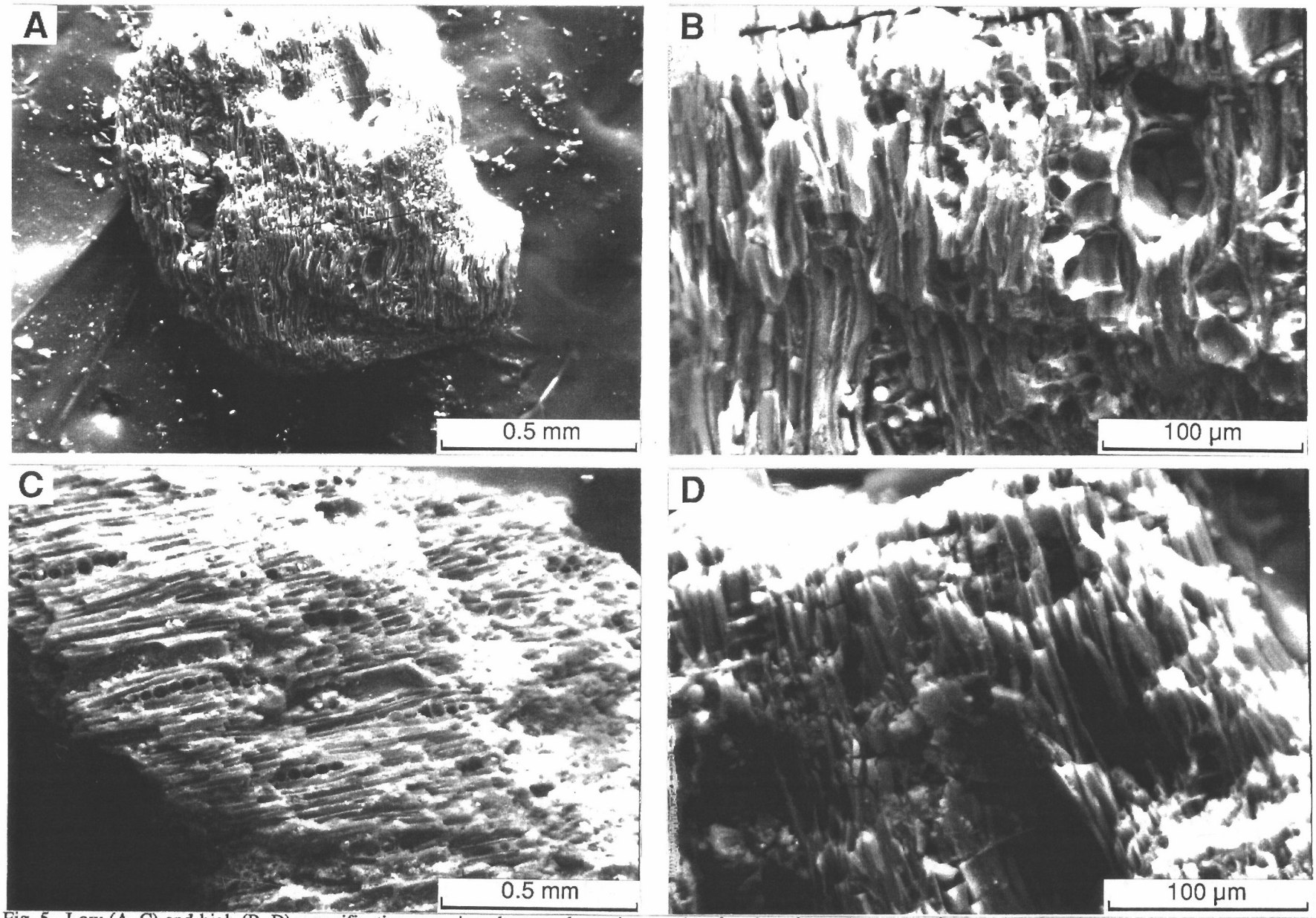

Fig. 5. Low (A, C) and high (B, D) magnification scanning electron photomicrographs of grains of pseudomorphs after amphiboles separated from soils of regolith Unit 2a. These grains are replaced by blade-shaped crystals of goethite. Energy dispersive X-ray (EDX) spectra indicated the presence of Fe confirming the presence of goethite, location 6891600N, 273350E.

Fig. 6A. Regolith Unit 2B: Lag of lateritic lithic fragments, pebbles after ferruginized saprolite and vein quartz over sandy clay loam soil, location 6891600N, 272800E.

Fig. 6B. Hand specimen of lag of lateritic lithic fragments (1), pebbles after ferruginized saprolite (2), and sporadic pisoliths (3). Sample 07-1313.

3.4.3 Residual Regimes

Unit 1 represents areas where the complete lateritic weathering profile, including the lateritic residuum, is preserved. In the Meatoa area, the unit is composed of the following subunits: friable brown (7.5 YR 4/4, moist) gravelly fine sandy loam to fine sandy clay loam soil, loose pisoliths/nodules, and nodular duricrust. Mottled zone material, which could be expected if the duricrust is locally eroded, was not recognized. Surface expression of this unit is shown in Fig. 7A.

The lag on this unit is mostly lateritic, however, some lithic lag also occurs. This lithic lag is related to pockets of saprolite exposed in the unit. Lateritic lag appears to have been derived from the breakdown of Fe-rich nodular duricrust and comprises reddish-brown (2.5 YR 4/4, dry) to black (2.5 YR 3/0, dry) coarse fragments (~40 mm) of nodular duricrust and reddish-brown, 5-10 mm pisoliths and nodules (Fig. 7B). Lithic lag consists of yellowish-brown to reddish-brown subangular to angular, 2-30 mm clay-rich lateritic lithic fragments. Some lateritic lithic fragments retain the primary rock fabric.

Soils in Unit 1 are brown (7.5 YR 5/4, moist), gravelly fine sandy loams to sandy clay loams and are slightly acidic. Generally hardpan is not present. The dominant (25-40 vol%) gravel component of these soils is 2- to 15-mm sized lateritic nodules and pisoliths. Occasionally, reddish-brown pseudomorphic grains are also present, but it is not clear whether these are after orthopyroxenes or amphiboles. The pseudomorphic grain shown in Figure 8 is about 4 mm in size and is completely replaced by a mixture of laths and platy crystals of Fe oxides and kaolinite. Qualitative chemical analysis of this crystalline aggregate shows the presence mainly of Fe with small amounts of Al and Si. Aggregates of similar morphology have been shown to develop from chemical weathering of orthopyroxenes in ultramafic rocks under lateritic conditions by Nahon and Colin (1982). These authors considered that lath shaped goethite is pseudomorphic after talc.

The *sand fraction* (25-35% vol%) largely consists of yellow to dark reddish-brown ooliths, quartz, black ferruginous granules, and yellowish brown lateritic lithic fragments. Magnetic ooliths and ferruginous granules are hematite-, goethite- and maghemite-rich with small amounts of kaolinite. The non-magnetic fraction contains large amounts of kaolinite, but maghemite was not detected. The ferruginous granules and ooliths are related to pisoliths and nodules of the gravel fraction and appear to have been derived from the breakdown of pisoliths and nodules. The lateritic lithic fragments largely consist of goethite and kaolinite. The presence of lithic fragments in these higlhy weathered soils suggests that the fragments are transported.

The *clay fraction* is largely dominated by kaolinite. Traces of chlorite, illite and mixed-layer minerals are also present.

The *lateritic residuum* is composed of varying proportions of matrix with lateritic pisoliths and nodules, but it was not possible to quantify the relative abundances using drill hole pulps. The cores of the nodules and pisoliths are dark reddish brown (5 YR 3/3, dry) through black (2.5 YR 3/0, dry) to red with thin, usually <2 mm, green coatings. Nodules, pisoliths and ooliths are present, however nodules are generally dominant. The nodules are subrounded to irregular in shape with a size range of 2-15 mm and are indurated by hematite, goethite, and maghemite. Similar nodules and pisoliths were also observed in the North Pit area and the characteristics of these were described in detail by Anand *et al.* (1989).

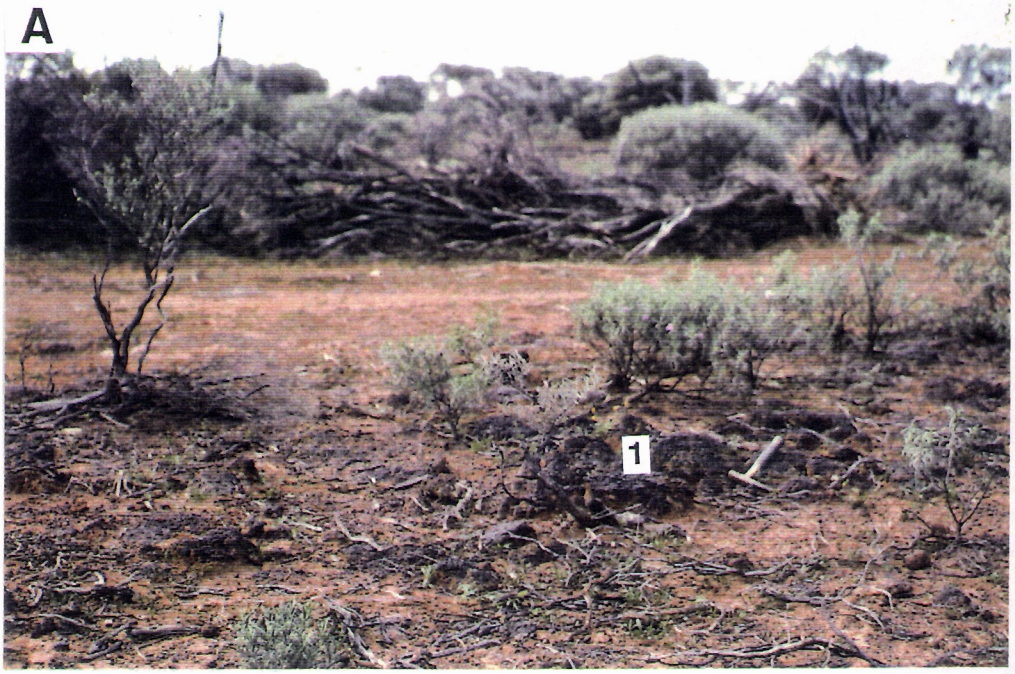

Fig. 7A. Regolith Unit 1: Fe-rich nodular duricrust (1) surrounded by sparse lateritic lag and mulga shrubs on crest, location 6891600N, 272720E.

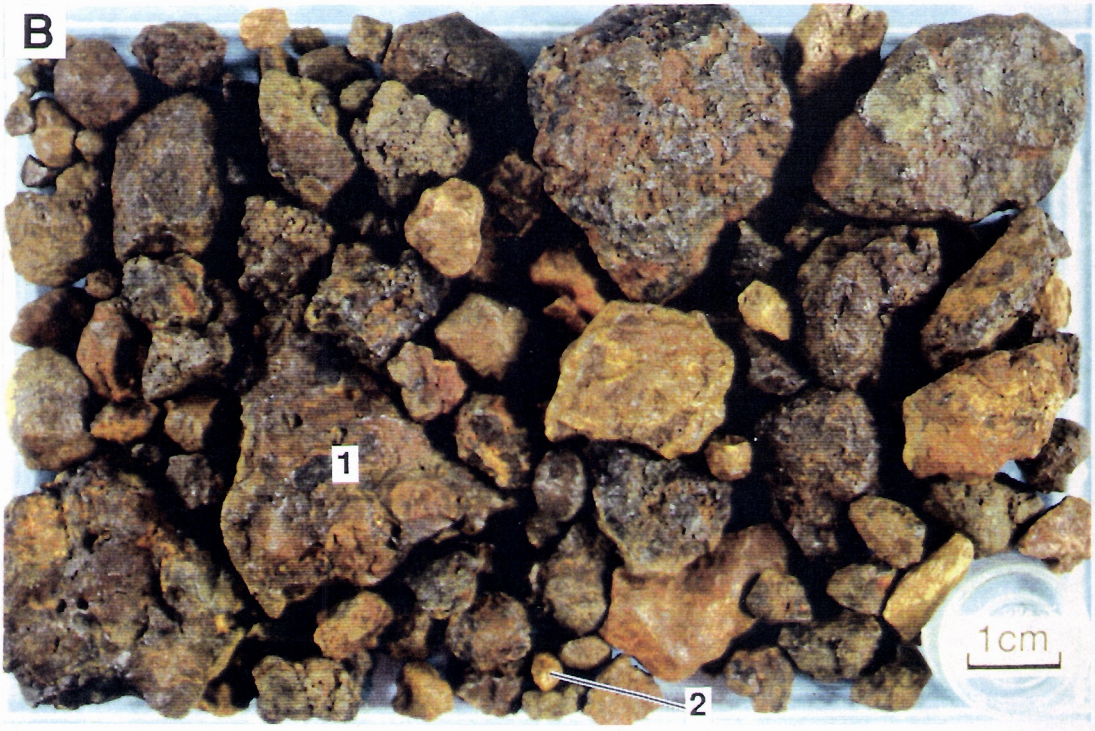

Fig. 7B. Hand specimen of lateritic lag showing fragments of Fe-rich nodular duricrust (1) and lateritic pisolith (2). Sample 07-1315.

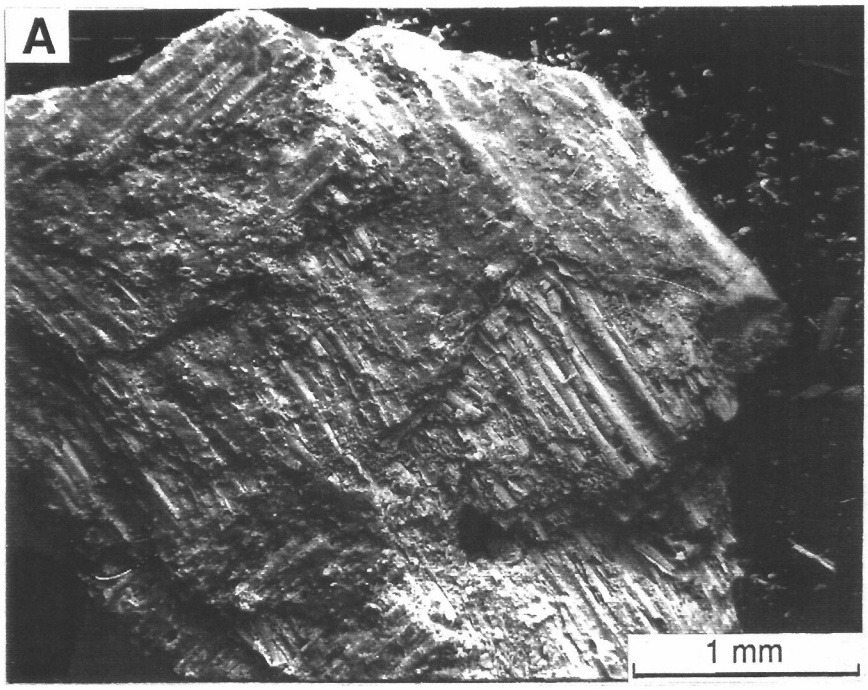

Fig. 8A. Low magnification scanning electron photomicrograph of separated grain of pseudomorph after orthopyroxenes (?) from soils of regolith Unit 1, location 6891600N, 272700E.

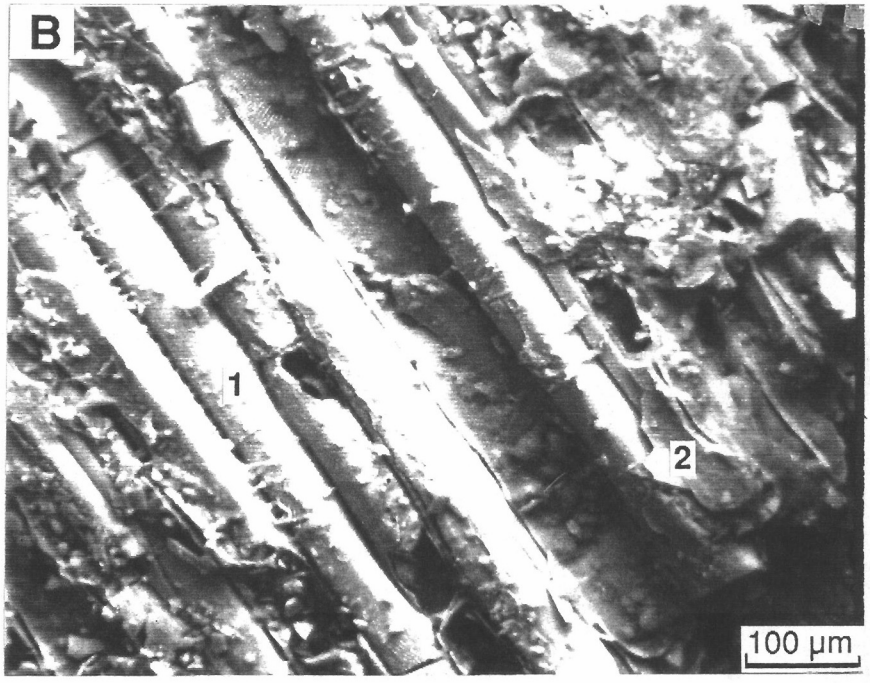

Fig. 8B. High magnification scanning electron photomicrograph of part of grain of Fig. 8A showing laths of goethite (1) and platy crystals of kaolinite (2).

3.4.4 Depositional Regimes

Much of the Meatoa area is characterized by unconsolidated colluvium and alluvium, a significant part of which has been derived from erosion of the lateritic weathering profile in upland areas. These depositional units commonly conceal extensive areas of complete lateritic weathering profiles.

Unit 6 - Colluvium
Two major types of colluvium are recognized in the Meatoa area. Unit 6a accounts for about 70% of the mapped Meatoa area.

Unit 6a
Unit 6a is a sand-silt-gravel colluvial unit which is well represented throughout the Lawlers district, and is believed to represent sheet wash and braided wash sediments derived from dismantling of adjacent lateritic and saprolitic uplands. In the Meatoa area, Unit 6a reaches 5 to 13 m in thickness and has resulted in burial of the West-sloping lateritic residuum and suppression of local relief of the partly-eroded lateritic surface. Hardpan due to cementation of the sandy clay/silty clay colluvial units is variable and reaches a maximum development within 2 m of surface.

Unit 6a has a vaneer of lag fragments in the 2-10 mm size range. This lag consists of lateritic lithic fragments (yellow, 10YR 6/8, dry), and dark reddish-brown, (5YR 3/3, dry), lateritic nodules, black ferruginous granules, and quartz fragments. The ferruginous granules appear to be derived from ferruginized saprolite and/or cores of black lateritic nodules. This lag typically overlies a gravelly red (10 R 4/6, moist) soil consisting of sandy clay loam to fine sandy light clay. The surface appearance of this unit is shown by Figs. 9A, B, C. The upper horizons of the colluvium are dominated largely by coarse gravels, the unit becoming finer with depth.

Gravel fractions of surface soils consist of a variety of clasts including lithic and ferruginous pebbles, quartz fragments and lateritic pisoliths and nodules. The clasts are subangular to angular, unsorted and reach 40 mm in diameter. The variety of clasts indicates their diverse origin, possibly from the breakdown of saprolite and lateritic duricrust.

The *sand-sized fraction* consists of rounded to subrounded shiny black and red ferruginous granules, black lateritic pisoliths, and grains of quartz. Both magnetic and non-magnetic granules are present. Many of the rounded ferruginous granules are transported.

The *clay-sized fraction* largely consists of kaolinite with small amounts of illite. Chlorite and mixed-layer minerals were not detected. Both goethite and hematite are present.

Unit 6b
Regolith Unit 6b characterizes areas which have a felsic substrate, but which have a mantle of colluvium derived from the adjacent mafic/ultramafic terrain. The lags of ferruginized saprolite, lateritic lithic fragments, and vein quartz derived from mafic terrain contrast with the quartzose and feldspar grits of the felsic detritus. Red friable fine sandy clay loams dominate the mafic detritus, while reddish-brown to brown gritty sandy loams are common soils on felsic detritus.

Unit 7 - Alluvium
Alluvium in the Meatoa area overlies lateritic duricrust or saprolite at depth and is in excess of 3 m thick. Alluvium accounts for about 10 % of mapped area at Meatoa. Unit 7 was divided into subunits as used elsewhere in the Lawlers district.

Fig. 9A. Regolith Unit 6a: Fine lag of mixed origin and eremophila shrubs and geranium herbs on colluvial outwash plains, location 6891600N, 271300E.

Fig. 9B. Close up of fine lag of mixed origin of Fig. 9A.

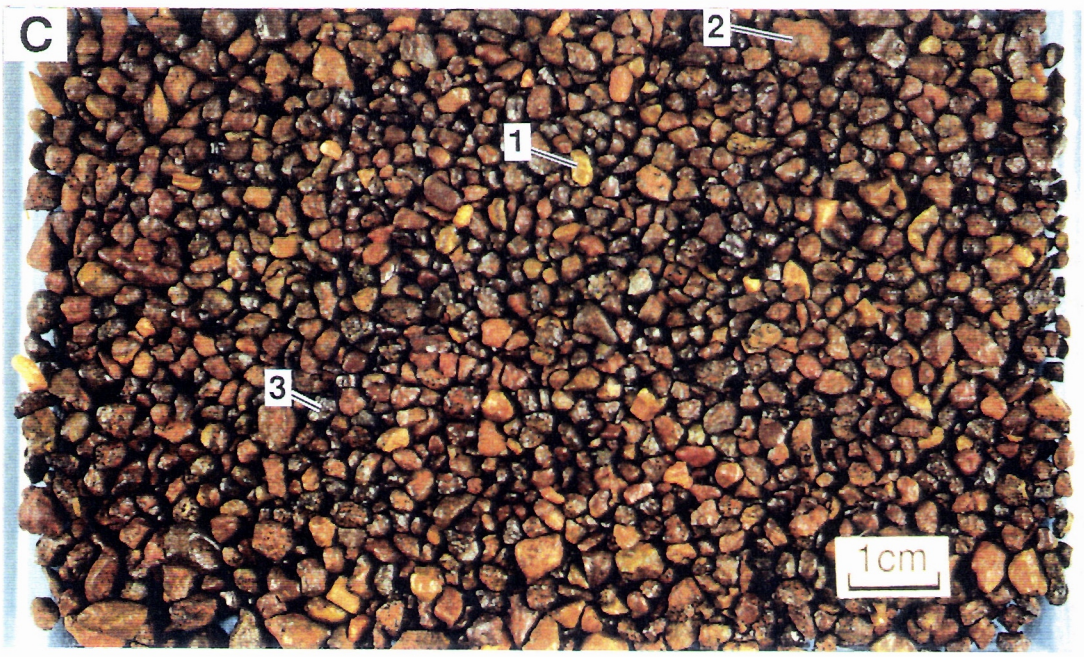

Fig. 9C. Detail of fine lag of mixed origin showing lateritic lithic fragments (1), lateritic pisoliths/ nodules (2) and ferruginous granules (3). Sample 07-1330.

Unit 7a - alluvium in minor tributaries
Red (10 R 4/6, moist) friable light clays are dominant. Lags are not common.

Unit 7b - alluvium in major tributaries
The dominate surface soil is a reddish brown (5 YR 3/3, moist), gravelly sandy clay loam varying to a light textured clay. Hardpan is developed at about 30 cm. There is very little lag on the surface.

3.5 Regolith/Landform Relationships

Field settings and airphoto interpretation show close relationships between regolith type and landforms. Regolith Unit 2 comprises a terrain within which erosion has removed the lateritic residuum, mottled zone and, in places, the saprolite. Subunit 2a is characterized by local undulating saprolitic terrain, comprising low stony hills and local valleys of mostly mafic rocks and shallow red friable light clay soils. Coarse lag of ferruginized saprolite and vein quartz is common. Pockets of calcrete have been worked into mounds by goannas.

Subunit 2b is characterized by terrain having long gentle slopes, often forming into wide amphitheatre with broad drainage floors. This subunit includes pediments and often is limited by breakaways and locally steep rocky slopes. Colluvial mantles are extensive, comprising friable sandy clay loam to fine sandy light clays derived from within Unit 2. Lag is relatively less abundant on this subunit and consists mainly of lateritic lithic fragments and ferruginized saprolite.

Regolith Unit 1, characterized by a complete laterite profile, forms on topographically higher parts of the area, and is a gently-undulating upland comprising broad crests flanked by long gentle slopes sometimes being elements of broad concavities (often referred to as backslopes). This unit, in part, is limited by prominent convex breaks of slope against the erosional regimes, such as the breakaway scarps. Downslope, the unit merges with the very long gentle sloping tracts of regolith Unit 6a. Broad crests are capped with Fe-rich nodular duricrust, the characteristics and origin of which are discussed in Section 7.0. Due to local truncation within areas mapped as Unit 1, patches of saprolite may be exposed, and in places are partially silicified. Pockets of silcrete may also occur. Fe-rich nodular duricrusts are important features of the crests within Unit 1, but there can also be scattered outcrops of saprolite.

Regolith Unit 6a is characterized by a terrain having long very gentle slopes, consisting of colluvium that had been largely derived from dismantling of the lateritic weathering profile. The slopes are commonly an extension of those of Unit 1. Unit 6a is characterized by a complex ridge-interridge microrelief with alternating bare areas and mulga groves typical of Wanderrie terrain (Mabbutt, 1963). The fine lag of mixed origin is widely distributed on colluvial slopes and becomes finer downslope. The upper elements of regolith Unit 6a merge with the paleofilled channel which exists to the east of the present-day drainage.

Regolith Unit 7a is expressed by floors of minor tributaries which merge laterally with adjacent Units 6 and 2b. Regolith Unit 7b is characterized by broad wash features of major tributaries occurring as broad drainage floors set slightly below the very long gentle slopes of Unit 6.

3.6 Synthesis

The landforms and regolith of the Meatoa area can be related to a complex physiographic history, including deep weathering, erosion, and deposition. Weathering of the mafic and ultramafic rocks has produced a thick, deeply-weathered mantle which shows vertical differentiation of developed horizons. The successive arrangement of these horizons, starting from the parent rock, follows this upward sequence: saprock-saprolite/ferruginized saprolite – mottled zone (weakly developed) – lateritic

duricrust – loose pisoliths/nodules. Primary minerals (amphiboles, feldspars, pyroxenes) weather into secondary products which in turn are transformed later and higher in the profiles into new products, amongst which iron oxides and hydroxides are the most abundant. The main characteristic feature of the lateritic weathering in the Meatoa profiles is the epigenetic replacement of kaolinite by Al-hematite in the upper part of the saprolite and ferruginous zones. This reaction is important since it involves the dissolution of kaolinite with the accompanying release of protons which may contribute to the dissolution and dispersion of gold (Ambrosi *et al.*, 1986; Colin *et al.*, 1989).

In the Meatoa area, differential stripping of the weathered profiles has resulted in an array of land surfaces apparently related to an older weathering profile. Erosion has affected some parts, while other parts such as broad crests and back slopes, remained relatively unchanged. Materials removed from the erosional areas have been deposited on lower slopes with consequent burial of deeply-weathered profiles and the reduction of local relief. Field relationships and subsurface information provided by drilling indicate that the present colluvial plains, for example, have had relatively higher relief before erosion. The occurrence of saprolite in the low hill areas suggests that the land surface was truncated by some 10 m or more. Perhaps the low hills were topographically higher than the present crests which are now capped with Fe-rich duricrusts and underlain by a complete laterite profile. If valleys and lower slopes were capped with Fe-rich duricrust, once hardened they would be resistant to erosion. Inversion of relief may have eventually caused Fe-rich duricrust to be located on ridge crests. The origin of these Fe-rich duricrusts is discussed in detail in Section 7.0.

Erosional regimes (Units 2a, 2b) are covered by red clay soils and coarse lags derived from ferruginized saprolite and have a much more immature weathering status based upon the presence of recognizable pseudomorphs after amphiboles and lateritic lithic fragments inherited from the saprolite. The residual regime (Unit 1) is dominated by gravelly soils and lags of lateritic gravels consistent with an origin by the breakdown of lateritic duricrust. Soils on the depositional areas (Units 6, 7) show slight increases in clay content and consist of heterogenous gravels, suggesting a transported rather than local origin. Lag gravels in the depositional areas are also of mixed origin and appear to have been derived from both the erosional and residual areas.

One of the main characteristic features of the soils in the erosional areas at Meatoa, and seen at other areas of Lawlers district, is the occurrence of friable acid red clays, which from drilling, are seen to overlie mafic lithologies. It might be expected that the soils developed from mafic lithologies would be calcareous and have significant amounts of smectite-type clay minerals, but these red clays lack carbonates and smectite. The non-calcareous nature and low level of smectite in these soils suggest that they have formed under generally mild to warm conditions, free drainage and sub-humid to humid climates with alternating wet and dry periods. These are the conditions interpreted to be necessary for leaching of carbonates and bases and the formation of kaolinitic clays that are acid and unsaturated with bases. Some Fe released on weathering has been mobilized and segregated as ooliths presumably during brief periods of partial saturation following heavy or prolonged rains. These observations do not support the general belief that these soils are the product of weathering of mafic lithologies during an arid climate in which they now occur. In arid climates, pedogenic processes such as the leaching of carbonates, do not occur due to the lack of water. However, the genesis of these red clays can be explained by the following: the acid red clay soils are recent residual soils formed in an arid climate from highly-leached kaolinitic mafic saprolite, the latter being a product of the earlier tropical weathering. Thus, kaolinization and leaching of bases and carbonates of mafic saprolite occurred in the earlier humid-tropical climates. Due to a general change to an arid climate during the mid-Tertiary, deep weathering ceased and vegetation changed, resulting in slope instability. Erosion removed the upper part of the weathering profile, including lateritic residuum, thereby exposing the leached saprolite. This leached saprolite then became the parent material of the red clays.

Both hardpan and calcrete are clearly much younger than the original lateritized surface. In the Meatoa area hardpan has developed in both *in situ* regolith and detritus resulting from the erosional modification of the old surface. Cementation of these materials by silica to form the hardpan is a relatively recent process, because the hardpanization is affecting colluvial units and some soil units. Calcrete in erosional areas is pedogenic in origin and has formed by the relative accumulation of carbonates due to the alteration of Ca-rich host materials in this case from mafic rocks.

The understanding of regolith relationships at Meatoa area has provided a framework for the geochemical sampling programme. In the residual regime (Unit 1), where the lateritic duricrust/loose nodules occur at or near the surface, sampling of lateritic nodules should be adequate to detect surface expression of mineralization. By contrast, in the erosional regime (Unit 2a) different sample media (e.g. red clay or saprolite) have to be employed because the lateritic residuum has been removed by erosion. Here in the erosional areas, saprolite is the parent material of red clays and the geochemical patterns in the red clays will closely resemble those of original saprolite, modified by the later processes, for example, leaching or calcrete formation. Hence soil geochemistry using BLEG techniques is effective, for example, within Unit 2a.

The understanding of regolith relationships at Meatoa has also provided a framework within which lag types will now be discussed. Ooliths that have developed in red clays must be distinguished from the lateritic pisoliths. The origins are different and they have different geochemical characteristics. In the depositional regimes (Units 6, 7), where the lateritic residuum is buried, it is necessary to drill for *in situ* samples, the nature of which will depend upon the degree of truncation of the profile before deposition. In drilling designed to detect buried laterite geochemical haloes, it is important to distinguish colluvial/alluvial units containing an abundance of lateritic pisoliths and nodules from lateritic residuum. The criteria for distinguishing between residual and transported laterite are discussed in detail in an earlier report by Anand *et al.* (April, 1989).

4.0 MORPHOLOGY, MINERALOGY AND GEOCHEMISTRY OF LAG GRAVELS, MEATOA AREA

4.1 Introduction

Section 4 addresses the objectives of gaining an understanding of lag types as a potential geochemical sampling medium pertinent to the Lawlers district. The approach was to systematically relate the type and characteristics of lag gravels to the regolith/landform framework of reference established from the research presented in Section 3 and thus gain an understanding of their origin. It could be expected that the findings established at Meatoa would then shed light upon the more general use of lag in exploration at Lawlers. It is not possible, however, in this concise study to carry out a comprehensive geochemical orientation. Lags described in this section refer to surface accumulations, fragments of regolith, rock and mineral particles resulting from removal of finer material by an aeolian and pluvial processes or by matrix removal through differential weathering. Other workers (e.g. Carver *et al.*, 1987) have shown that such materials in many situations are predominatly bedrock-derived and can be effectively used as a sampling medium in exploration programmes for Au and base metals in arid and semi-arid terrains of Western Australia.

The lag gravels which occur over most ground surfaces at Meatoa contain a variety of clast types including lateritic lithic fragments, ferruginous granules, pebbles and cobbles, fragments of Fe-rich duricrust, lateritic nodules and pisoliths, and white vein quartz. The various clast types are mixed, but their general distribution can be related to source material, such as regolith substrate or upslope outcrops, and to landform position. Coarse lag gravels tend to dominate the erosional areas (regolith Units 2a, 2b) to the east, whereas fine lag dominates the regolith Unit 6. In the Meatoa area, four major categories of lag have been recognised in the field and are described below in Section 4.3.

4.2 Sampling And Analytical Procedures

4.2.1 Sample Collection

Twenty-three samples of lag from line 6891600N were chosen for detailed study, out of a total of 80 samples which also covered parts of lines 6891800N, 6892000N, and 6894000N. The samples of lag were taken at 50 to 100-m intervals, depending on the type of lag and the mapped regolith/landform units. For comparison, three Fe-rich duricrust samples are also included. At each sample site, about 1.5 kg of the loose surface material was swept from an area of 0.25-1 m^2 using a plastic dustpan and brush. Coarse lag, such as fragments of Fe-rich duricrust, were collected by hand. Vein quartz in the pebble and cobble-size range was discarded.

4.2.2 Laboratory Methods

Attention was focussed upon the plus 2-mm fraction of lag gravels. In order to obtain this, samples were passed through a 2-mm non-metallic sieve to separate sand, silt and organic debris. The minus 2-mm fraction was stored for possible future work. The plus 2-mm fraction was washed with water to remove the soil and fine organic debris attached to the surfaces of lag gravels and dried at <50° C. A small, representative portion of each sample was selected for future reference, slicing and petrogrpahic examination, the remainder was crushed and ground using non-metallic methods described by Smith (1987). Oversize materials, particularly coarse lags, were reduced to minus 8 mm by crushing between zirconia plates in an automated hydraulic press with the undersize then being processed through an epoxy resin line disc grinder with alumina plates and reduced to minus 1 mm. Final milling was done in a motorized agate mill.

Analytical Methods

Chemical methods
A combination of chemical analytical methods including inductively coupled plasma spectroscopy (ICP), X-ray fluorescence (XRF) and atomic absorption spectrophotometry (AAS) were used to analyse 32 elements. Table 2 shows the elements analysed, method used and lower limits of detection.

Petrography
Samples were sliced for petrographic study of the colour and major fabric under a binocular microscope. Polished sections of selected samples were prepared and examined using a reflected light petrographic microscope in order to provide information on mineralogy and internal fabrics.

X-ray Diffraction
XRD patterns of pulverized representative samples of lag gravels were obtained using Cu Kα radiation with a Philips vertical diffractometer and graphite diffracted beam monochromator. The diffraction peaks were recorded over the 2θ range of 3-65° and data collected at 0.02° 2θ intervals. The semi-quantitative abundance of minerals in each sample was estimated using a combination of XRD and chemical analyses of bulk samples. The relative proportions of constituent minerals were estimated from peak intensities of selected characteristic lines on XRD traces. This approach provides a reconnaissance assessment of relative mineral abundance. The following diffraction lines were used - (111) and (110) lines of goethite, (012) and (202) lines of hematite, (313) and (220) lines of maghemite, (001) of kaolinite, (101) of anatase, (110) of rutile and (101) of quartz.

Aluminium substitution in Fe-oxides
The type, crystallinity, and Al substitution of Fe oxides are influenced by pedogenic environments (Fitzpatrick and Schwertmann, 1982; Schwertmann, 1985). Because of its identical valency and its similar size (r = 0.67 Å for Al and 0.76 Å for Fe) the Al atom can replace Fe in its octahedral position in Fe (III) oxides. An important characteristic of Al substituted Fe (III) oxides is their smaller unit cell size (shift in XRD peaks) caused by the slightly smaller size of Al. In lag samples, the concentration of goethite and hematite was high enough to be easily detected by XRD without any pre-treatment. For Al substitution measurements a NaCl or quartz internal standard was added. Measurement errors of the position of peaks were estimated and the positions of diffraction lines corrected. Aluminium substitution in goethite was determined from the (111) reflection using the relationship of mole % Al = 2086–850.7d (111) as established by Schulze, (1984). Aluminium substitution in hematite was calculated from the a dimension of the hematite unit cell as obtained from the d(110) using the relationship mole% Al = 3109–617.1a (Schwertmann et al., 1979). Aluminium substitution in maghemite was determined from the spacings of the (220) reflection and a calibration curve given by Schwertmann and Fechter (1984).

Scanning electron microscopy
The micromorphology and qualitative energy dispersive analysis of materials in polished sections of hand picked clasts from the gravels were carried out using a JEOL Geo SEM 2.

Microprobe analysis
Geochemical analysis of each bulk sample provided the average chemical composition of that lag type. However a variety of clast types generally occurs within each sample of lag. The chemical composition of individual grains however, can be determined by microprobe analysis which also provides information on the association of elements within particular mineral species. Selected mineral grains in polished sections were thus analysed using a Cameca SX-50 microprobe (specimen current 100 nA beam, accelerating voltage 25 kV). A suite of major and minor elements including Si, Al, Fe, Ti, Mg, Ca, Na, K, As, Cr, Cu, Mn, Ni, V, and Zn were determined.

Table 2. Analytical methods and lower limits of detection

Element	Reported as	Method	Detection Limit
SiO_2	wt%	ICP	0.2
Al_2O_3	wt%	ICP	0.04
Fe_2O_3	wt%	ICP	0.03
MgO	wt%	ICP	0.004
CaO	wt%	ICP	0.007
Na_2O	wt%	ICP	0.007
K_2O	wt%	ICP	0.06
TiO_2	wt%	ICP	0.003
Mn	ppm	ICP	15
Cr	ppm	ICP	20
V	ppm	ICP	5
Cu	ppm	AAS	2
Pb	ppm	XRF	2
Zn	ppm	AAS	2
Ni	ppm	AAS	4
Co	ppm	AAS	4
As	ppm	XRF	2
Sb	ppm	XRF	2
Bi	ppm	XRF	2
Mo	ppm	XRF	1
Ag	ppm	XRF	0.1
Sn	ppm	XRF	2
Ga	ppm	XRF	4
W	ppm	XRF	4
Ba	ppm	ICP	5
Zr	ppm	ICP	5
Nb	ppm	XRF	2
Se	ppm	XRF	2
Be	ppm	ICP	1
Au	ppm	Graphite furnace AAS Aq req.	0.001

ICP = inductivity coupled plasma optical spectroscopy, Si, Al, Fe, Ti, Cr, V after an alkali fusion, others after $HCl/HClO_4/HF$ digestion.

XRF = X-ray fluorescence

AAS = Atomic absorption spectrophotometry, after $HCl/HClO_4/HF$ digestion

4.3 Morphology

Lags were classified into four groups based mainly upon the nature of the lag (e.g saprolitic vs lateritic) and regolith/landform framework. Each class is described below in terms of its mesoscopic and micromorphological characteristics. The five-character codes given in parentheses are those of the *Terminology, Classification and Atlas* of Anand *et al.* (August, 1989).

4.3.1 Lag of ferruginous cobbles and pebbles after ferruginized saprolite (LG 206, 203)

The external appearance of this lag type is generally black, subrounded to subangular and ranges in size from 20 to 150 mm. Ferruginous cobbles (LG206) exceeding 100 mm are common. This lag is typically non-magnetic. It is significant that the ferruginous cobbles/pebbles do not show any development of cutans. These cobbles and pebbles are examples of extreme ferruginization. They are characterized by the disappearance of the parent rock fabric and are now composed of micro-crystalline hematite and goethite. Sliced surfaces show the interiors to be reddish-black through reddish-brown to weakly-red mixtures of fine-grained hematite and goethite. Dissolution cavities are filled with brownish-yellow secondary goethite and traces of kaolinite (Fig. 10A). Some cavities are lined with chalcedonic silica. Colours reflect the differences in the crystallinity and abundance of Fe oxides. Petrographic examination of the ferruginous cobbles show that they have simple fabrics and Fe-oxide mineralogies that are dominated by fine-grained hematite and goethite. Several generations of Fe oxides may occur. Pre-existing minerals, principally layer-silicate clays, have been impregnated and/or replaced by Fe oxides.

This lag type occurs largely on erosional areas (regolith unit 2a, 2b) in the east and appears to have been derived from the mafic feruginized saprolite.

4.3.2 Lag of Lateritic Lithic Fragments

The lateritic lithic lag differs from the lag of ferruginized saprolite in its yellow-brown colour, has less Fe and has a mottling with small incipient nodular structures. The lateritic lithic fragments are brownish yellow to yellowish brown, 10-50 mm in size and show abundant dissolution pits which are filled with goethite and kaolinite. Interior surfaces display a variety of colours including yellow, reddish brown, and dusky red indicating a range of hematite content (Fig. 10B). Numerous irregular and mammillated to regular and subrounded voids are lined and in places, filled with yellow fine-grained material. X-ray diffraction analysis of microsamples of materials from the voids indicates the occurrence of Al-goethite and well-crystallized large crystals of kaolinite. Under the petrological microscope, a gradual transition can be observed between red matrix in which hematite is more abundant than goethite and the yellow matrix in which goethite dominates or is the only Fe-oxide. Some lateritic lithic fragments are dominantly red, homogeneous and hematite-rich. In places it appears that kaolinite has been completely replaced by hematite in lateritic lithic fragments. During this transformation, the former crystal organization of kaolinite is obliterated. Some lateritic lithic fragments also show the development of incipient yellowish-brown nodules/pisoliths which are goethite and kaolinite rich with kaolinite present as microcrystallites, generally smaller than 1 μm.

Most lateritic lithic fragments consist of a mixture of fine grained microcrystalline kaolinite, goethite, and hematite (Fig. 11A). The interstices between kaolinitic clays are filled with spongy fine-grained goethite. Hematite occurs as irregular discrete grains (20-30 μm) and in places coalescing to form aggregates 200-500 μm across. Both solution-deposited (colloform structure) and residual goethite exist (Fig. 11B). Colloform goethite is younger and probably occupies the void spaces created by the weathering of primary minerals. A few lateritic lithic fragments also contain pseudomorphs after mica, some of which have split along their cleavages and are replaced by mixture of goethite and kaolinite

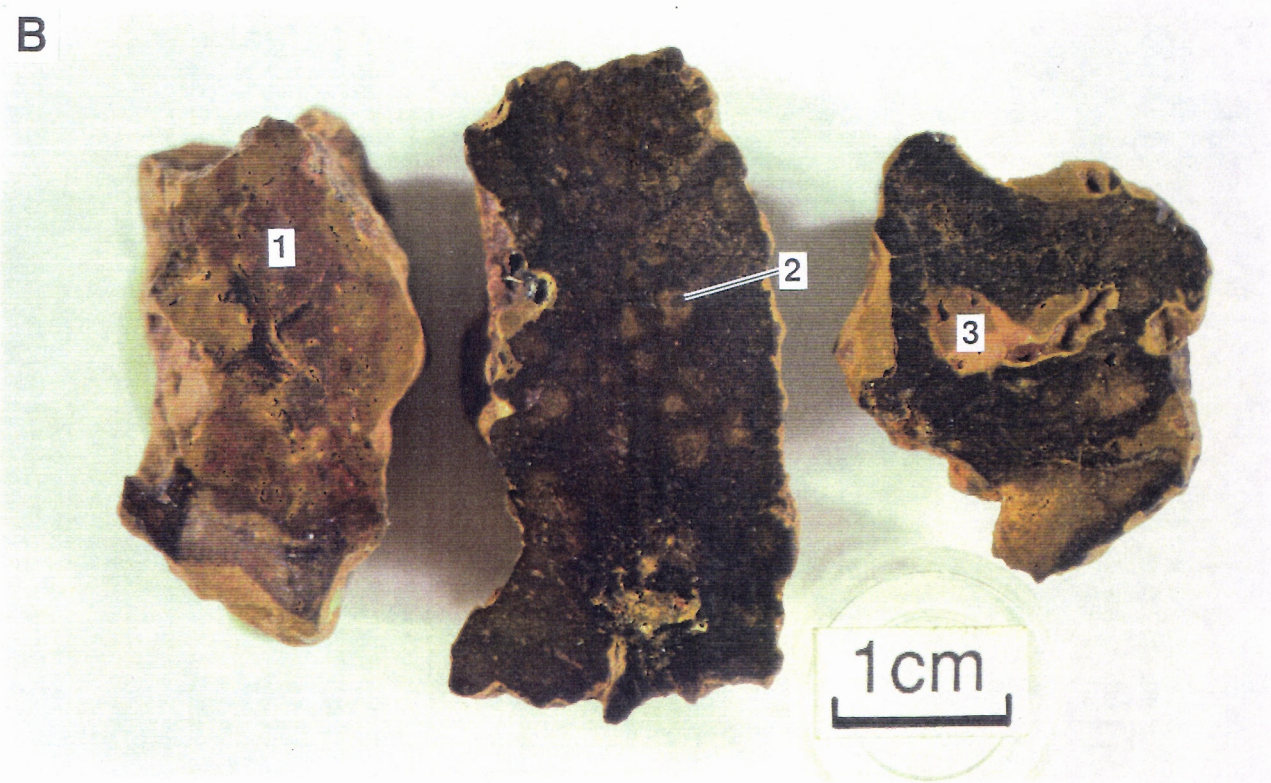

Fig. 10A. Sliced surfaces of lag of ferruginized saprolite from regolith Unit 2a showing relatively uniform reddish brown to black matrix. Sample 07-1310.

Fig. 10B. Sliced surfaces of lag of lateritic lithic fragments from regolith Unit 6a showing diffuse mottles (1), incipient nodular structures (2), and vermiform voids filled with kaolinite and goethite (3). Sample 07-1326.

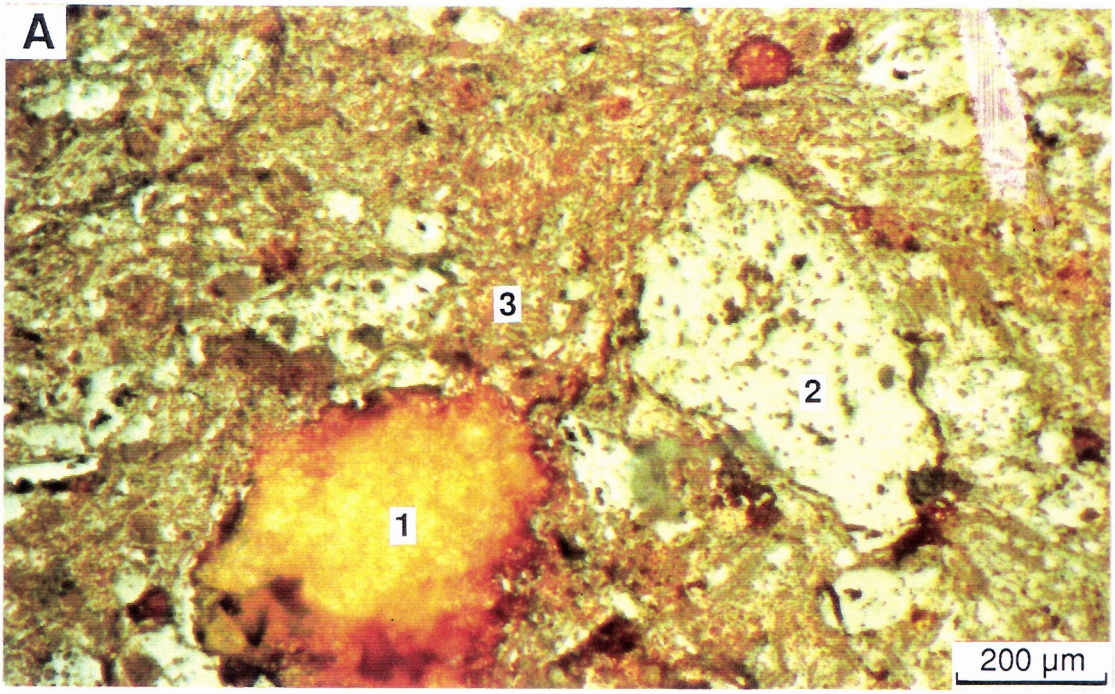

Fig. 11A. Polished section of a lateritic lithic fragment from regolith Unit 1 showing anatase (1) and grains of hematite (2) set in a fine-grained mixture of goethite and kaolinite (3).

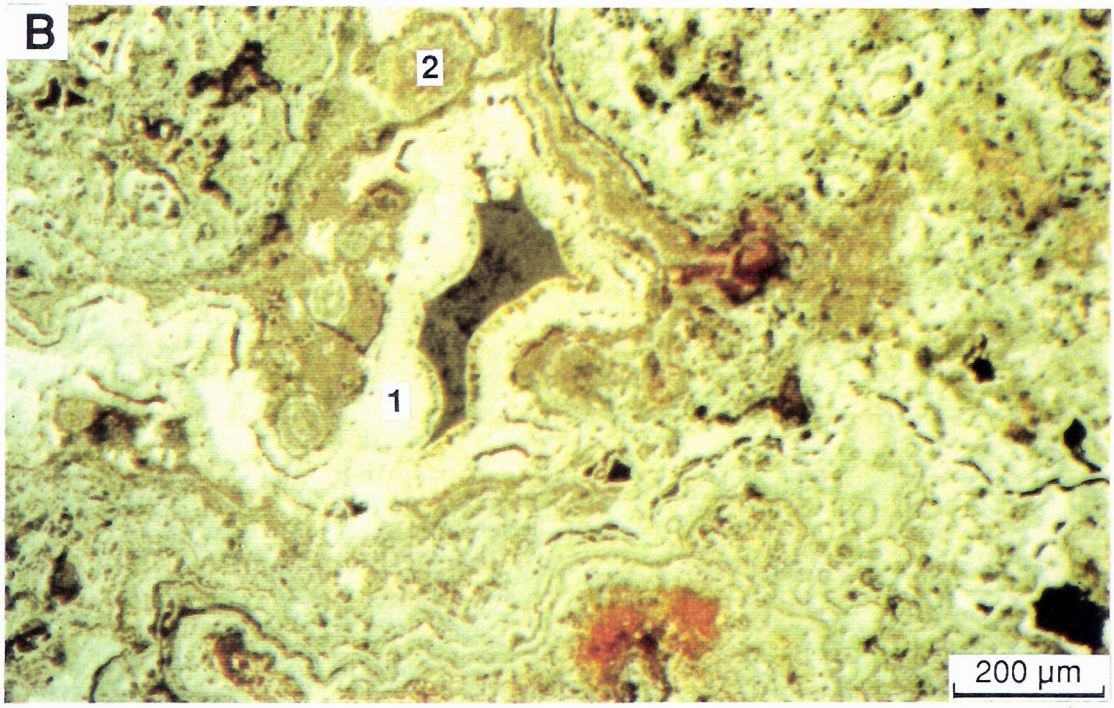

Fig. 11B. Polished section of a lateritic lithic fragment from regolith Unit 2b, showing colloform goethite (1) set in fine-grained residual goethite (2).

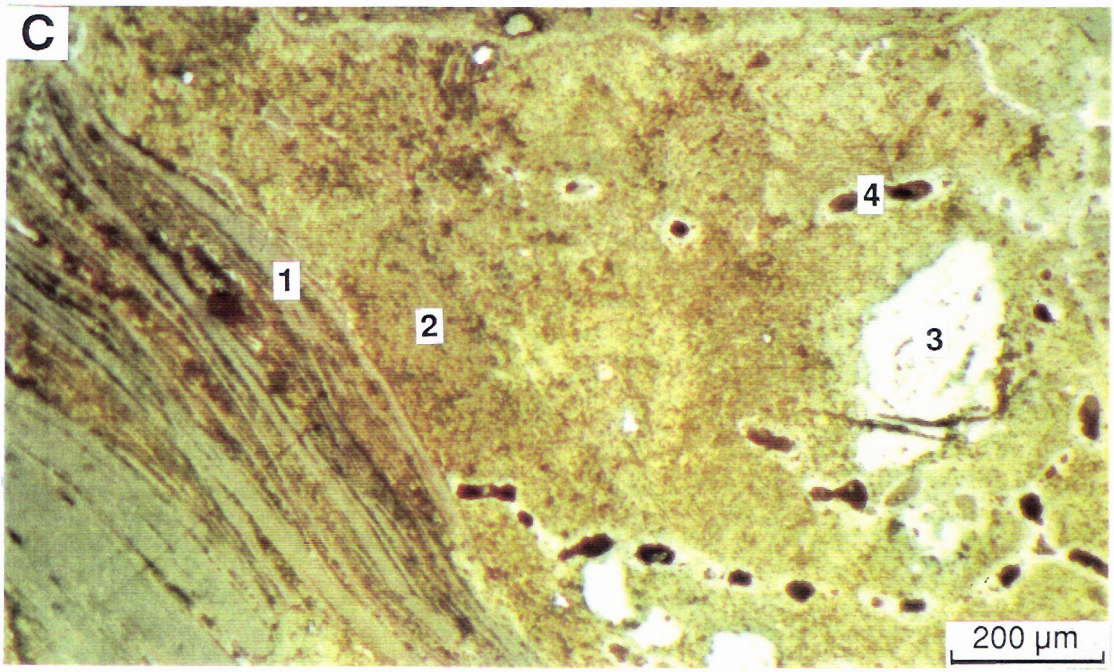

Fig. 11C. Polished section of lateritic lithic fragment from regolith Unit 2b, showing mica relics (1) set in fine-grained goethite (2) with a few hematite grains (3) and small voids (4).

(Fig. 11C). In some samples weathered ilmenite grains, now anatase, occur as porous irregular grains (Fig. 11A).

The lateritic lithic lag occurs on areas from which lateritic residuum has been removed. These include parts of Unit 2b, pockets within Unit 1 (where the lateritic residuum is locally absent), and in Unit 6. This lag is derived from the dissolution and breakdown of the upper saprolite, and could include parts of a mottled zone, if present.

4.3.3 Lateritic lag (LG100)

This lag comprises lateritic pisoliths/nodules and fragments of Fe-rich duricrust. The external appearance of fragments of the Fe-rich nodular duricrust is black, subrounded to subangular and this duricrust comprises reddish black hematite-rich subrounded to subangular nodules and similarly coloured ooliths set in a small amount of microcrystalline hematite-rich weak-red matrix (Fig. 12A). Nodules in the fragments are generally magnetic. There are at least two generations of Fe oxides in the core of some of the nodules. The core often contains several dissolution cavities which are filled with bright yellow microcrystalline goethite. Loose nodules/pisoliths (not shown) have dark reddish-brown to black cores, are subrounded to irregular in shape, with a size range of 2-12 mm. Cores of nodules show the development of oval voids, which have greenish (<1 mm thick) cutans of kaolinite and goethite and infill of kaolinite, goethite, and silt-sized detrital quartz. The occurrence of greenish cutans on the outer surfaces of pisoliths/nodules is typical of residual nodules/pisoliths of the Lawlers area. Compound nodules enclosing small pisoliths and nodules are also present.

Lateritic lag occurs on regolith Unit 1 where the complete or nearly-complete lateritic profile is preserved and is mainly derived from the breakdown of Fe-rich nodular duricrust and nodular duricrust (low in Fe).

4.3.4 Fine lag of mixed origin (LG221, LG103, LG201)

The fine lag is a very heterogenous material containing lateritic lithic fragments of various colours, lateritic pisoliths/nodules, and ferruginous granules (Fig. 12B). The lateritic lithic fragments are derived from saprolite and are yellow, yellowish brown, reddish brown, greyish brown or red, subrounded to angular, 2-6 mm in size and are generally non-magnetic. Outer surfaces of the fine lag have a varnished appearance and lack cutan development. Fabrics of some lateritic lithic fragments preserve their mafic and ultramafic origin. However, extreme ferruginization has generally produced lateritic lithic fragments of almost uniform red or black colour which have completely lost the fabric and these may look similar to pebbles of ferruginized saprolite. The kaolinitic clay has been replaced by fine grained hematite. Coarse lateritic lithic fragments, consisting of microcrystalline kaolinite and goethite, show abundant syneresis cracks which are lined with hematite. Irregularly shaped ilmenite or weathered ilmenite (leucoxene) grains occur in some lateritic lithic fragments. Some lateritic lithic fragments contain recognizable pseudomorphs of primary minerals such as amphiboles/pyroxenes.

The lateritic pisoliths and nodules are yellow to red, rounded to subrounded in shape with a size range of 3-5 mm and they consist of black to reddish brown hematitic cores with greenish goethite-rich cutans. Nodules with black cores are generally magnetic because of presence of maghemite.

This lag is abundant on the colluvial regolith Unit 6a. The variety of components in the fine lag indicate their diverse origin, possibly derived upslope from the breakdown of lateritic duricrust, large lateritic lithic fragments, and ferruginized saprolite. The components of the fine lag are inherited from large lithic fragments, nodular duricrust, and ferruginized saprolite. For example, pisoliths and nodules related to lateritic duricrust have hematite-rich black cores with yellow goethite-rich cutans. These

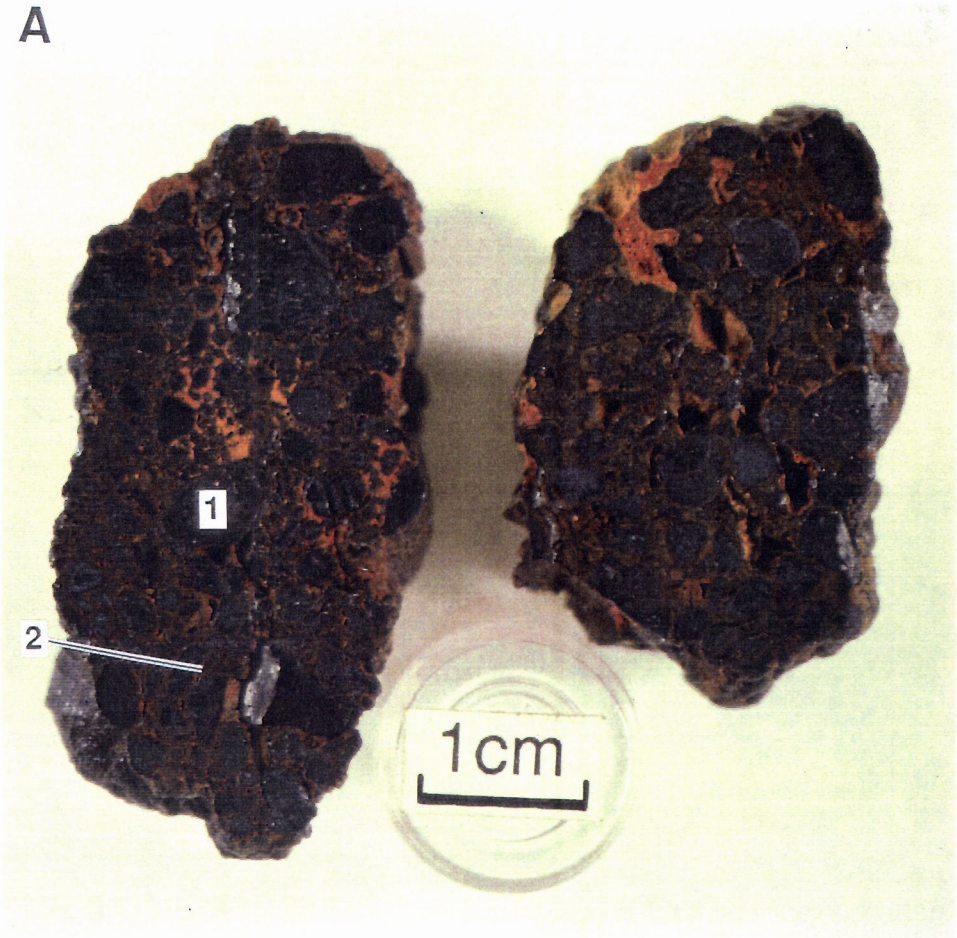

Fig. 12A. Sliced surfaces of fragments of Fe-rich duricrust from regolith Unit 1 showing reddish black nodules (1) set in a hematite-rich weak red matrix (2). Sample 07-1315.

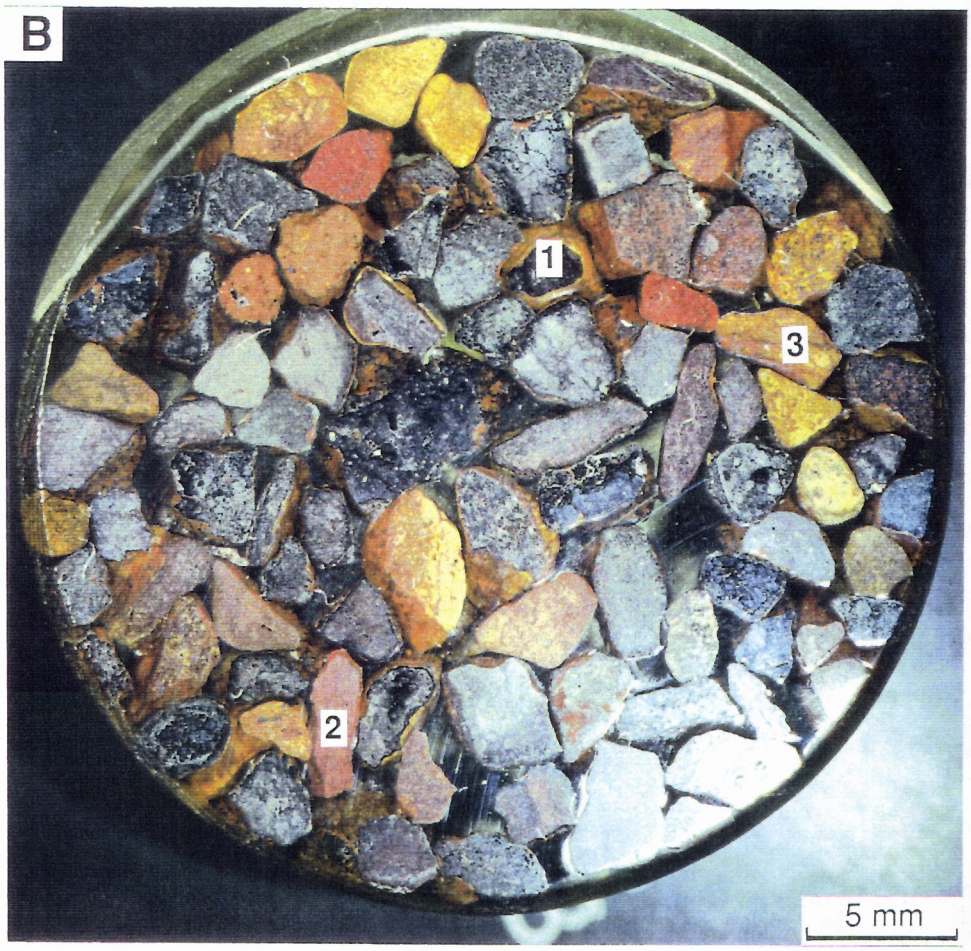

Fig. 12B. Sliced surfaces of lag of mixed origin from regolith Unit 6a showing a variety of clasts comprising lateritic pisoliths (1) and lithic fragments of several internal colours (2, 3). Sample 07-1330.

pisoliths are commonly observed in lateritic residuum of regolith Unit 1. A few black subangular to angular granules without any cutans are related to ferruginized saprolite of regolith Unit 2. Yellow reddish-brown and red lateritic lithic fragments are related to the large lateritic lithic fragments of erosional areas described in Section 4.3.2.

4.4 Mineralogy

The semi-quantitative mineralogical data for various types of lag gravels are plotted as a traverse along line 6981600N in Fig. 13, and in terms of the relative proportions of hematite, goethite, kaolinite, and maghemite are plotted on ternary composition diagrams in Figs. 14 and 15. For comparison a few samples of Fe-rich duricrust are also included. The range of values for each category of lag are presented in Table 3.

The lag of ferruginous cobbles and pebbles after ferruginized saprolite on regolith Unit 2a largely consist of mixtures of hematite and goethite with very small amounts of poorly-crystalline kaolinite and quartz. Hematite and goethite are present in almost equal proportions. Maghemite was not detected. Hematite dominates the lateritic lag, fine lag of mixed origin, and Fe-rich duricrust. The ratio of hematite to goethite is almost 2:1 in these samples. Besides hematite and goethite, these samples also contain higher concentrations of maghemite. Kaolinite also occurs in significant amounts in the fine lag, mainly within the yellow lateritic lithic fragments and greenish cutans of pisoliths. The lag of lateritic lithic fragments is richer in goethite and poorer in hematite compared to the other lag types. It is also richer in kaolinite. Quartz is present in small amounts in all lag types.

Evidence for few other minerals is seen on X-ray diffraction charts of the samples studied. Anatase and rutile are present in appreciable amounts in lateritic lag and petrographically are seen to be the products of ilmenite weathering. Small amounts of these minerals were also detected in a few samples of other lag types. The presence of talc and chlorite were recorded in one sample of lateritic lag. Traces of gibbsite occurred in a few samples of lateritic lag and the fine lag of mixed origin.

4.5 Aluminium Substitution in Fe-oxides

The values of Al substitution in goethite, hematite, and maghemite are plotted for sample sites along line 6981600N (Fig. 16) and the range of values for the various categories of lag gravels are presented in Table 4.

The Al substitution of goethites ranged from 2 to 22 mole%. Goethites in the lag consisting of ferruginized saprolite on regolith Unit 2a show lowest Al substitution (values less than 5 mole%). In contrast, goethites in the lag consisting of lateritic lithic fragments and in the lateritic lag contain moderately-high levels of Al subsitution. A wide range of Al subsitutions occurs for goethites of the fine lag of mixed origin on regolith Unit 6a. A similar trend is observed for Al substitution in hematites for all lag types.

These differing levels of Al substitution in goethite between the lag types suggest different environments and/or mechanism of their formation. Very low Al substitution in the goethite of the ferruginized saprolite indicates that they must have grown in an environment almost free of accessible Al. On the other hand, goethite of lateritic lithic fragments is formed in an Al-rich environment as indicated by the presence of kaolinite.

Ferruginized saprolite, comprising mixtures of goethite and hematite, occurs as discrete bodies at several levels within the saprolite horizon of laterite profiles in Meatoa. Ferruginized saprolite is also well exposed in the walls of the McCaffery Pit, a location chosen for systematic study of the characteristics and

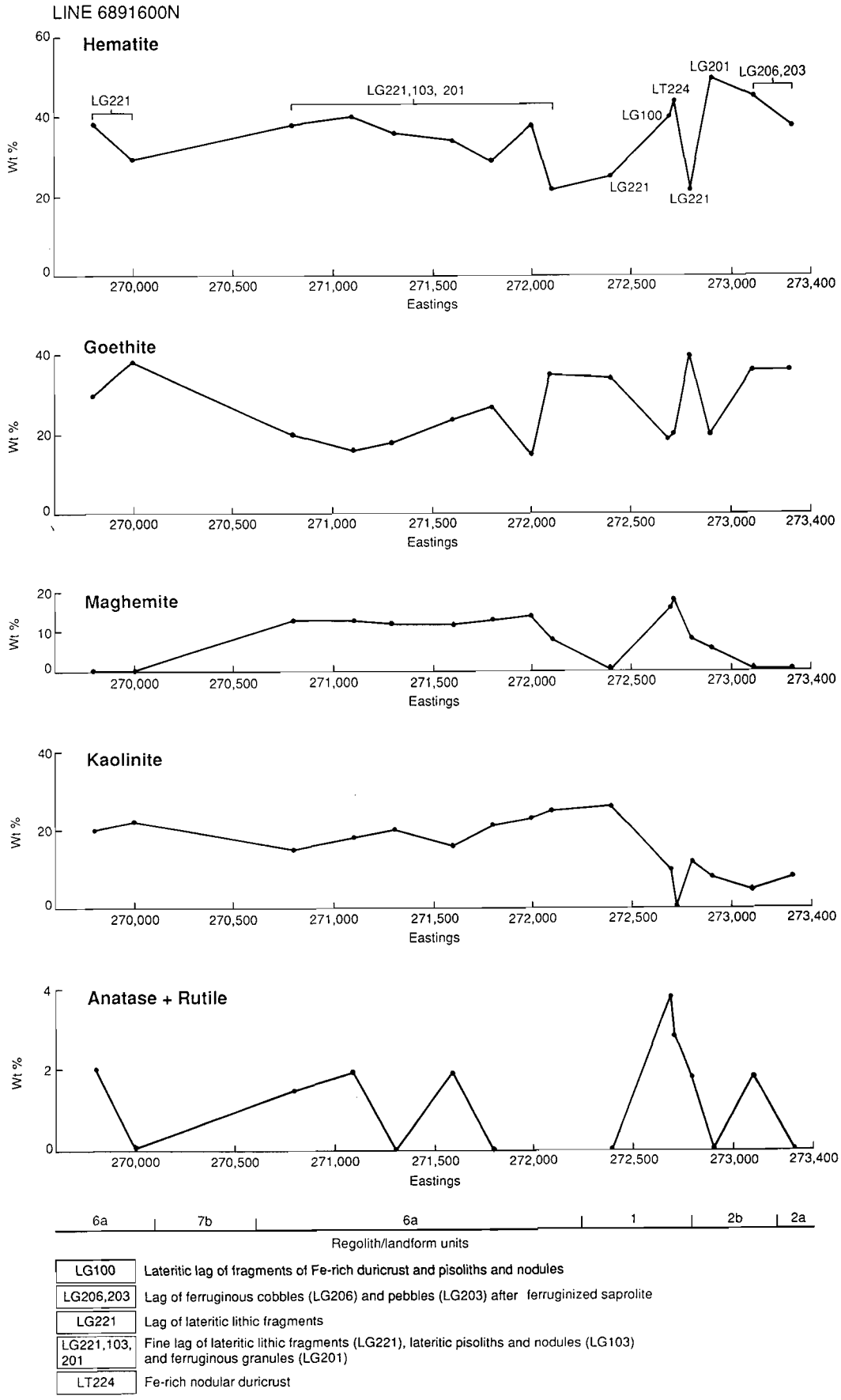

Fig. 13. Traverse along 6891600N showing the distribution of hematite, goethite, maghemite, kaolinite and anatase + rutile in lag gravels of the various regolith units.

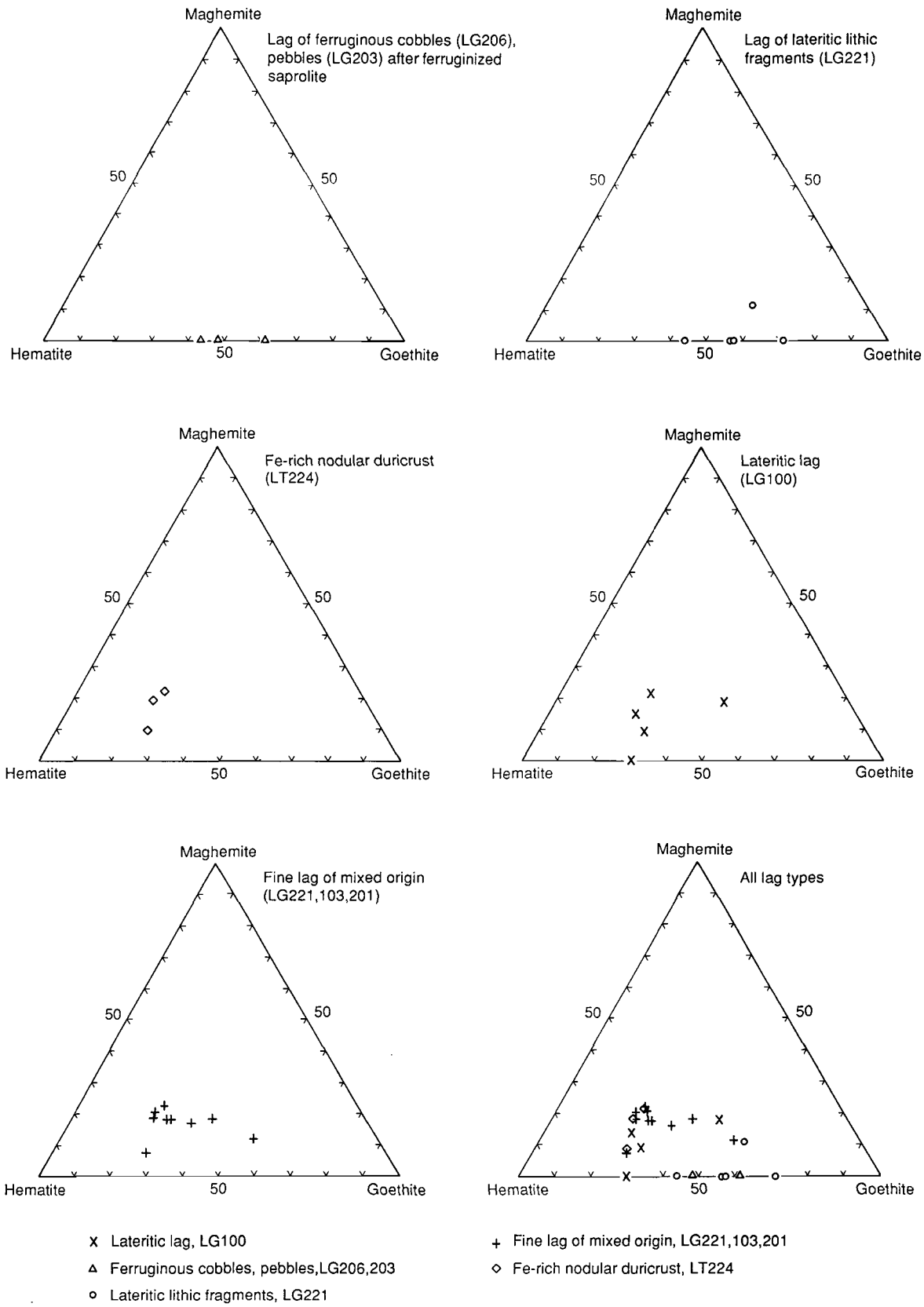

Fig. 14. Triangular diagrams showing compositions of four lag types, in terms of the dominant iron oxide minerals. For comparison, three samples of Fe-rich duricrusts are also included.

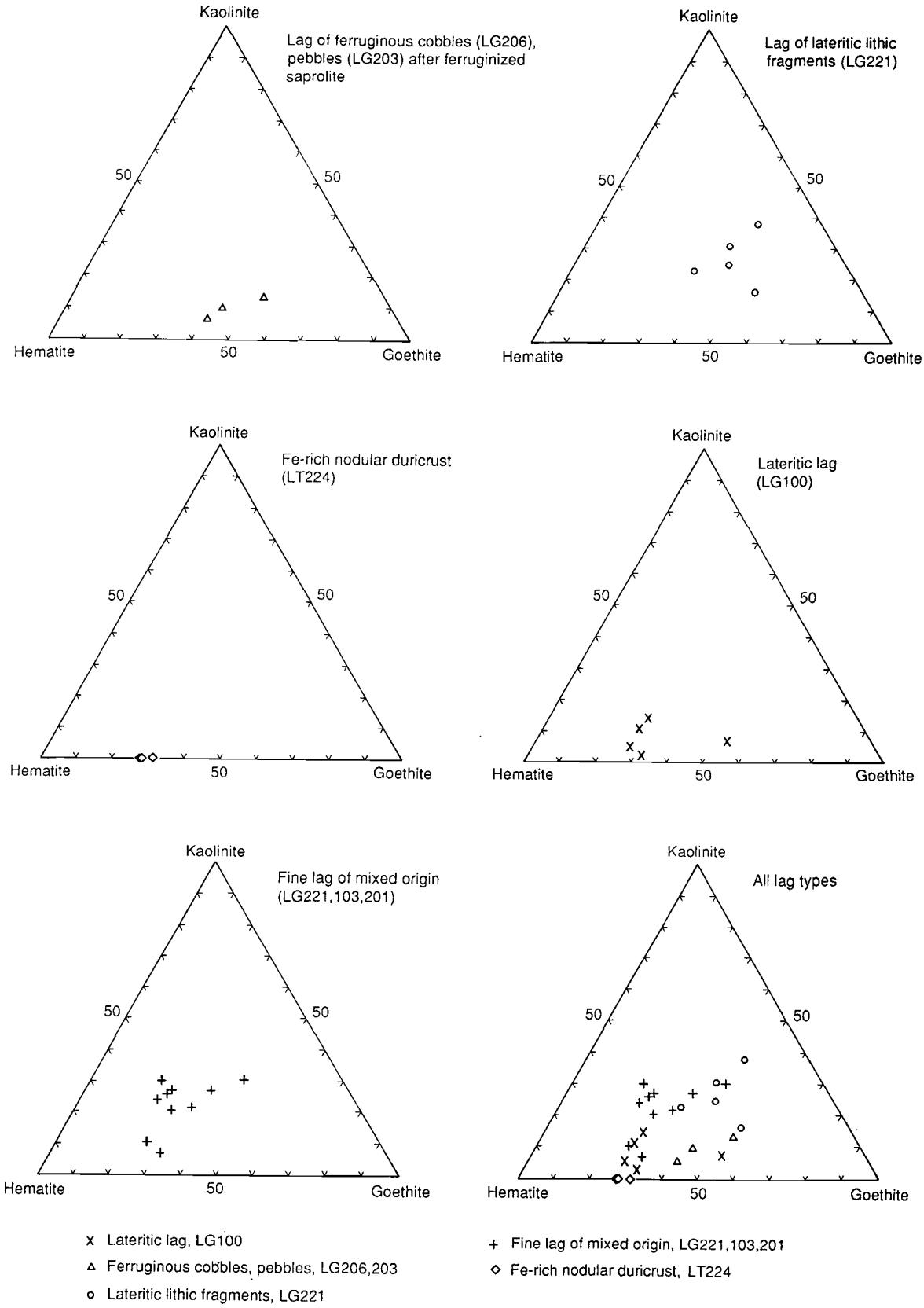

Fig. 15. Triangular diagrams showing compositions of four lag types, in terms of hematite, goethite and kaolinite. For comparison, three samples of Fe-rich duricrusts are also included.

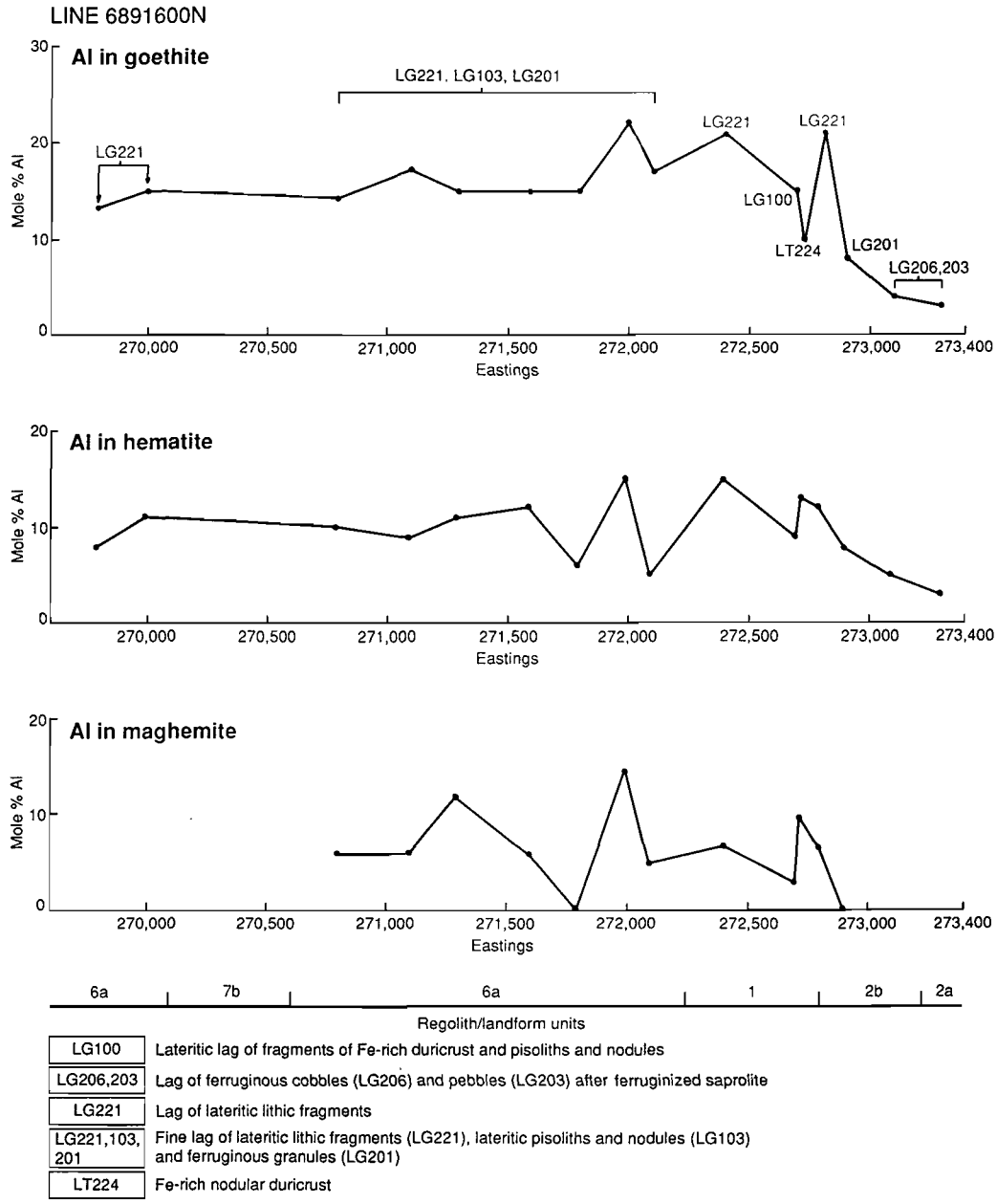

Fig. 16. Traverse along line 6891600N showing the distribution of Al-substitution in goethite, hematite and maghemite in lag gravels of the various regolith units.

Table 3. Range of values of mineral contents for various categories of lag gravels

	Lag of ferruginous cobbles, pebbles after ferruginized saprolite (LG206, LG203) N = 3			Lag of lateritic lithic fragments N = 5			Lateritic Lag (LG100) N = 5			Fine lag of mixed origin (LG221, LG103, LG201) N = 10		
wt%	Min	Max	Mean	Min	Max	Mean	Min	Max	Mean	Min	Max	Mean
Hematite	30	46	38	15	38	26	26	56	45	22	50	37
Goethite	36	48	40	30	40	36	19	35	25	15	35	21
Maghemite	0	0	0	0	8	2	0	16	10	6	15	12
Kaolinite	5	12	8	12	32	22	2	10	6	5	25	17
Quartz	3	12	8	0	4	3	2	3	3	0	10	5
Rutile	0	1	<1	0	5	1	0	3	2	0	2	<1
Anatase	0	1	<1	0	2	<1	0	5	3	0	2	<1
Talc	0	0	0	0	0	0	0	5	1	0	0	0
Gibbsite	0	0	0	0	0	0	0	2	<1	0	3	<1

Table 4. Range of values of Al substitution (mole%) in goethite, hematite and maghemite for various categories of lag gravels

	Lag of ferruginous cobbles, pebbles after ferruginized saprolite (LG206, LG203) N = 3			Lag of lateritic lithic fragments N = 5			Lateritic Lag (LG100) N = 5			Fine lag of mixed origin (LG221, LG103, LG201) N = 10		
wt%	Min	Max	Mean	Min	Max	Mean	Min	Max	Mean	Min	Max	Mean
Goethite	3	5	4	13	21	18	6	20	12	2	22	13
Hematite	3	4	3	8	20	13	5	13	9	4	15	9
Maghemite	0	0	0	0	7	3	0	7	3	0	15	6

genesis of the ferruginization. This research shows that the goethites of ferruginized saprolite, at McCafferys and elsewhere in the Lawlers district are characterized by a very low level of Al substitution, possibly due to an absolute accumulation of Fe under hydromorphic conditions in an environment almost free from available Al. This follows the conclusions of Fitzpatrick and Schwertmann (1982) and Schwertman and Latham (1986) that goethites formed by absolute accumulation of Fe contain low (<10 mole %) Al substitution. It therefore seems likely, that many of these ferruginized saprolites in the Lawlers district were formed under the influence of at least some hydromorphic concentration of Fe within the saprolite horizon in the past, although now they occur on areas which are presently freely drained. The lower substitution of Al in the Fe-oxides under hydromorphic conditions may partly be due to a high pH which decreases the activity of Al, and consequently a lower availability of Al for incorporation into the goethite structure as it forms (Fitzpatrick and Schwertmann, 1982). Therefore, in as much as goethites are formed by oxidation of mobilized Fe^{2+}, Al is not equally mobile. This is supported by high Mn values in the Fe oxides (discussed in section 4.6) of ferruginized saprolite which underline their low degree of leaching. This, in turn, would also explain why the Al substitution of goethite in ferruginized saprolite is significantly lower than that of goethites from non-hydromorphic environments (e.g. lateritic lithic fragments).

At Lawlers, Al substitution in hematite and maghemite is generally lower than in goethite in the same sample which is in keeping with findings of other researchers (e.g. Schwertmann and Latham, 1986; Anand and Gilkes, 1987). These authors conclude that since both minerals are assumed to have crystallized in the soil, this difference is probably a consequence of the lower capacity of hematite to accommodate Al.

4.6 Geochemistry

Analytical data for the lag gravels from Meatoa are plotted for line 6891600N (Figs 17, 19, 20, 21) and minimum, maximum and mean values for all lag types are given in Table 5. Analytical data on individual samples and correlation coefficient matrices are given in Appendix I and II respectively.

4.6.1 Major and Minor Elements

SiO_2, Al_2O_3, Fe_2O_3

The compositions of various types of lag in the terms of three major components of Fe_2O_3, Al_2O_3 and SiO_2 are also plotted in the triangular diagrams in Fig. 18. Silica and Al_2O_3 are present in higher concentrations in lags of Unit 6a, whereas Fe_2O_3 tends to dominate in the lag gravels of Units 2a and 2b and 1 at the east end of the traverse. With the increase in Fe_2O_3, there is a concomitant decrease in SiO_2 and Al_2O_3. By far the most abundant constituent is Fe_2O_3 with mean values greater than 70 wt% in the lag consisting of ferruginized saprolite and in the lateritic lag. Silica and Al_2O_3 are thoroughly leached in the lateritic lag and in the ferruginized saprolite. The remaining Al_2O_3 and SiO_2 are in kaolinite, some Al in goethite and Si in quartz. In general, the Al_2O_3 and SiO_2 contents of the fine lag of mixed origin and the lag of lateritic lithic fragments are significantly higher than in lags of ferruginized saprolite and lateritic lag reflecting the presence of numerous clay-rich lateritic lithic fragments in the fine lag of mixed origin and in the lateritic lithic lag.

For the group of 27 lag samples analysed, negative, highly-significant correlations of Fe occur with Al (r=-0.95), Si (r=-0.88), Cu (r=-0.68) and positive correlations with Ti (r=0.61), V (r=0.47), Mo (r=0.53) and Sn (r=0.50). This suggests the adsorption of Ti, V, Mo, and Sn on goethite.

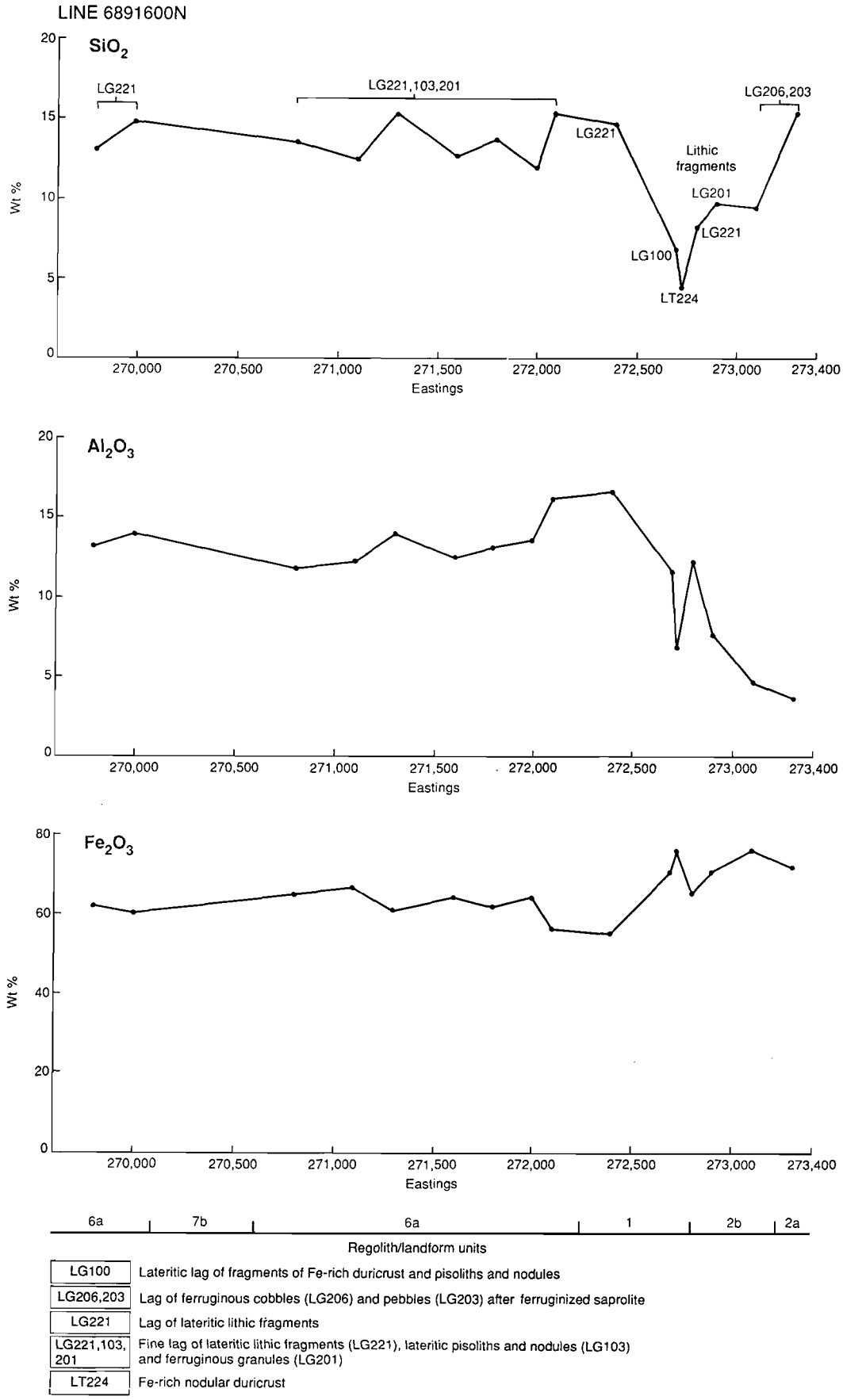

Fig. 17. Traverse along line 6891600N showing the distribution of SiO_2, Al_2O_3 and Fe_2O_3 in lag gravels of the various regolith units.

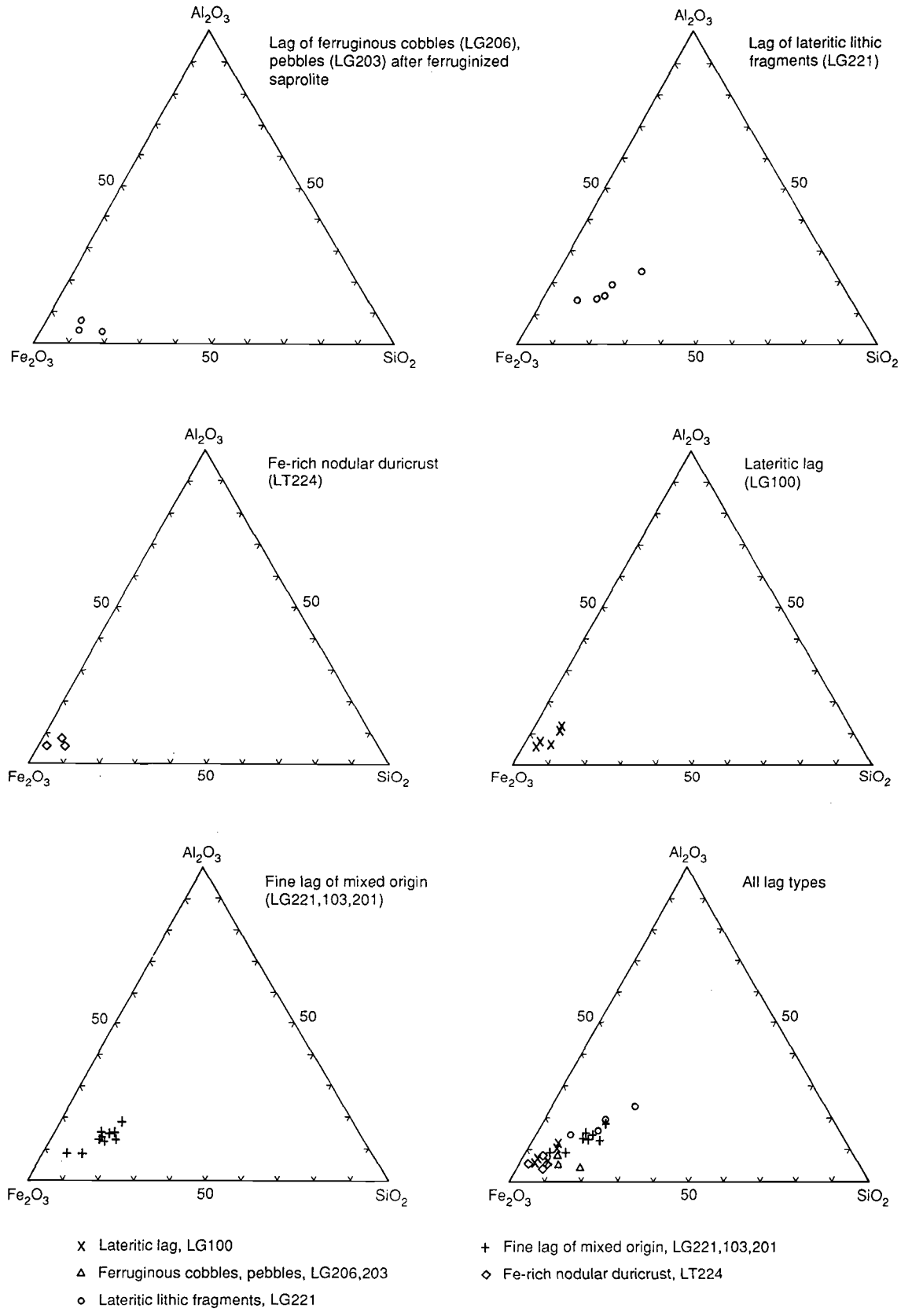

Fig. 18. Triangular diagrams showing compositions of four lag types, in terms of Fe_2O_3, SiO_2 and Al_2O_3. For comparison, three samples of Fe-rich duricrusts are also included.

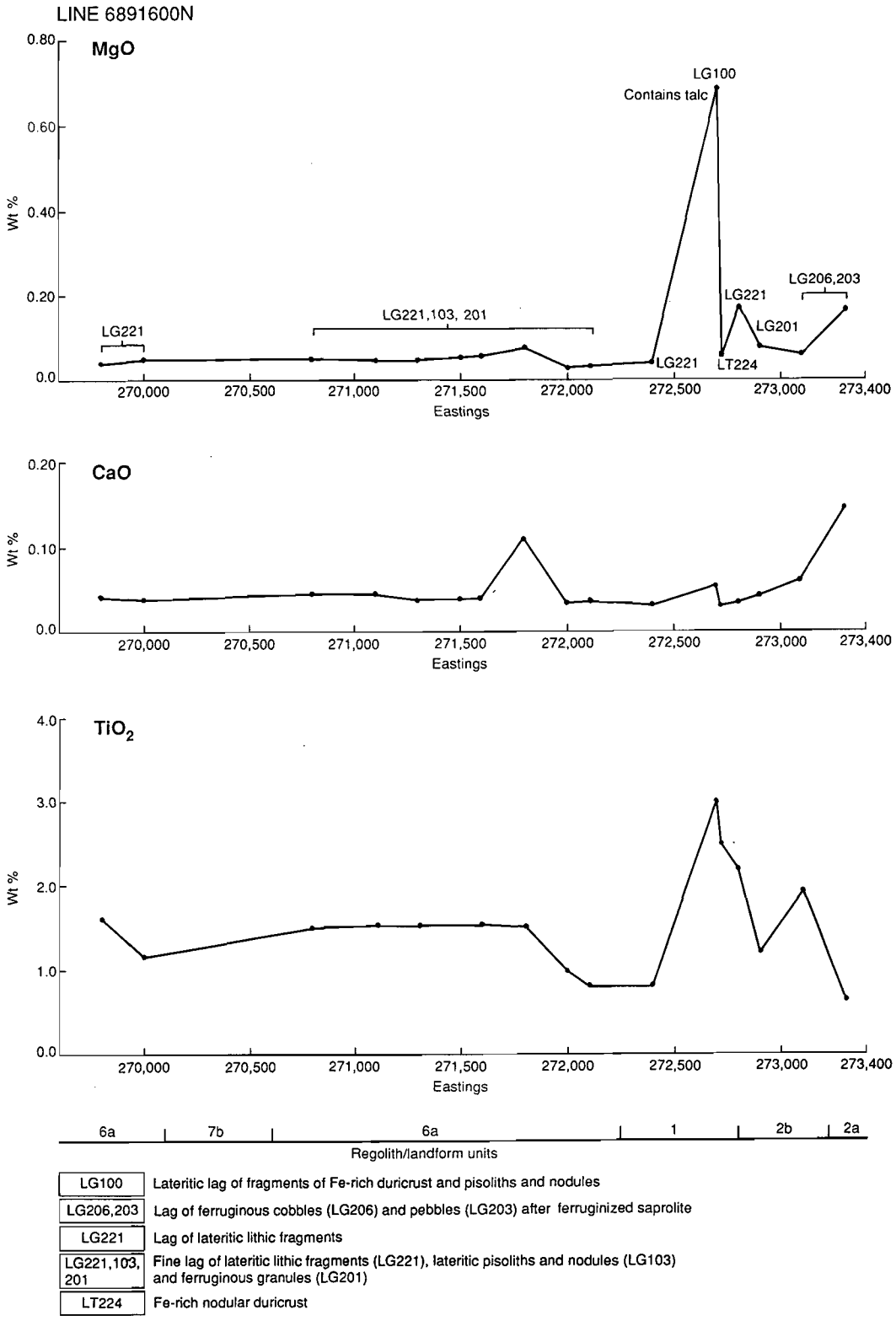

Fig. 19. Traverse along line 6891600N showing the distribution of MgO, CaO and TiO_2 in lag gravels of the various regolith units.

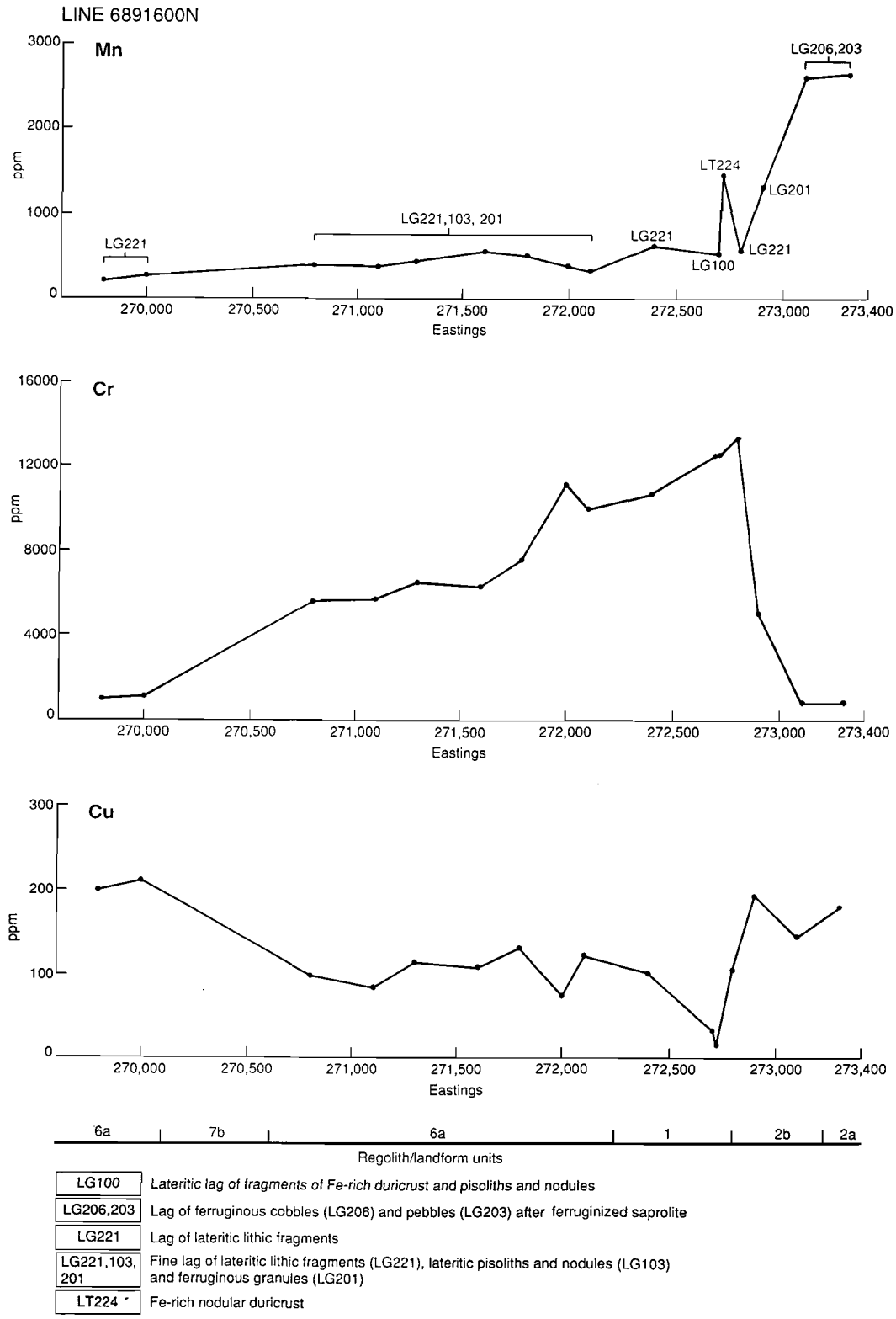

Fig. 20. Traverse along line 6891600N showing the distribution of Mn, Cr and Cu in lag gravels of the various regolith units.

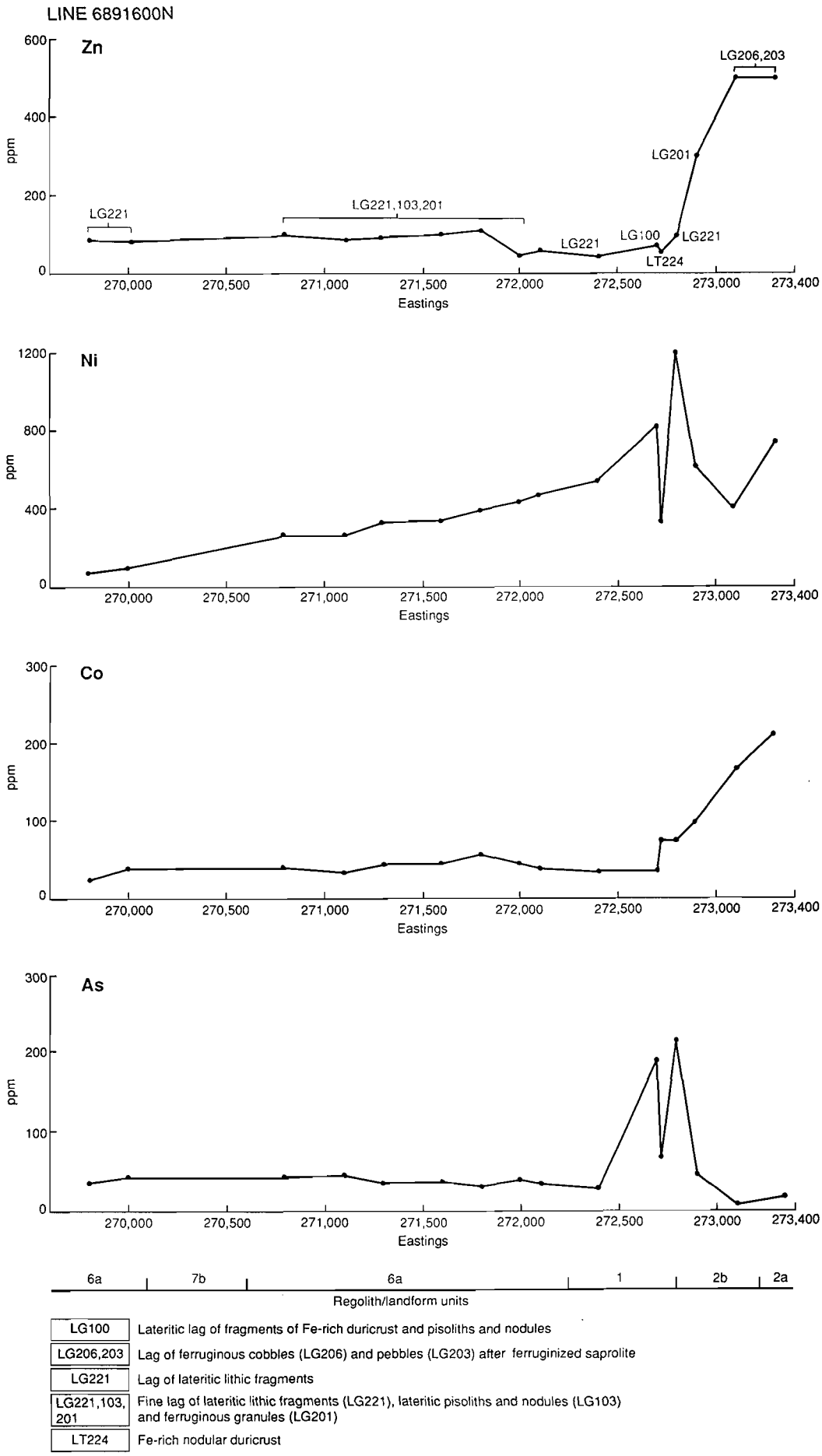

Fig. 21. Traverse along line 6891600N showing the distribution of Zn, Ni, Co and As in lag gravels of the various regolith units.

Table 5. Range of values for various categories of lag gravels

ELEMENT	Lag of ferruginous cobbles, pebbles after ferruginized saprolite (LG206, LG203) N = 3			Lag of lateritic lithic fragments N = 5			Lateritic Lag (LG100) N = 5			Fine lag of mixed origin (LG221, LG103, LG201) N = 10		
wt%	Min	Max	Mean	Min	Max	Mean	Min	Max	Mean	Min	Max	Mean
SiO_2	8.10	15.50	11.00	8.30	19.70	14.12	3.20	6.90	5.30	6.10	17.10	12.81
Al_2O_3	3.85	7.12	5.22	12.36	20.20	15.31	5.14	10.30	7.33	7.86	16.17	12.17
Fe_2O_3	71.77	76.55	73.74	46.11	65.54	58.04	69.86	77.63	74.21	56.50	75.46	65.08
MgO	0.030	0.165	0.086	0.039	0.177	0.070	0.027	0.690	0.183	0.032	0.075	0.049
CaO	0.035	0.146	0.081	0.028	0.040	0.035	0.041	0.055	0.049	0.034	0.112	0.048
Na_2O	0.013	0.014	0.014	0.010	0.017	0.014	0.014	0.017	0.015	0.011	0.084	0.020
K_2O	0.020	0.020	0.020	0.020	0.020	0.020	0.020	0.020	0.020	0.020	0.020	0.020
TiO_2	0.615	1.952	1.428	0.656	2.202	1.294	3.003	8.291	5.068	0.827	3.453	1.558
ppm												
Mn	336	2640	1868	218	548	347	259	419	341	337	1314	554
Cr	482	956	782	1057	13400	5983	342	12600	6806	3903	11100	6936
V	394	1028	697	564	1573	1054	1176	3365	2208	670	1632	1140
Cu	65	180	130	105	250	174	17	74	36	50	145	106
Pb	<2	22	11	12	22	16	8	125	40	12	32	22
Zn	240	500	413	46	95	76	40	90	66	46	300	111
Ni	100	740	413	70	1200	448	50	820	280	160	610	357
Co	54	210	143	24	78	50	28	74	45	34	98	49
As	7	13	9	16	220	69	10	195	77	18	48	36
Sn	<2	3	2	<2	5	3	2	12	6	<2	4	2
Ga	18	42	32	18	135	86	78	195	115	28	78	48
W	4	6	5	1	12	6	1	18	9	1	16	5
Ba	13	302	120	15	32	20	11	34	25	13	65	27
Zr	27	58	45	21	68	46	40	91	70	68	129	103
Au	0.000	0.001	0.001	0.002	0.034	0.015	0.000	0.003	0.001	0.000	0.003	0.001

MgO, CaO, Na_2O, K_2O

These minor oxides are strongly leached in the lag gravels. A significant amount of MgO (0.692 wt%) is present in only one sample of a lateritic lag within regolith Unit 1. Talc was seen in the XRD trace for this sample suggesting derivation from a Mg-rich bedrock.

TiO_2

The fourth highest concentration after Fe_2O_3, Al_2O_3, and SiO_2 is TiO_2. The concentrations of TiO_2 are higher in the lags of Units 1 and 2 in the east and drop sharply to the west. The lateritic lag is highest in TiO_2 averaging 5% compared with 1.3-1.6% TiO_2 for the other lag types. This may indicate that the lateritic lag is derived from the weathering of Ti-rich basic rocks such as gabbros. However, knowledge of bedrock relationships are presently inadequate to prove this. Strong correlations of Ti occur with V(r=0.90), Ga (r=0.94), Mo (r=0.83) and Nb (r=0.98). Petrographic and SEM studies of these lag gravels have shown that Ti mainly occurs as anatase and rutile. However, some Ti is also found to bound within Fe oxides where Ti substitutes for Fe^{3+} in goethite/hematite.

4.6.2 Trace Elements

Mn

The lag of ferruginized saprolite on regolith Unit 2a has significantly higher levels of Mn than the other lag types which is in keeping with findings generally over the Yilgarn Block. Iron-rich duricrust samples also show high concentration of Mn. Strong correlations of Mn occur with Zn (r=0.88) and Co (r=0.73), but the correlation of Mn with Fe is weak (r=0.28). This suggests that Mn is not associated with Fe-oxides and occurs as discrete Mn-mineral species. However, discrete Mn-oxide phases were not found, but more careful analytical work is needed to confirm this.

Cr

The lag over the residual regime, Unit 1, shows particularly high values of Cr, with values exceeding 1%. These levels are greater than the 98th percentile of statistics from samples in the Laterite Geochemistry Group's Yilgarn database. It is almost certain that these high-Cr laterites are derived from Cr-rich bedrock. It is interesting to note, that the Cr levels fall gradually from east to west and that there is a large range in the values of Cr in the fine lag of mixed origin on regolith Unit 6a. This variation in Cr between samples of fine lag seems clearly due to various proportions of lag gravels of different origins derived from upland areas. Some clasts are derived from the mafic rocks, whereas others are derived from ultramafic rocks.

In strong contrast are the Cr levels of the lag of ferruginized saprolite on regolith Unit 2a, for which Cr lies in the 480 to 780 ppm range. This is close to the range so far established for ferruginized mafic saprolite in the Lawlers district. Drilling shows that both ultramafic and mafic lithologies are present.

Chromium is well correlated with Ni (r=0.50), As (r=0.63) and Sb (r=0.47). Chromium can substitute for Fe^{3+} in goethite because of similar ionic radius and therefore can concentrate in iron oxide rich materials. SEM and electron-microprobe work on the Meatoa lag gravels has shown that this is so, and that Cr also occurs as chromite.

V

The distribution of V is similar to that of Cr in the four lag types however, levels in the range 3000 to 4000 ppm are relatively lower than Cr. Lateritic lag on regolith Unit 1 has the highest concentration of V. The lag consisting of ferruginized saprolite shows a lower V content than the lag consisting of lateritic lithic fragments and the fine lag of mixed origin.

Cu

Copper is enriched in the lags consisting of lateritic lithic fragments and ferruginized saprolite relative to lateritic lag and the fine lag of mixed origin. Copper corrrelates well with Si (r=0.76), Al (r=0.53), and Zn (0.40), suggesting anomalous concentrations in the clay-rich lateritic lithic fragments.

Pb

The levels of Pb are low with little variations. However, Pb is slightly enriched in lateritic lag relative to the other lag types. One sample of lateritic lag shows values up to 125 ppm.

Zn

The distribution of Zn follows that of Mn. The lag of ferruginized saprolite on regolith Unit 2a to the east has much higher concentrations of Zn than the lateritic lithic lag, lateritic lag and the fine lag of mixed origin. Zinc correlates well with Mn (r=0.88) and Co (0.63).

Ni

Nickel generally is following the Cr distribution, but Ni levels are lower in the east and fall gradually westwards. This westward decrease results in a large range in Ni values in lag of mixed origin on regolith Unit 6a. Despite these variations, the mean values of Ni are not significantly different for each of the lag types.

Nickel correlates well with Cr (0.49), Mg (r=0.53) and Co (r=0.50) suggesting a likely strong association of these elements with ultramafic bedrock sources.

Co

The mean content of Co is much higher in the lag of ferruginized saprolite on regolith Unit 2a relative to the other lag types.

As

The lag of ferruginized saprolite on regolith Unit 2a and the lag of mixed origin on regolith Unit 6a show low contents of As which rises sharply in lateritic lag. Arsenic correlates well with Mg (r=0.70), Cr (r=0.63), and Ni (r=0.63).

Sb, Bi, Sn, Ge

Most of the data lie below or close to the detection limit. The mean concentration of Sn is slightly higher in lateritic lag (6 ppm) compared with other lag types (2 ppm)

Ga

The lateritic lag shows a significantly higher mean value of Ga than the other lag types which suggests the association of Ga with Fe. Gallium is negatively correlated with Si (r=-0.68), Al (-0.43) and positively correlated with Fe (r=0.52), Ti (r=0.94) and V (r=0.92).

W

The mean levels of W are low for all lag types and are not significantly different from each other. However, the lateritic lags show some relatively-higher values of W (up to 18 ppm)

Ba

Care is needed in the interpretation of Ba values up to about 250 ppm because Ba is an unwanted impurity in the alumina disk grinding plates. However, the lag of ferruginized saprolite shows significantly high values of Ba (to 300 ppm). Scanning electron microscopy shows that Ba occurs as barite ($BaSo_4$) in voids, in some such samples.

Zr

The mean levels of Zr are relatively lower in the lag consisting of ferruginized saprolite and in the lateritic lag than in lags of lateritic lithic fragments and that of mixed origin. Zirconium is probably bound to clays as is suggested by good correlation between Al and Zr.

Nb

Niobium is enriched in lateritic lag relative to the other lag types. It seems to be associated with Fe oxides. Strong correlations of Nb occur with Fe ($r=0.61$), Ti ($r=0.98$), V ($r=0.89$), and Ga ($r=0.93$).

Se

The levels of Se are low, however some samples of lag of mixed origin reach a value of 9 ppm.

Be

Almost all the Be data is below or close to the detection limit.

Au

The levels of Au are low and range from 0 to 0.034 ppm.

4.7 Microchemistry

Chemical analyses and X-ray diffraction data for bulk samples of lag gravels are important in characterization, but do not provide information at the micron scale. Electron microprobe analysis of optically-identified secondary minerals provides the only practical means to study changes in the composition of different generations of minerals. Microprobe analysis of secondary minerals contained within the lateritic lithic fragments and lateritic nodules of fine lag of mixed origin are set out in Table 6. Each spot analysis is from a volume of about 1 to 2 μm in diameter and a depth slightly greater than this.

The matrix of lateritic lithic fragments is composed of variable mixtures of SiO_2, Al_2O_3, and Fe_2O_3 corresponding to mixtures of kaolinite and goethite. These secondary minerals produced by weathering of primary minerals are very fine grained and tend to be a mixture, even at the sub-micron scale. The yellow colour of the lateritic lithic fragments is due to the presence of goethite as minute spots associated with clay. The cores of black lateritic nodules are Fe-rich with little Al and Si. These black nodules in the fine lag of mixed origin are related to the lateritic duricrust. Four discrete mineralogical facies were identified within the matrix of the lateritic lithic fragments and black nodules. These are Al-hematite + Al-goethite, Al-goethite, Al-goethite + kaolinite, and kaolinite. *In situ* geochemical analysis of these mineralogical facies demonstrates an orderly succession of mineralogical and structural transformations. It appears that kaolinite is progressively replaced by goethite and/or hematite and that these transformations result in formation of goethite-hematite-rich lateritic nodules. A general relation between Fe accumulation, destruction of kaolinite and formation of lateritic nodules has also been documented by other workers (Muller and Bocquier, 1986; Fankel and Bayliss, 1966).

XRD data for whole samples of lag gravels provide an assessment of bulk mineralogy and, in the case of goethite and hematite, an indication of chemical composition in the sense of an average Al-substitution. Given that kaolinite is the only layer silicate clay mineral present, and that no gibbsite is recorded in the sample, the Al/Si ratios indicate that all areas have Al above that accounted for by admixed kaolinite (Table 6). The excess Al is regarded as a measure of Al-substitution in the oxide structure. Goethite in the lateritic lithic fragments contains up to 8% Al. Black nodules contain mixtures of hematite, goethite, and maghemite and therefore Al subsitution in goethite could not be determined from the data.

Table 6 - Electron Microprobe Analyses of Lag Gravels

Grain Type	Mineralogy	Sample Analysis		Wt %								ppm							Wt %
				SiO2	Al2O3	Fe2O3	TiO2	MgO	CaO	Na2O	K2O	As	Cr	Cu	Mn	Ni	V	Zn	Total
Yellow L.L.F.	Gt,Ka	07-1330	15314	17.38	21.30	47.76	2.60	0.05	0.02	0.02	0.01	183	958	597	314	210	1538	653	89.14
	Ka,Gt	07-1330	15315	23.05	25.50	38.45	0.04	0.06	0.03	0.03	0.03	124	886	407	40	136	587	196	87.19
	Gt,Ka	07-1330	15316	17.60	20.39	47.73	0.17	0.04	0.02	0.05	0.02	158	1106	600	1443	342	919	881	86.02
Yellow L.L.F.	Ka,Gt	07-1330	15317	21.40	27.93	28.74	0.81	0.12	0.11	0.02	0.10	309	17025	318	40	1416	720	50	79.23
	Ka,Gt	07-1330	15318	25.31	32.28	28.02	0.57	0.11	0.09	0.02	0.09	50	16409	166	40	1026	645	50	86.49
Green L.L.F.	Gt,Ka	07-1330	15319	18.09	22.98	48.15	0.31	0.09	0.05	0.03	0.05	50	612	30	40	224	986	50	89.75
Green L.L.F.	Ka,Gt	07-1330	15320	33.98	34.36	21.68	0.16	0.10	0.03	0.04	0.05	50	612	64	91	137	361	50	90.40
Greyish Brown L.L.F.	Gt,Ka	07-1330	15321	21.53	23.85	45.13	0.25	0.02	0.02	0.03	0.02	50	813	143	40	76	1173	50	90.85
Greyish Brown L.L.F.	Gt,Ka	07-1330	15322	12.05	14.49	67.62	0.24	0.02	0.02	0.05	0.01	50	927	98	40	25	2072	50	94.50
Yelowish brown L.L.F.	Gt,Ka	07-1330	15329	22.41	31.10	33.87	0.20	0.03	0.02	0.02	0.03	50	3734	88	40	220	561	50	87.68
	Gt	07-1330	15330	6.25	18.26	64.16	0.37	0.06	0.03	0.04	0.02	50	3993	215	40	103	1399	50	89.19
Yellow L.L.F.	Ka,Gt	07-1330	15331	27.18	34.12	23.52	0.38	0.04	0.02	0.01	0.01	50	7963	167	40	775	484	50	85.28
Black Nodule	Hm,Gt,Mgh	07-1330	15323	1.08	9.10	79.20	1.52	0.02	0.02	0.01	0.01	50	16723	30	123	133	5105	50	90.96
	Hm,Gt,Mgh	07-1330	15324	1.14	7.31	81.05	2.22	0.01	0.04	0.01	0.01	50	15100	30	210	157	5117	50	91.79
Black Nodule	Hm,Gt,Mgh	07-1330	15325	4.50	9.82	81.26	0.55	0.04	0.03	0.01	0.01	148	2077	30	40	25	2506	50	96.22
	Ka	07-1330	15326	35.53	39.39	17.35	0.02	0.17	0.08	0.02	0.07	50	1270	137	102	199	544	50	92.63
	Il	07-1330	15327	0.02	0.00	40.24	54.74	0.03	0.28	0.01	0.01	50	148	30	10826	25	17503	255	95.33
Black Nodule	Hm,Mgh,Gt	07-1330	15328	3.08	9.94	79.34	0.95	0.04	0.04	0.01	0.02	50	1730	75	40	184	2505	50	93.42
Black Nodule	Hm,Gt,Ka	07-1330	15312	14.84	16.48	62.50	0.42	0.02	0.02	0.01	0.02	50	3776	30	40	89	2302	50	94.31
	Ka	07-1330	15313	41.22	40.51	3.44	0.02	0.01	0.01	0.02	0.02	50	408	95	40	454	40	50	85.25
Yellow L.L.F.	Ka,Gt	07-1313	15332	18.42	28.39	38.55	1.49	0.09	0.04	0.06	0.05	129	7956	91	40	486	1358	140	87.09
	Gt	07-1313	15333	0.97	16.71	68.22	0.43	0.03	0.01	0.01	0.01	309	24932	168	353	793	4724	144	86.39
	Ka	07-1313	15334	39.07	29.09	3.22	0.03	5.69	0.05	0.01	0.04	222	1746	52	40	508	93	50	77.20
	Ka,Gt	07-1313	15335	21.11	30.59	29.99	1.16	0.14	0.11	0.01	0.05	211	40958	30	40	747	948	50	83.16
Yellowish Brown L.L.F.	Gt,Ka	07-1313	15337	14.22	21.71	54.01	0.74	0.11	0.02	0.04	0.03	1202	7044	434	267	990	539	50	90.88
	Gt	07-1313	15338	2.38	5.11	76.66	0.38	0.15	0.01	0.01	0.01	1214	15080	313	400	2773	728	179	84.71
	Gt	07-1313	15339	3.12	3.26	61.36	0.48	0.02	0.01	0.01	0.01	725	9912	215	243	1470	421	125	68.27
	Ka,Gt	07-1313	15347	22.52	28.56	35.96	0.54	0.09	0.01	0.02	0.04	867	5252	259	40	540	397	50	87.74
Black Nodule	Hm,Gt,Mgh	07-1313	15336	2.96	3.36	81.00	3.61	0.03	0.03	0.01	0.02	50	5454	30	40	25	3959	50	91.02

Hm= Hematite Gt=Goethite Ka=Kaolinite Mgh=Maghemite Il=Ilmenite L.L.F.=Lateritic lithic fragment

One microprobe spot analysis in the yellow lateritic lithic fragments has an MgO value of 5.69% which is probably present in talc.

Trace element data on lag gravel clearly indicate that lateritic lithic fragments and lateritic nodules of similar morphology and colour in single specimens have different origins (Table 6). Some clasts originated from mafic rocks, whereas others originated from ultramafic rocks. This is indicated by the distribution of Cr and Ni. However, it is interesting to note that high values of Cr are not always accompanied by high values of Ni for the lag gravels originating from ultramafic rocks. This may indicate that behaviour of the Ni is quite complex.

Trace elements which are either adsorbed or incorporated into goethite and kaolinite structures by isomorphous replacement show a wide range in their abundance levels (Table 6). Analyses of geothites within lateritic lithic fragments show values of As up to 1200 ppm and the highest level of Ni. Generally, higher concentrations of Mn, Cu, and Zn occur in lateritic lithic fragments containing goethite and kaolinite than in black nodules. Strong correlations occur between Mn and Zn ($r=0.83$), Mn and Cu ($r=0.64$), and Zn and Cu ($r=0.73$).

Ilmenite grains occurred in the matrix of some black nodules and had values of 40.2% Fe_2O_3 and 54.74% TiO_2 which are quite close to the values for pure ilmenite. Manganese contents reach 10,000 ppm suggesting that Mn is substituting for Fe^{3+}.

4.8 Discussion

The general distribution of lag gravels can be understood in terms of regolith/landform relationships. In the erosional regimes, coarse black lags of ferruginized saprolite, or where stripping is less extensive lag of lateritic lithic fragments, appear to be largely the result of present-day *in situ* weathering of the landscape. In the same sense, lateritic lag is the *in situ* product of present-day weathering of lateritic duricrust. These lags may have been concentrated at the surface by a variety of processes including deflation, removal of matrix, burrowing action of termites, ants and rabbits, etc. and these processes have been discussed in detail by Mabbutt (1977) and Carver *et al.* (1987). These *in situ* lags have been further subjected to physical and chemical weathering and dispersion processes. Lateral dispersion of these lags by the action of water has resulted in a layer of fine lag comprising a variety of clasts on the adjacent colluvial outwash plains. The increase in the abundance of fine lag in the lower slopes is probably related to the colluvial sedimentation and fractionation of the lag as it passes downslope and away from the source whereas the large fragments of ferruginized saprolite and Fe-rich duricrusts show lesser dispersion. Fine lag is therefore allochthonous and does not relate to the immediately underlying lithology.

Morphological characteristics and regolith/landform framework allowed separation of the lag gravels into four types described above: lag of ferruginized saprolite, lag of lateritic lithic fragments, lateritic lag, and fine lag of mixed origin. These four types were shown to have different mineralogical and geochemical characteristics. Some lag gravels preserve the primary rock fabric, and this information combined with the geochemistry and mineralogy, allows one to predict the underlying lithology.

Although the lateritic lithic lag, ferruginized saprolite, and lateritic lag are either directly derived or the products of weathering of saprolite, there are significant differences in the chemical composition between the lag types. These differences may be due to the nature of the bedrock, degree of weathering, and mechanism of accumulation of the secondary weathering products. For example, the Fe_2O_3 contents of the lag of ferruginized saprolite are comparable with those of the lateritic lag, but there are strong geochemical distinctions between the two types. Lateritic lag is depleted in Mn, Zn, and Co relative to the mean values of ferruginized saprolite which is consistent with findings generally over the Yilgarn Block.

Conversely, the lateritic lag at Meatoa carries significantly higher levels of As, Pb, W, and TiO_2. These geochemical differences between the two lag types are attributed to the different mechanism of their formation. The lag of ferruginized saprolite appear to have formed by absolute accumulation of Fe under reducing conditions as is also shown by its low level of Al substitution in goethites and hematites. In reducing conditions, Fe and Mn are mobile in the form of Fe^{2+} and Mn^{2+} respectively. The metals Zn and Co released from the weathering of primary minerals also occur in diavalent forms in reducing conditions and may substitute for Fe^{2+} and Mn^{2+} (Tiller, 1963). The strong correlations of Zn and Co with Mn, but the poor correlation with Fe suggest their occurrence in Mn minerals rather than in Fe oxides. However, Mn minerals were not detected by XRD, but more careful analytical work is needed to prove this. Because of the relatively high levels of Mn, Sn, and Co in samples of ferruginized saprolite, it is important to treat the regolith formed by absolute accumulation and relative accumulation separately when calculating thresholds, otherwise genuine anomalies in the regolith formed by relative accumulation may be regarded as background fluctuations because their magnitude is small by comparison with values in regolith formed by absolute accumulation.

Many of the chalcophile elements exhibit slightly-lower levels of abundance in the lag of lateritic lithic fragments to those in the lateritic lag. These differences are probably related to the nature and degree of weathering. Lateritic lithic lag is relatively less weathered compared to the lateritic lag as is shown by the relatively large amounts of kaolinite and goethite and moderate levels of Al substitution. The elements As, Pb, V, and perhaps Sn, likely to be associated with Fe oxides, are relatively lower in abundance in the lateritic lithic lag. However, Cu levels are significantly higher in the lateritic lithic lag and were found to be strongly associated with kaolinite.

The research on lag gravels highlights the importance of understanding their origin, particularly in terms of their regolith/landform history when planning, executing and interpreting an exploration geochemical survey in this style of deeply weathered terrain. The absence of known mineralization underneath prevents one from making conclusions about the choice of the lag type as a sampling medium at this stage. However, the genetic understanding of these lag gravels from the Meatoa area should act as a guideline for their use as a sampling medium in the exploration programme.

5.0 REGOLITH RELATIONSHIPS IN THE AGNEW-McCAFFERY AREA

5.1 Introduction

Detailed regolith/landform relationships for the North Pit area were earlier reported by Anand *et al.* (1989). The work presented here extends the research north of McCafferys to cover much of airphoto Run 4/9544 (6.12.88). The aim is to establish regolith relationships in the Agnew-McCaffery areas and identify the pattern of occurrence and morphological, mineralogical, and geochemical characteristics of the lags and soils.

5.2 Regolith And Landforms

The surface distribution of regolith units in the Agnew-McCaffery area is shown in Fig. 22 as an overlay to airphoto 4/9544. The units delineated in this diagram have been mapped onto a three-times enlargement, that is, at a scale of 1:8333. In order to compare the regolith and characteristics of an area characterized by lateritic residuum at surface with those from an area that has been modified by stripping processes, a traverse was selected for detailed study some 3.5 km east-north-east of Agnew, immediately south of the Agnew-Leinster road (Fig.22). The location comprises two parallel minor valleys. In the more northerly valley, smooth gentle slopes on either side of the valley extend down from a broadly-convex crest to a broadly-concave unchannelled floor. Southward, the smooth slopes rise to another broadly convex crest forming the interfluve to the adjacent valley. This crest is flanked to the south by a low breakaway from which the pediments slope gently downwards to a flat valley floor.

A regolith/landform model for this area is shown in Fig. 23A. Changes in regolith stratigraphy and soil types along the traverse AB are shown in Fig. 23B. The dominant features of the regolith of the study area are related to the occurrence of lateritic gravels and duricrust (Unit 1) on broad crests and backslopes, subcropping saprolite (Unit 2) on the breakaway and upper pediments and colluvium/alluvium (Unit 7) dominating the valley floors. However, locally-derived colluvium also occurs in the valley floors. The regolith of the northern valley is characterized by gravelly sandy loam to sandy clay loam soils which overly lateritic residuum. For the purpose of discussion, it can be referred to as a residual area. The regolith of the southern valley, by contrast, is characterized by gravelly sandy clay loam soil overlying saprolite. It is interpreted that lateritic residuum once covered most and possible all of the area and the main regolith/landform features are due to partial truncation by erosional processes which continue today.

Details of the regolith at sample sites along the transect are given in Table 7. Nodular duricrust and medium to coarse (4-12 mm) yellowish-brown lateritic pisoliths and nodules dominate the lags of the broad crests (Unit 1a), forming a divide between the valleys. Down the slopes of the more northern valley, gravels become finer and dominantly comprise lateritic pisoliths and nodules (Unit 1b). Nodules forming the lateritic gravels on the broad crests have black or reddish brown cores, each having a yellowish-brown cutan (Fig. 24A). Downslope in the northern valley, the gravels with dark brown to brownish-black surfaces become increasingly more common. The pediments below the breakaway of the southern valley are mantled by a coarse lag containing yellowish-brown lateritic lithic fragments similar to those at Meatoa (Unit 2). These lags also become finer downslope, they are a mixture of clasts with yellowish brown surfaces and others that are black. Cutans are not present on these clasts. The interiors of some lateritic lithic fragments have diffuse mottles and incipient nodules (Fig. 24B). The contact between the yellow kaolinitic and goethitic matrix and reddish brown hematitic-kaolinitic incipient nodules is not clear, whereas that between the yellow matrix and hematitic black nodules is sharp. Petrographic examination has shown that the hematite black nodules develop at the expense of the reddish-brown incipient nodules, and the latter themselves develop at the expense of the yellow kaolinitic and goethitic matrix. The result is the development of hematitic nodules gradually destroying yellow

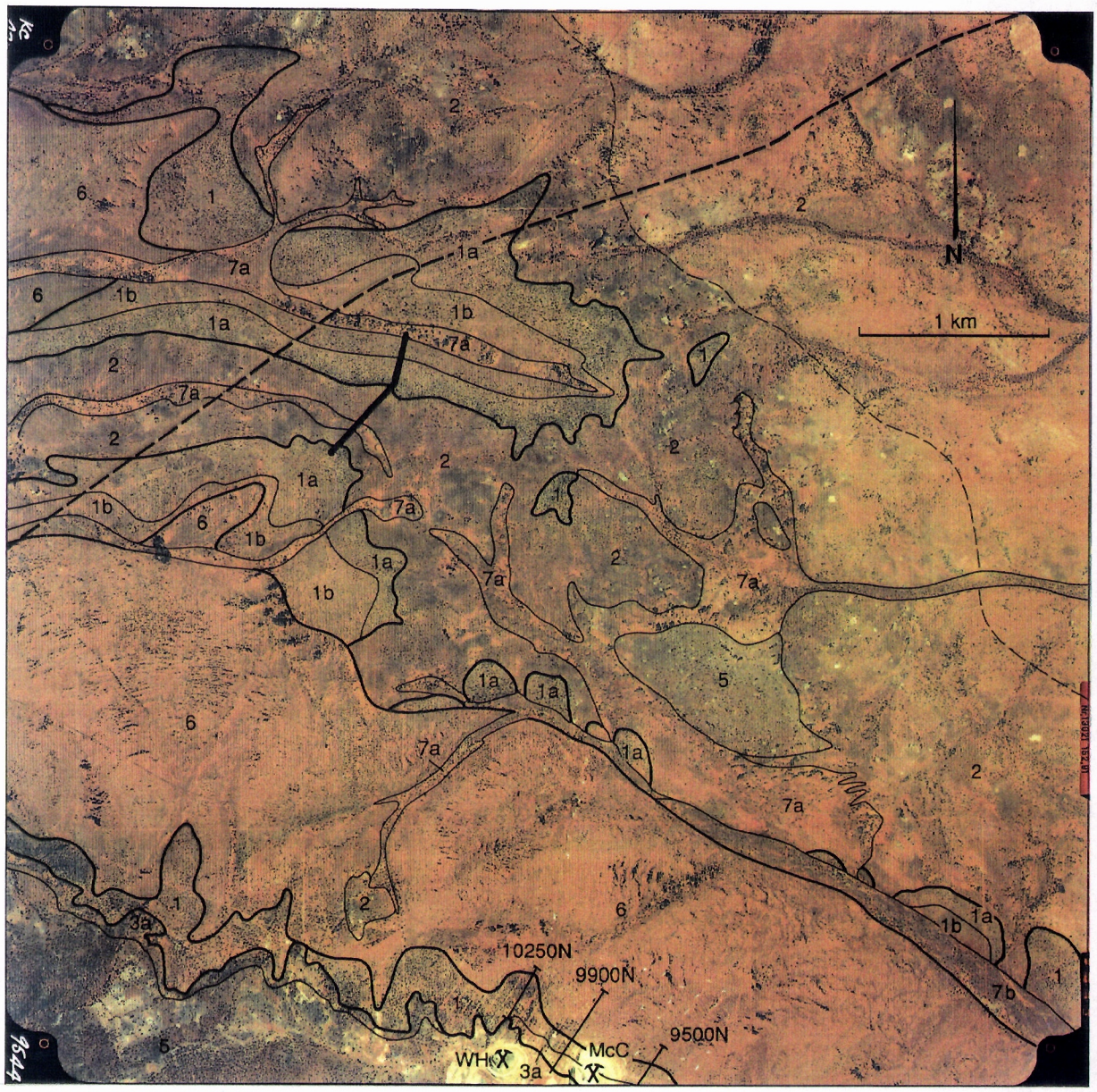

EROSIONAL REGIMES

- 2 Soil, lag, on saprolite
- 3a Mottled zone saprolite
- 5 Subcrop of bedrock

RESIDUAL REGIMES

- 1 Lateritic residuum
  - 1a duricrust
  - 1b gravel

DEPOSITIONAL REGIMES

- 7 Alluvium
  - 7a in minor tributaries
  - 7b in major tributaries
- 6 Colluvium as sheet wash

Traverse

Regolith cross sections from Anand et al (1989)

McCaffery and Weight Hill mine pits

Fig. 22. Map showing the surface distribution of regolith units and vegetation for the Agnew-McCaffery area. Bedrock lithologies are mafic and ultramafic. Aerial photograph 4/9544, 6.12.88, Kevron Aerial Surveys, published with permission of Homestake Gold of Australia Limited.

A

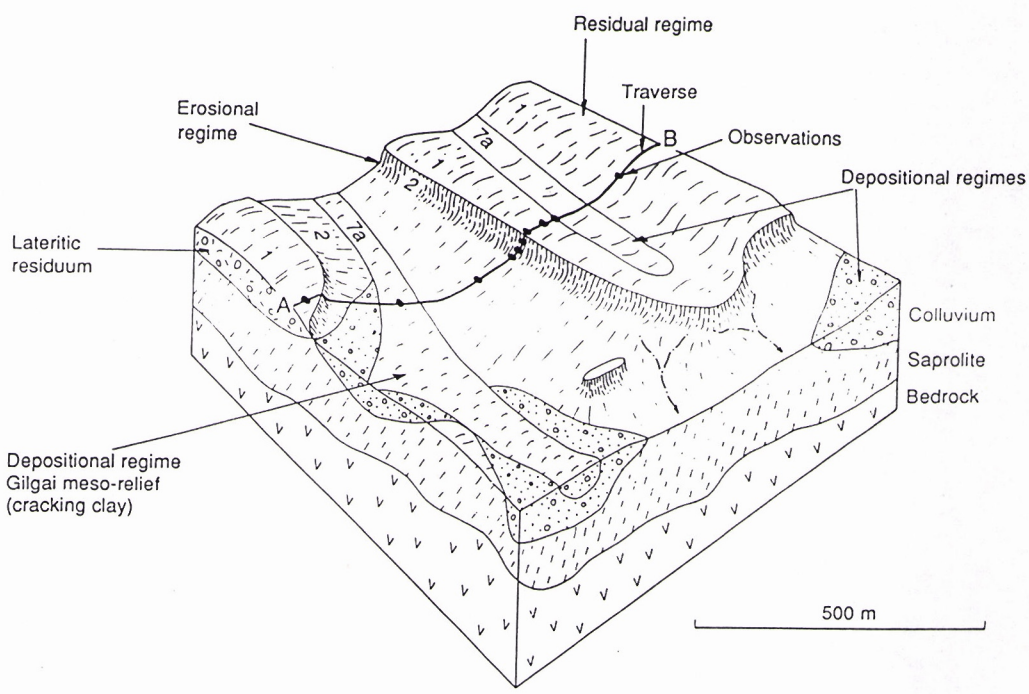

Fig. 23A. Generalized regolith/landform model based upon the Agnew-McCaffery study area.

B

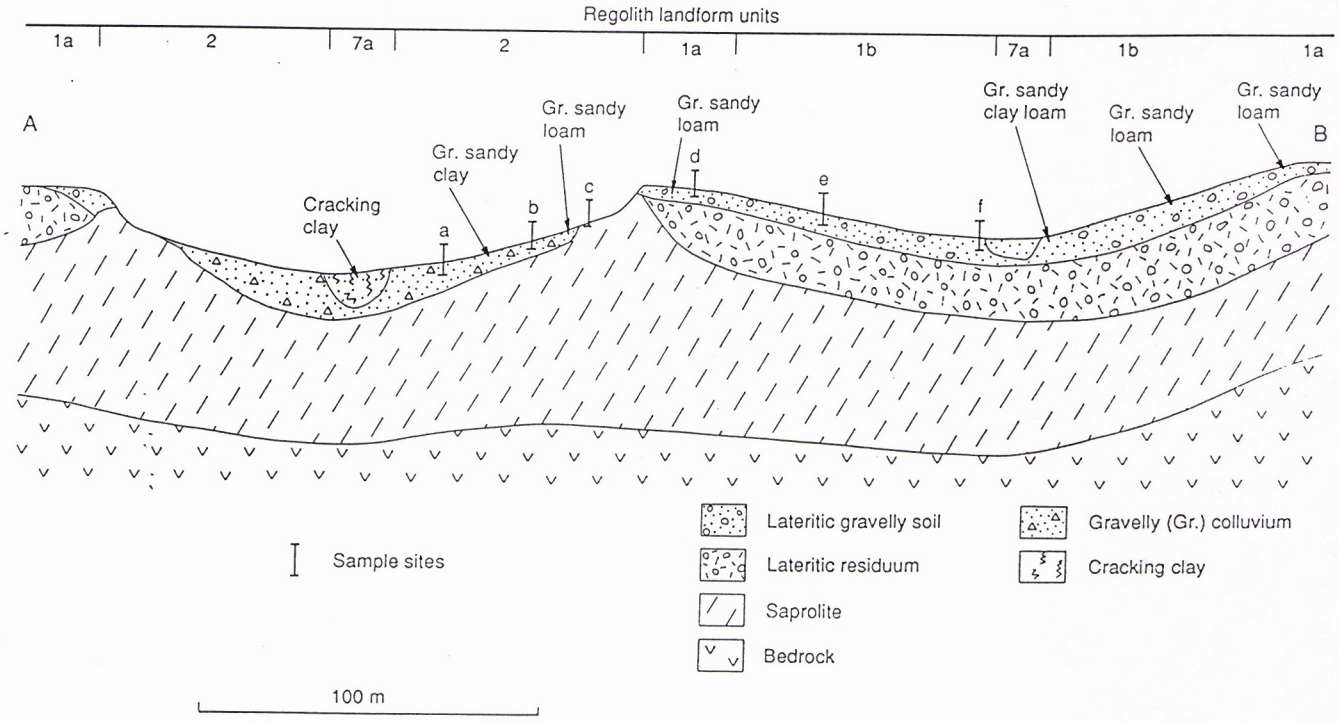

Fig. 23B. Schematic regolith cross-section showing trends in soil and regolith stratigraphy for the traverse shown in Fig. 23A.

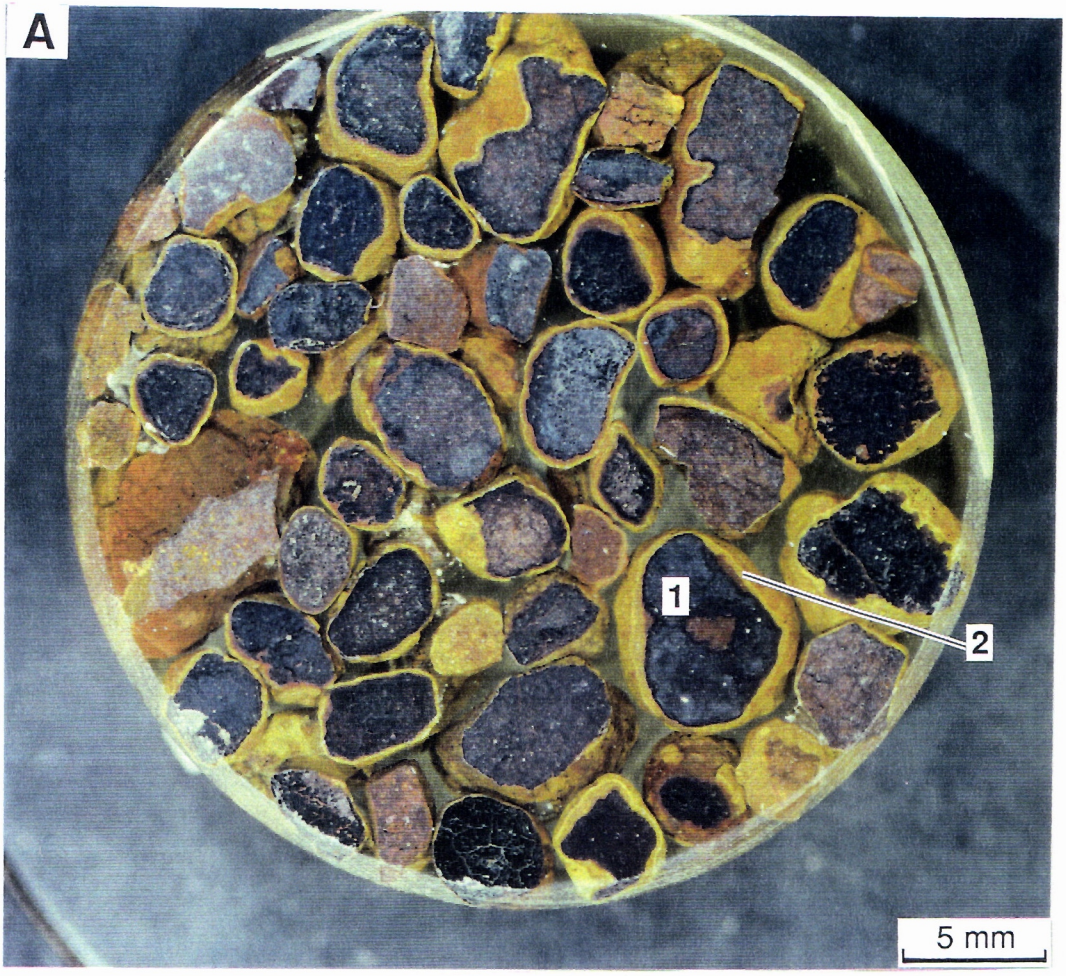

Fig. 24A. Loose lateritic pisoliths from regolith Unit 1 showing black hematite-rich core (1) and yellowish brown goethite-rich cutan (2). Sample 07-1393.

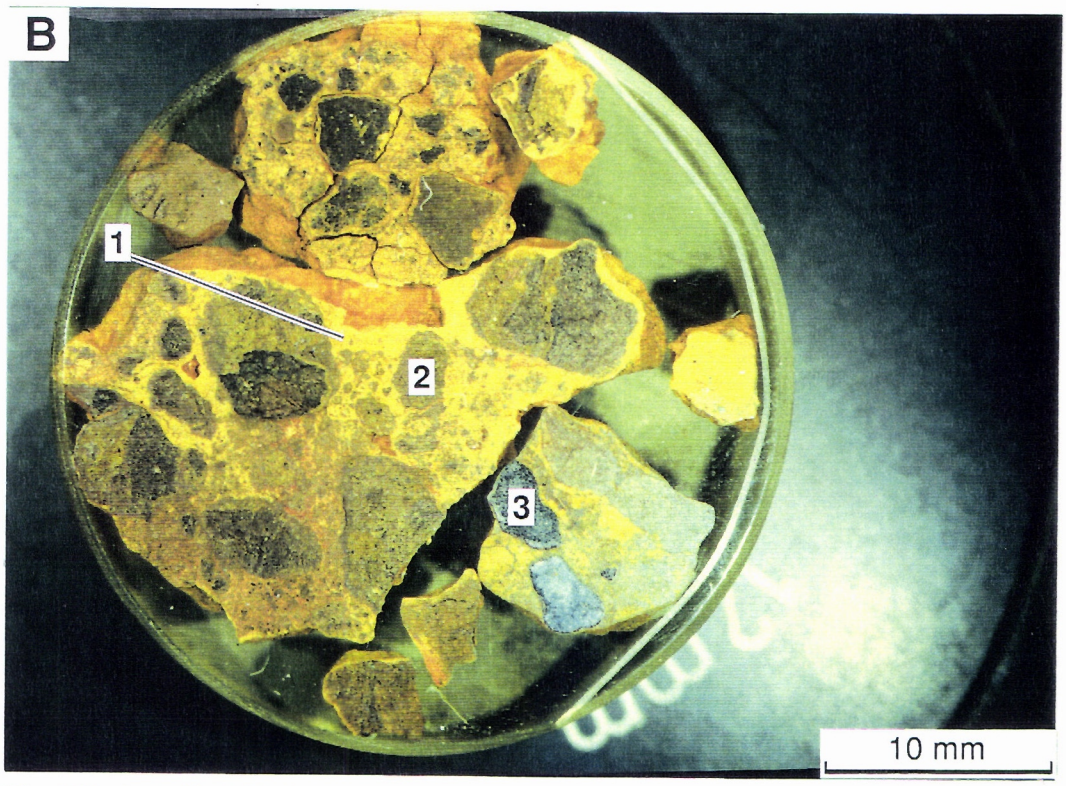

Fig. 24B. Lateritic lithic fragments from regolith Unit 2 showing yellow goethite-rich matrix (1), incipient nodule (2) and black hematite-rich nodule (3). Sample 07-1397.

Table 7. Regolith characteristics, Agnew-McCaffery Area

SAMPLE SITES (See Fig. 23B)	a	b	c	d	e	f
REGOLITH UNIT AT SURFACE	2	2	2	1a	1b	1b
TYPE OF REGIME	Erosional	Erosional	Erosional	Residual	Residual	Residual
LANDFORM	Valley floor	Upper pediment	Breakaway scarp	Broad smooth crest	Smooth gentle slopes "back slopes"	Valley floor
LAG	Lag of mixed origin (ferruginous pebbles/ granules after ferruginized saprolite, lateritic nodules)	Lateritic lithic fragments	Lateritic lithic fragments	Lateritic lag	Lateritic lag	Lateritic lag
SOILS	Gravelly red fine sandy clay	Reddish-brown gravelly fine sandy loam	-	Gravelly reddish brown fine sandy loam	Gravelly reddish brown fine sandy loam	Gravelly brown fine sandy clay loam
COLLUVIUM	Gravelly colluvium	Gravelly colluvium		-	-	Gravelly colluvium
HARDPAN	Present within a metre	Present within a metre	-	-	Some	Some
LATERITIC RESIDUUM	-	-	-	Nodular duricrust	Nodular duricrust (?)	Nodular duricrust (?)
SAPROLITE	Ferruginized and clay-rich saprolite (?)	Ferruginized and clay-rich saprolite	Ferruginized and clay-rich saprolite	Ferruginized and clay-rich saprolite (?)	Ferruginised and clay-rich saprolite (?)	Ferruginized and clay-rich saprolite (?)

matrix. An incipient nodule is a transitional feature in which Al-hematite replaces kaolinite and Al-goethite.

On the crests (Unit 1a) the soils are reddish brown (7.5-5YR 5/6, moist), friable fine sandy loams. Down the smooth slopes, there is a slight but perceptible increase in the clay fraction leading to fine sandy loams and fine sandy clay loams. On the upper pediments, the soils are red brown (5YR 5/6, moist) sandy loams, but merge downslope to red (5YR 4/6, moist) sandy light clays. Deep, cracking, self-mulching, red, heavy clays associated with gilgai mesorelief occur in the floor of the southern valley.

5.3 Mineralogy of Lag Gravels

Mineralogy of the lag samples along the traverse, on a semi-quantitative basis, is shown in Fig. 25. Hematite, goethite, maghemite, kaolinite, and quartz (not shown) are the dominant crystalline minerals in all lags. However, the relative abundance of these minerals varies widely between the lag types and particularly as a function of the regolith/landform unit. Hematite and maghemite are more abundant in lateritic lag gravels on the broad crest (Unit 1a) forming a divide between the valleys. This suite of minerals also dominates the backslope and valley floor of the northern valley (i.e. the residual regime). By contrast, goethite is the dominant mineral in lags containing lateritic lithic fragments of the southern valley, where stripping is suggested by the absence of lateritic residuum. Kaolinite is relatively more abundant in lateritic lithic fragments than in lateritic lag gravels. The differences in mineralogy between the lateritic lag and lateritic lithic fragments are due to differences in the degree of weathering. Lateritic lithic fragments are derived from the breakdown of upper parts of saprolite, while lateritic nodules/pisoliths are the product of breakdown of nodular/pisolitic duricrust. Lateritic lithic fragments have experienced a lesser degree of weathering compared with those of lateritic gravels as is shown by the large amounts of goethite and kaolinite in lateritic lithic fragments.

5.4 Aluminium Substitution in Fe-Oxides

Aluminium substitution in goethite, hematite and maghemites for all lag types is from presented in Fig. 26. Aluminium substitution in goethite, hematite, and maghemite of lateritic lag gravels from the northern valley (residual area) is different from that in the lateritic lithic fragments of erosional area (southern valley). Goethites of lateritic gravels show much higher levels of Al substitution (up to 30 mole %) than those of lateritic lithic fragments. High substitution reflects weathering in an environment with a high degree of Al availability which is then incorporated in the goethite structure. The somewhat lower substitution (13-18 mole %) in lags containing lateritic lithic fragments of the southern valley is in line with a lower degree of weathering as also indicated by the mineralogy.

As has generally been found, the levels of Al substitution in hematite and maghemite are much lower than those for goethites in the same sample (e.g. Anand and Gilkes, 1987; Fitzpatrick and Schwertmann, 1982).

5.5 Geochemistry of Lag Gravels

The major and trace elements composition of lags are presented in Figs 27, 28, 29. Analytical data on individual samples is given in Appendix III. By far the most abundant constituent is Fe_2O_3, with values greater than 75% in lateritic lag gravels and averaging about 55% in the lateritic lithic fragments. The Fe_2O_3 , SiO_2, and Al_2O_3 values show strong inverse relationships. The apparently-close similarity between the SiO_2 , Al_2O_3 curves indicates that these are mainly present in the same mineral, i.e., kaolinite. However, some Si is present as quartz, and some Al is present in goethite and hematite. The minor oxides Mg, Ca, K (not shown) are strongly depleted. The levels of TiO_2 do not show any variation between the lag types.

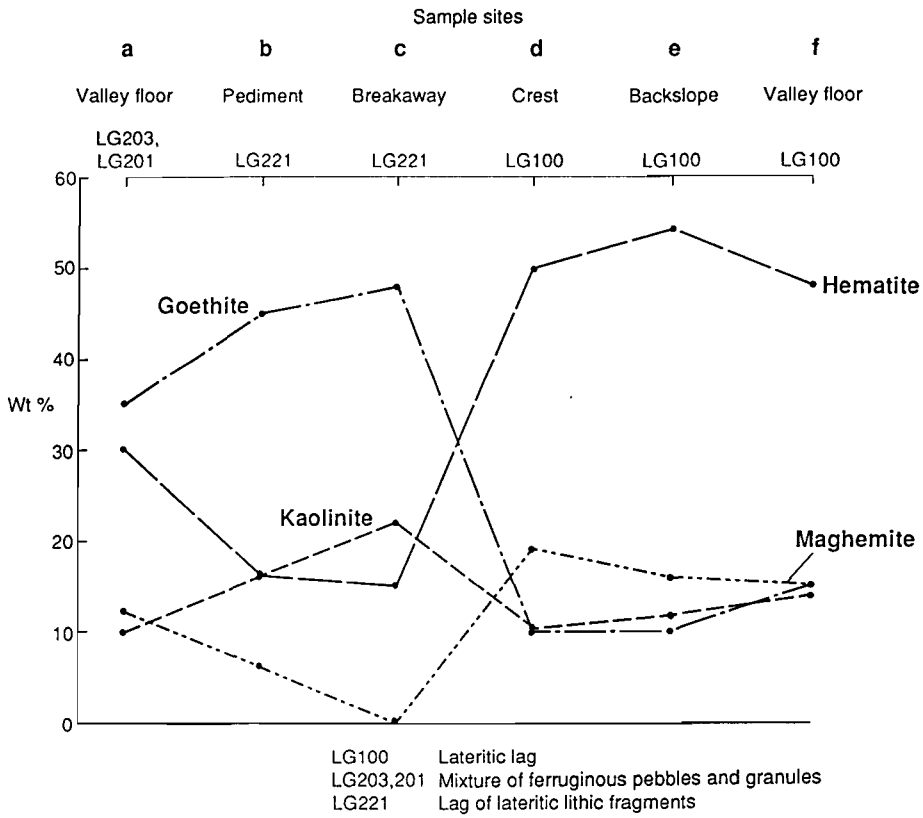

Fig. 25. Distribution of goethite, hematite, maghemite and kaolinite in lag gravels for the sample sites shown in fig. 23B.

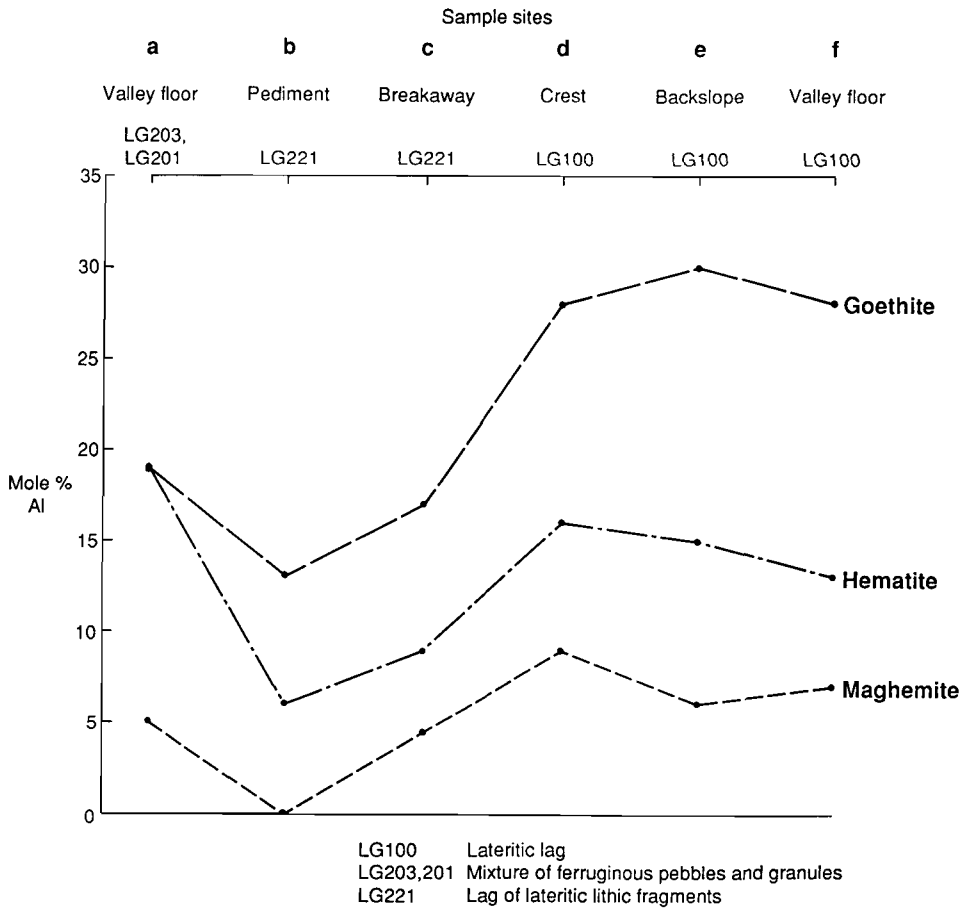

Fig. 26. Distribution of Al-substitution in goethite, hematite and maghemite in lag gravels for the sample sites shown in fig. 23B.

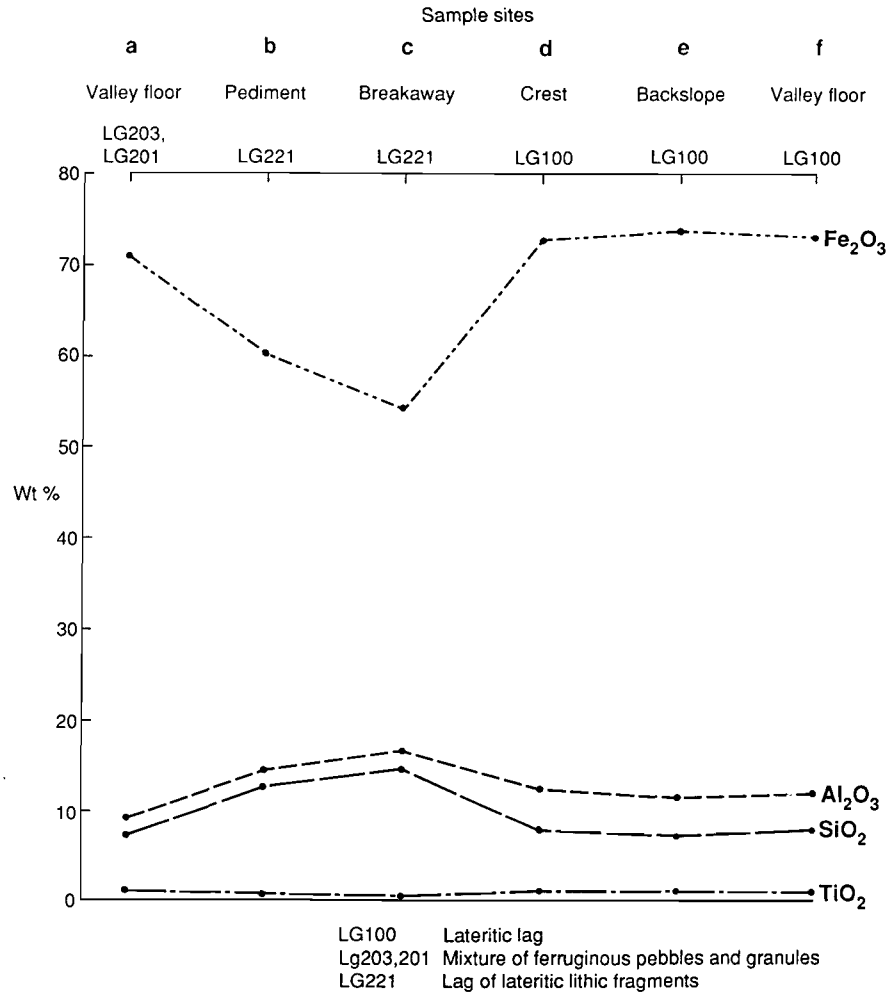

Fig. 27. Distribution of Fe_2O_3, Al_2O_3, SiO_2 and TiO_2 in lag gravels for the sample sites shown in Fig. 23B.

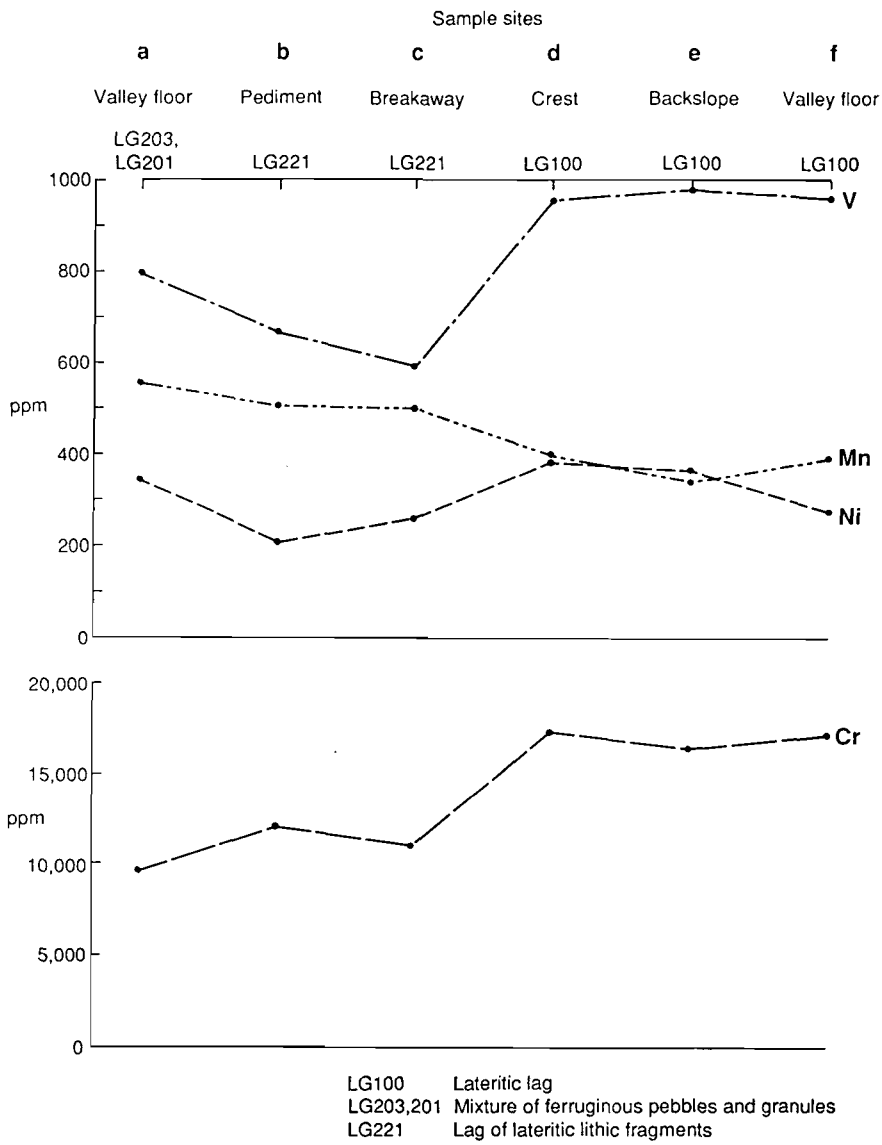

Fig. 28. Distribution of V, Mn, Ni and Cr in lag gravels for the sample sites shown in Fig. 23B.

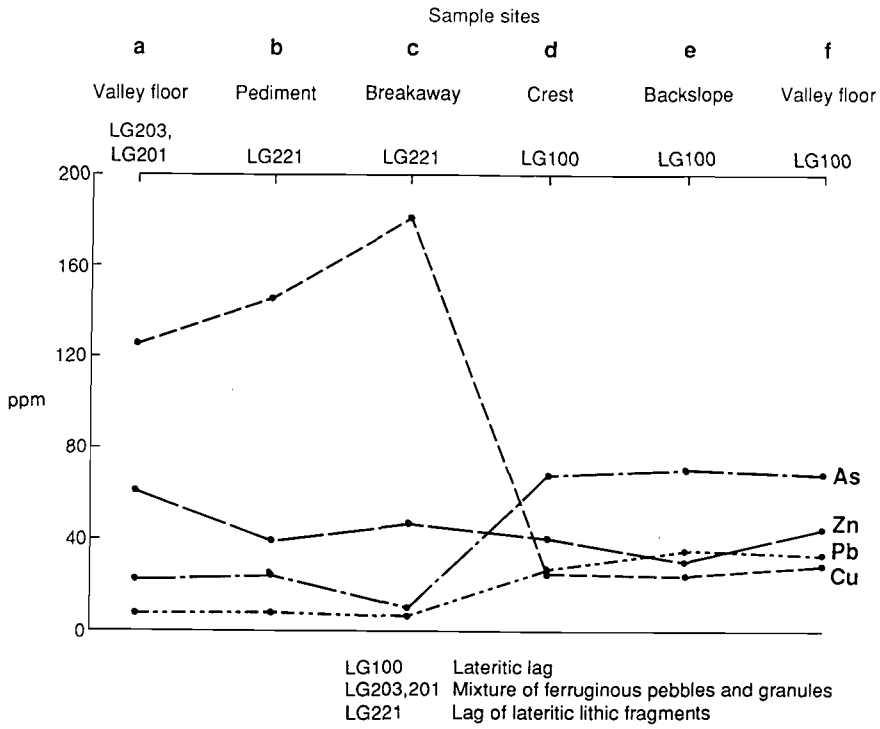

Fig. 29. Distribution of As, Zn, Pb, and Cu in lag gravels for the sample sites shown in Fig. 23B.

The trace elements V, Mn, Cr, As, Pb, Ga, Zr are more abundant in lateritic lag gravels of the residual area of the northern valley. Copper and Ni, in contrast, are more abundant in the lateritic lithic lags of the erosional area of the southern valley. Zinc and Co do not show appreciable variations. Other elements, namely Mo, Sn, Ge, W, Nb, Se, Ag, and Au, are present in very small amounts. Part of the distribution of trace elements in the lag gravels of the two valleys may simply reflect the differences in the nature of the bedrock from which these gravels are derived. However, direct knowledge on bedrock for this area is not available. Another factor which may influence the distribution of trace elements is the nature of the lag itself. The lags of the residual area are lateritic, while those of erosional area are lithic. These lags differ in their Fe contents. Vanadium, Mn, Cr, As, and Pb appear to follow the Fe_2O_3 curve. However, this relationship does not hold true for the Fe-rich lags on the floor of the southern valley. This may be due to the mixed origins of these lag gravels as is dicussed in Section 5.2.

5.6 Clay Mineralogy

The clay mineralogy of the soils of the regolith units on various topographic positions is shown in Table 8. The clay fraction was sedimented on to glass slides and saturated with Mg, with and without glycerol, to confirm the identity of smectites. XRD traces of these indicate that kaolinite is the dominant soil mineral of the crest and breakaway/pediments while Mg-smectite dominates soils on the floor of the southern valley. However, it is of interest to note, that small to moderate amounts of smectite are present in all the samples. Chlorite occurs in significant amounts in the floor of the southern valley. Small amounts of interstratified clays and illite are also present in a few samples.

Kaolinite is generally a product of weathering of well-drained highly-weathered soils (Dixon, 1977). Its formation is not favoured in the current overall soil chemical environment for this arid area since the leaching conditions are not optimum. Kaolinite in these soils is thus related to more severe leaching conditions during the paleoweathering regime. It can then be concluded, that the soils under investigation on the crests and breakaways have developed on remnants of the old lateritic profile which were formed under warm humid climate.

Soils on the floor of the southern valley are largely developed in colluvium/alluvium derived from the erosional areas. Smectite development in these soils is compatible with the truncated provinence areas being more labile. In addition, poor drainage conditions in the valley floor would further lead to the formation of smectite. Because of the lack of stripping in the northern valley, the presence of small to moderate amounts of smectite cannot be explained by the mechanism described for the southern valley. The occurrences of smectite may be relics from the humid climate in the past, or may relate to biocycling of Mg.

5.7 Conclusions

The present study has shown that within a local area of some 25 square kilometres where the climate, parent rock, and vegetation are similar, the regolith and its characteristics show wide variation. The variations in characteristics of regolith observed between the two valleys could be related to the distinct geomorphic position. Highly-weathered regolith, such as lateritic duricrust or lateritic gravels, occurs on residual areas, while relatively less weathered and less disaggregated materials such as saprolite are exposed on erosional areas. The nature and characteristics of lag are controlled by regolith/landform history and by their nature and degree of weathering. The degree of Al substitution in goethite appears to relate to the maturity of the regolith, level of truncation, and may also reflect the environments in which it has formed.

Table 8. Clay mineralogy of soils of various regolith/landform units

Sample Sites	Landform	Kaolinite	Smectite	Chlorite	Interstratified	Illite
a	Valley floor	+ +	+ +	+ +		+
c	Breakaway	+ + + +	+		+ +	
d	Crest	+ + + +	+ (?)			
f	Valley floor	+ + + +	+ +			
cracking clays	Gilgai meso-relief	+	+ + + +	+ +	+	

+ + + + = Dominant

+ + = Sub-dominant

+ = Minor

6.0 REGOLITH RELATIONSHIPS IN THE BRILLIANT AREA

The Brilliant area was selected in order to clarify some of the regolith/landform relationships observed in the Meatoa area and to allow further extrapolation of regolith relationships at the district scale. The Brilliant area, 14.5 km NE of Agnew, was chosen to be that covered by airphoto 3/9505 (6.12.88), occupying approximately 30 km^2 in the Lawlers district. Figure 30 shows the surface distribution of regolith units for the area. Their boundaries are based on interpretation of 1:25,000 colour air photography substantiated by ground traverses. The regolith/landform model derived from the study area is depicted in Fig. 31. The dominant features of the distribution of regolith units are the occurrence of erosional regimes (Units 2a, 2b) on low stony hills in the central zone, and residual areas (Units 1a, b) on broad crests/backslopes and depositional regimes (Units 6, 7) on colluvial/alluvial outwash plain areas in both the eastern and western sides of the figure. Drainage in the erosional regimes finds its way through gaps between residual and depositional regimes to the main regional drainages. The data show that regolith relationships in the Brilliant area are similar to those described for the Meatoa area in Section 3.0. These relationships therefore will not be described in detail here. However, the features that differ from those of Meatoa area are as follows:

- An erosional regime (Units 2a, 2b) occupies the central zone. It is flanked by residual Units 1a, 1b and depositional Units 6, 7 on either side of the study area. This relationship was not observed in the Meatoa area where the erosional regimes (Units 2a, 2b) are flanked by exposures of the felsic bedrock to the east and residual and depositional regimes to the west.

- The residual regime (Unit 1) has been subdivided largely on the basis of the nature and size of the lateritic materials and topographic characteristics. Unit 1a is mantled by Fe-rich duricrust and coarse lateritic gravels, whereas Unit 1b is dominated by fine lateritic gravels. Unit 1b generally merges downslope with Unit 6. In the Meatoa area, the differences in the clast-size of gravels were not apparent and therefore Unit 1 was not subdivided.

- Outcrops of mafic/ultramafic rocks forming low hills have been mapped as Unit 5 at Brilliant. These features were not prominent at Meatoa.

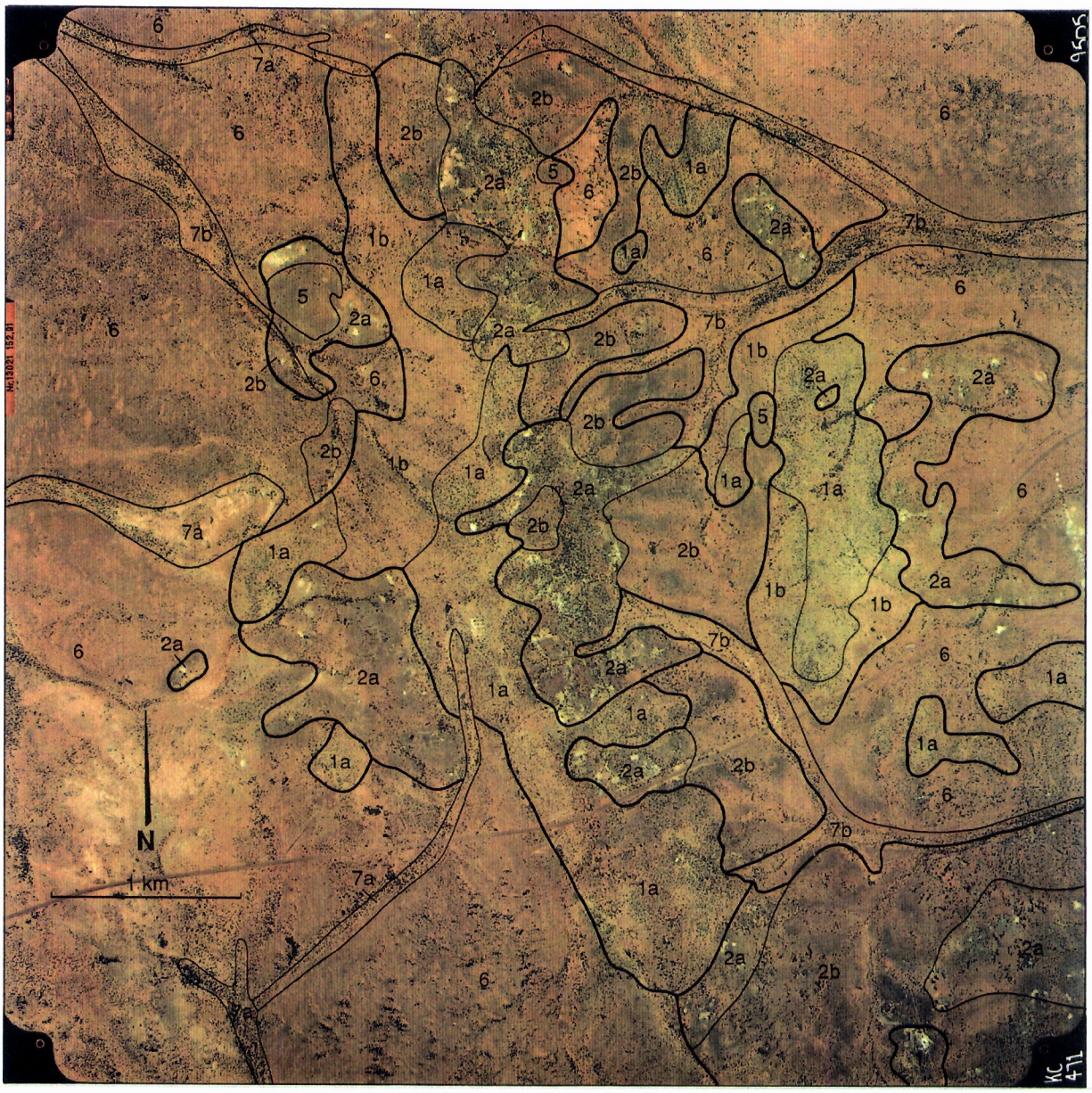

EROSIONAL REGIMES

Saprolite
- 2a — Sandy light clay soil,coarse black lag on saprolite, pedogenic calcrete
- 2b — Sandy clay loam soil, coarse lag on saprolite
- 5 — Subcrop of bedrock

RESIDUAL REGIMES

Lateritic residuum
- 1a — Sandy clay loam soil, Fe-rich duricrust, coarse lateritic gravels
- 1b — Sandy clay loam soil, fine lateritic gravels

DEPOSITIONAL REGIMES

Colluvium
- 6 — Sandy light clay soil, fine mixed lag, colluvium as sheet wash

Alluvium
- 7a — Light clay soil, alluvium in minor tributaries
- 7b — Light clay soil, alluvium in major tributaries

Fig. 30. Map showing the surface distribution of regolith units and vegetation for the Brilliant area as an overlay to the colour air photograph (Kevron Aerial Surveys Run 3/9505, 6.12.88) published with permission of Homestake Gold of Australia Limited.

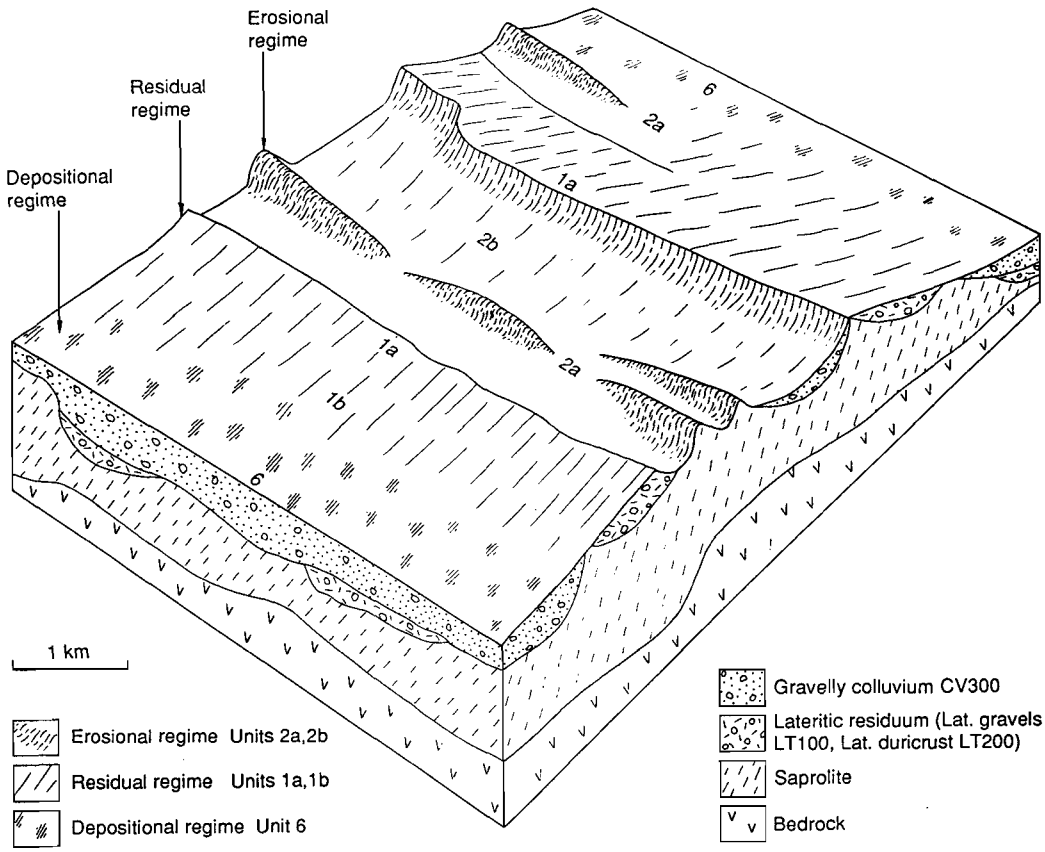

Fig. 31. Generalized regolith/landform model based on the Brilliant study area.

7.0 THE Fe-RICH DURICRUST

7.1 Introduction

Fe-rich duricrust is the nomenclature used in this report in the sense of Anand et al. (1989) for dense, black duricrusts with greater than 70% Fe_2O_3. In the Lawlers district, they characteristically have a nodular, nodular-pisolitic or oolitic fabric, being categories LT 224, LT 223, and LT 221 respectively. They are sporadically distributed throughout the Lawlers district and commonly occur on topographically elevated areas (Fig. 32). The objective of the present study is to understand the possible relationships of Fe-rich duricrust with the underlying lithology, nodular/pisolitic duricrust (low in Fe), and the period of lateritic weathering. Bedrock can profoundly influence the nature of the lateritic duricrust. However, at present knowledge of the distribution of bedrock types for the non-outcropping, regolith covered parts of the Lawlers district is apparently scarce and is inadequate for a definitive study of the genesis of the Fe-rich duricrusts. The following progress has been made within these limitations.

Samples of Fe-rich duricrust collected in the vicinity of Meatoa, Brilliant, and the Agnew gravel pit were investigated for petrological, mineralogical, and geochemical characeristics which are described below.

7.2 Morphology And Petrology

The Fe-rich duricrusts are coherent weathering crusts comprised of accumulations of ferruginous nodules/pisoliths/ooliths cemented by Fe oxides. Three broad categories were identified on the basis of their fabric and microstructure: nodular duricrust, piolitic nodular duricrust, and oolitic duricrust. Nodular duricrust is the most common type. The outer surfaces of all three types of duricrusts may have a pebbly appearance.

Nodular duricrust consists of abundant subrounded to irregular, 2-15 mm dark reddish-brown/reddish-black (5R 2.5/1, dry) hematite-rich nodules set in a fine grained, uniform weak red (5R 4/3, dry) hematite-goethite-rich matrix (Fig. 33A). Nodules up to 35 mm in size may also occur. A few pisoliths are also commonly present in the nodular duricrusts. Matrix generally occurs in small amounts. The ratio of nodules to matrix ranges from 60:40 to 80:20; most samples having a ratio close to 80:20. The boundary between nodules and matrix is not well defined and nodules do not show the development of cutans. Nodules are generally magnetic because of the presence of maghemite which may occur around the margins or within cores of nodules. There is commonly more than one form of Fe-oxide present (hematite, goethite, maghemite) in nodules and, in some samples, several generations of Fe oxides (e.g. goethite) can be recognized.

Pockets of nodules having weak red colour appear to have been further enriched with Fe to give a rim of reddish-black colour (Fig. 33A-1). This enrichment began at the borders of the grain or along cracks and proceeded inwards to give reddish-black grains containing isolated weak red areas (Fig. 33A-2) and finally nodules of reddish-black colour consisting of hematite and maghemite (Fig. 33A-3). Red colouration is provided by hematite. The cores of nodules can have oval voids and cracks, some of which have infilling of grey goethite and small quartz grains. The cracks may have developed during the dehydration of goethite to hematite.

Weathered ilmenite grains consisting of pseudorutile and anatase are included in the cores of nodules (Fig. 34A). These grains are subrounded, 10-40 μm in size and are randomly oriented. They were identified using a scanning electron microscope. Dark areas of ilmenite grains are Ti-rich whereas light areas are Fe-rich.

Fig. 32. Fe-rich duricrust on crest and low breakaway face (1). On the pediment occur coarse lag of ferruginized saprolite (2), local pockets of pedogenic calcrete (3) and saprolite (4), location 4.7 km SE of Brilliant.

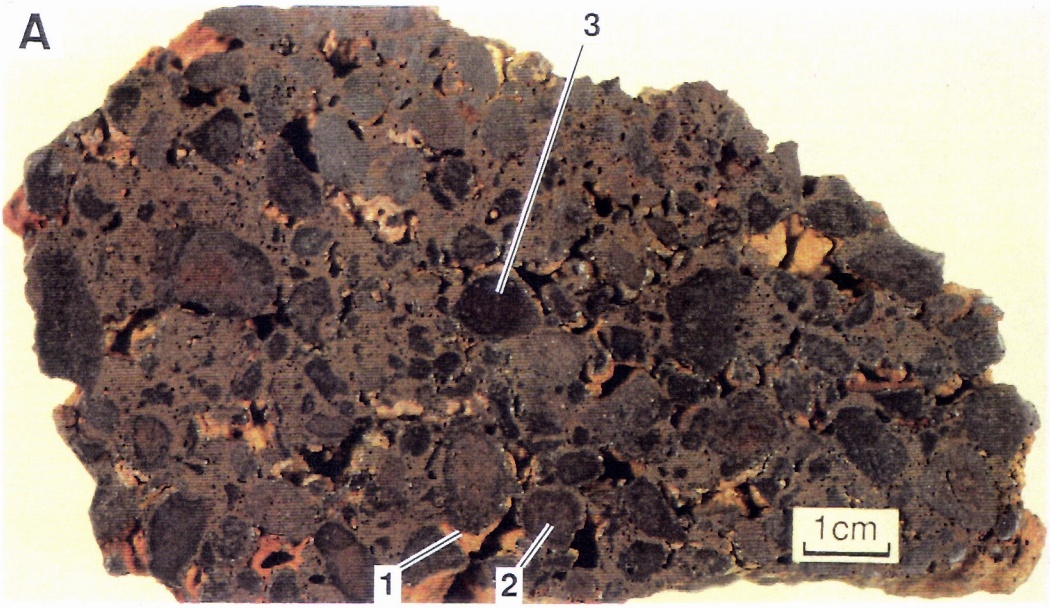

Fig. 33A. Slice through an Fe-rich nodular duricrust showing various stages of fabric development. Weak red areas enriched with Fe to give a reddish black rim (1), reddish black grains with isolated weak red areas (2) and finally reddish black grains (3). Sample 07-1314.

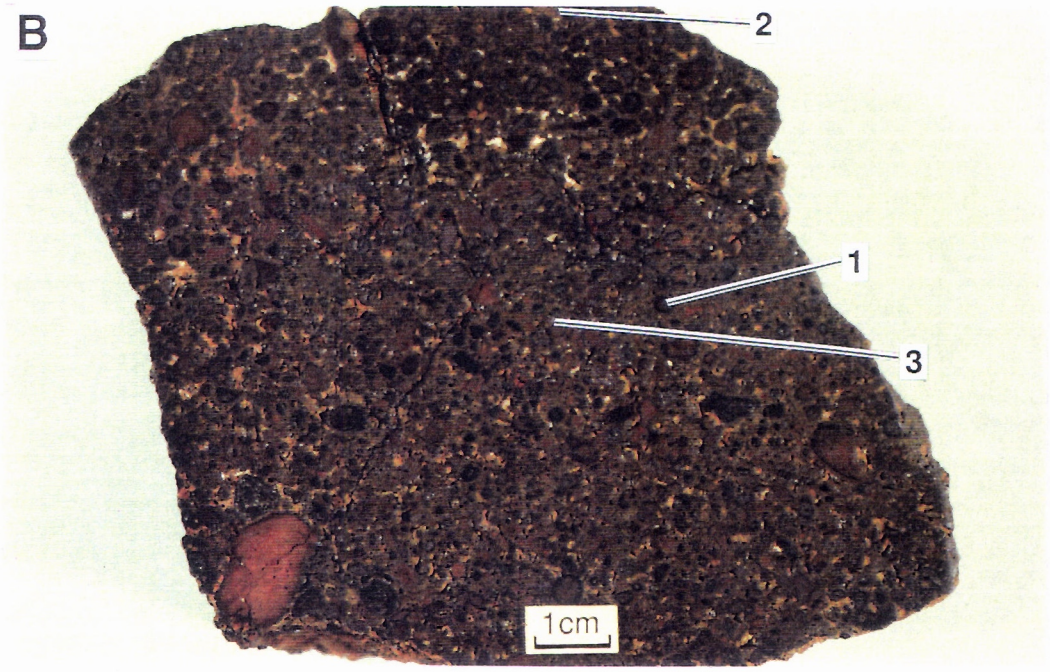

Fig. 33B. Slice through an Fe-rich oolitic duricrust showing ooliths (1) and lithic fragments (2) set in a sandy clay matrix (3). Sample 07-1390.

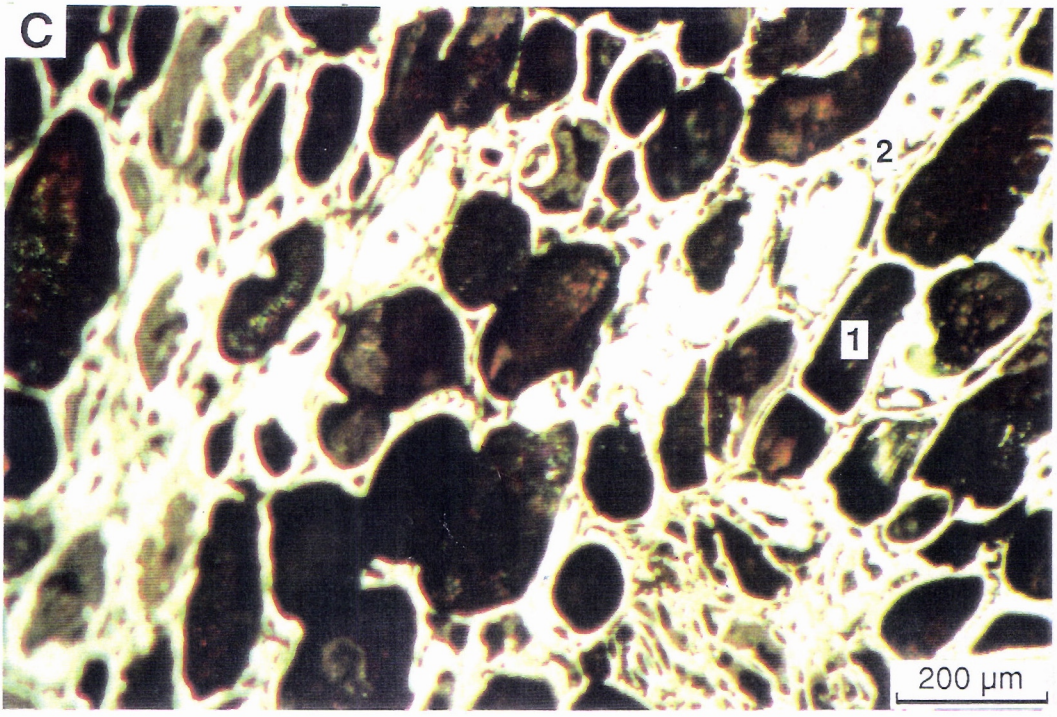

Fig. 33C. Polished section of part of an oolith in the Fe-rich nodular duricrust (shown above) showing slightly ferruginized charcoal fragments (1) within a goethite-rich core. Sample 07-1390.

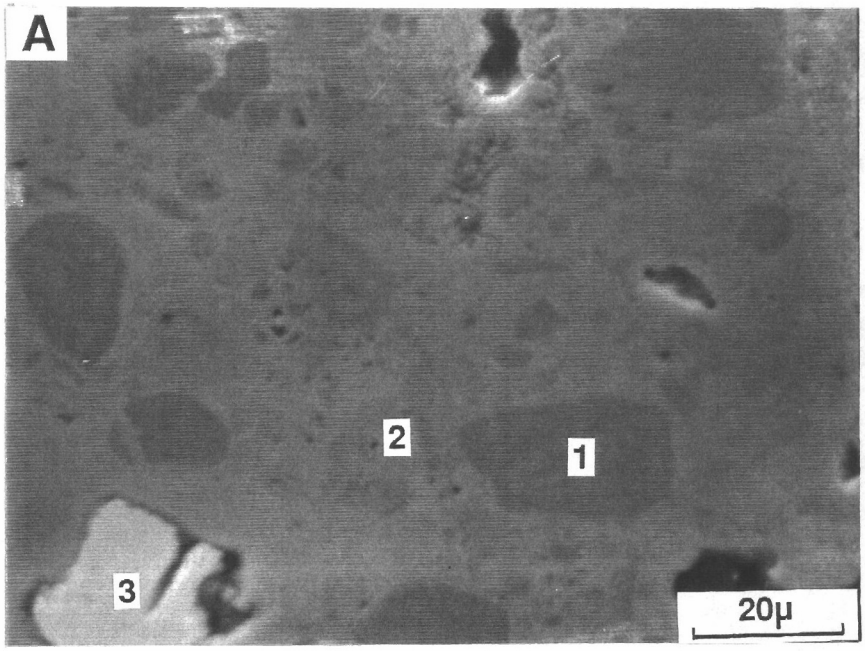

Fig. 34A. Scaning electron photomicrograph of part of a nodule in an Fe-rich nodular duricrust showing a weathered ilmenite grain (1) in a hematite-rich core (2). Barite grain (3) occurs in a void. Sample 07-0825.

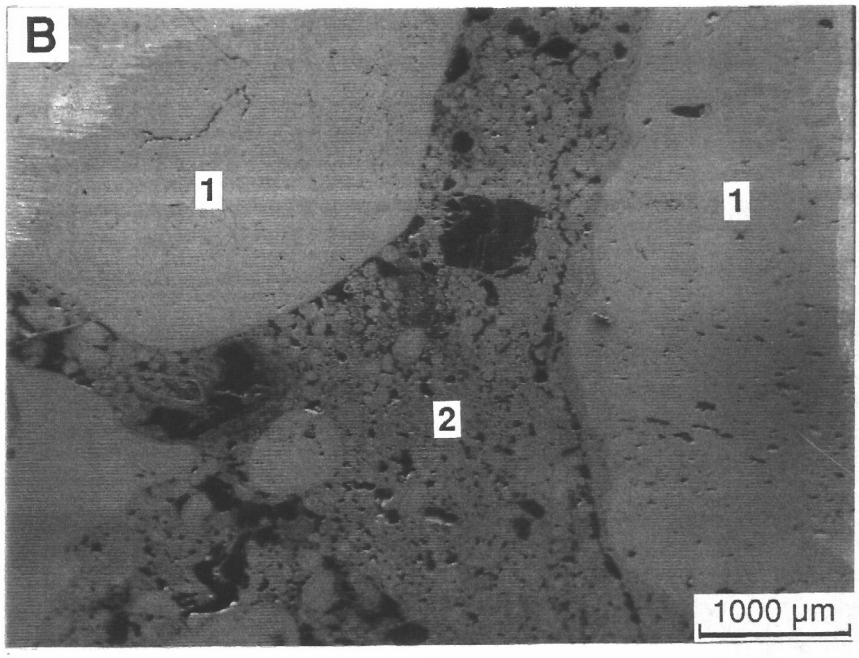

Fig. 34B. Low magnification scanning electron photomicrograph of parts of an Fe-rich duricrust showing nodules (1) set in a Ti-rich oolitic matrix. (2) Sample 07-0922.

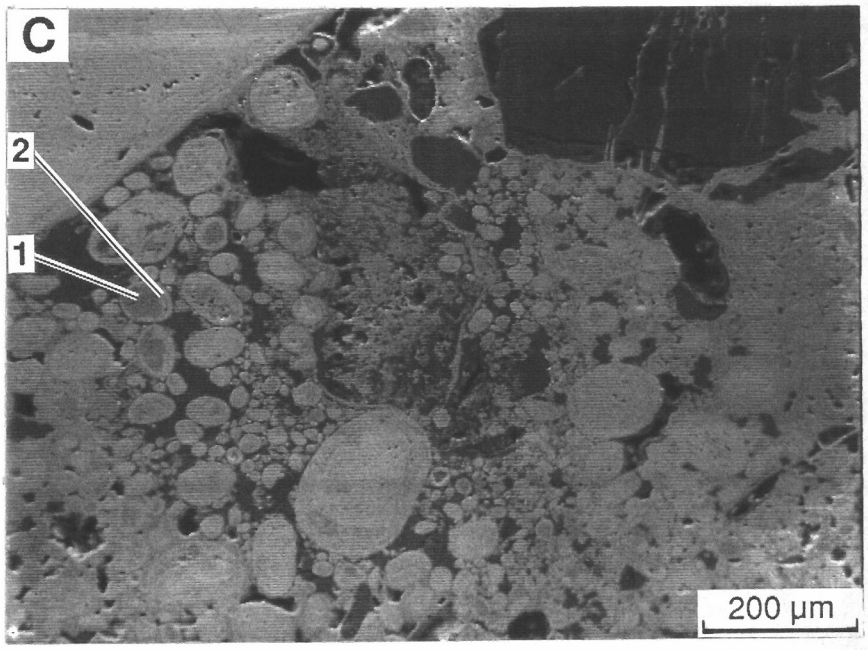

Fig. 34C. High magnification scanning electron photomicrograph of the matrix shown in Fig. 34B. The dark cores of ooliths are Ti-rich (1) and the light areas are Fe-rich (2).

The matrix has consistent characteristics with numerous cavities showing dissolution to the stage where only nodules are left with no matrix. Cavities generally contain small quartz grains. The fabric and mineralogy of the matrix is very similar to the weak red areas of nodules. Occasionally, Ti- and Fe-rich ooliths (2-40 μm) were seen concentrated in the matrix (Fig. 34B), apparently having crystallized from solution. The dark cores of the ooliths are Ti-rich and the light areas are Fe-rich.

Oolitic duricrusts shown in Fig. 33B have abundant hematite-goethite rich reddish black (5 R 2.5/1, dry) magnetic ooliths separated by a very small amount of weak red (5 R 4/3, dry) matrix. A few pisoliths up to 5 mm in diameter are also present. Several irregular to angular lithic fragments of variable degree of ferruginization occur in the matrix. In polished sections, *pseudomorphed wood fragments* are conspicuous and occur in a finely crystalline matrix of hematite and goethite (Fig. 33C). In the ooliths, many pieces of wood are replaced by Fe oxides so completely, that in sections the cell structures can readily be seen.

The cores of ooliths are weak red which are further ferruginized to give rims of reddish-black colours. A similar process of Fe enrichment was seen in nodular duricrust and is described above. Ooliths have multiple thin light grey/dark grey cutans, which are a series of depositional layers usually of goethite. Cutans show at least three generations of goethite.

Goethite which has in-filled irregularly-shaped voids is common and there are rare small (0.5 mm) quartz grains.

The most characteristic features of Fe-rich durcrists are:

- The boundaries between nodules/ooliths and matrix are not well defined in sliced surfaces, despite the pebbly appearance of weathered surfaces
- The matrix and nodule compositions are not significantly different and both are Fe-rich.
- The volume of matrix between the nodules is small.
- Nodules generally lack cutans.
- Microscopic examination and XRD suggest the absence of clay minerals and gibbsite.
- Weathered ilmenite grains and slightly-ferruginized charcoal fragments commonly occur within the ooliths.

7.3 Fabric Development

Based upon their fabrics, possible processes involved in the formation of the Fe-rich duricrusts may be explained by two alternative scenarios:

(i) The duricrust had originally a weak red/dusky red uniform matrix which has been modified by enrichment of Fe under appropriate conditions to give rise to reddish black nodules. Enrichment of Fe evolved into three discrete facies: pale weak red, weak red/dusky red or reddish black. The enrichment of weak red areas began along cracks or at the borders and proceeded inwards to give reddish-black grains containing isolated weak red areas and finally reddish-black nodules.

(ii) The duricrust originally had reddish-black nodules which have been weathered/leached out to give a matrix of pale red/weak red colours. Reddish-black nodules split up by leaching into a weak red matrix retaining the same facies. The latter are thus residues of the original reddish-

black nodules. Leaching necessitates dissolution of Fe constituents. Voids developed by leaching serve as secondary "reception" structures of highly crystalline goethite.

7.4 Mineralogy and Aluminium Substitution in Fe-Oxides

The mineralogical compositions of Fe-rich duricrusts and Al substitution of their Fe-oxides are given in Tables 9 and 10. Hematite, goethite, and maghemite are the major minerals and are present in all the samples. Rutile and anatase, weathering products of ilmenite, are present in all samples and range from 1 to 9%. However, pseudorutile identified petrographically was not detected by XRD. Kaolinite and gibbsite are either absent or present in trace amounts. Talc was recorded in two samples. Quartz occurs in small amounts.

A range in the ratio of hematite/hematite + goethite (0.35-0.84) indicates variable amounts of hematite and goethite in samples. Hematite is dominant in nodular duricrusts and goethite in oolitic duricrust. This variation may reflect conditions during Fe oxide formation. The relative concentrations of goethite and hematite in pedogenic environments are strongly influenced by the initial valence of the Fe source and the concentration of Fe in solution, and factors such as temperature, moisture activity, pH, Eh, presence of organic matter, and the ionic environment – including the activity of Al in soil solution (Schwertmann, 1985). Low temperature, high water activity, and high organic matter concentrations favour goethite formation. Bushfires commonly convert goethite to hematite by locally heating exposed soils or duricrust at temperatures up to 600-800° C. In the intimate presence of organic matter under such conditions, goethite may transform to highly magnetic Fe-oxide – maghemite (Schwertmann, 1985, Anand and Gilkes, 1987). Alternatively, hematite may form from goethite by dissolution and reprecipitation under appropriate conditions (Schwertmann, 1985).

X-ray diffraction studies of Fe-rich duricrusts show that the goethite generally has a low degree of Al substitution (3-10 mole%) and that it is even lower in hematite and maghemite. By contrast, goethites of duricrust/loose pisoliths and nodules low in Fe from the North Pit and Meatoa areas contain much higher levels of Al substitution (19-26 mole%). Fitzpatrick and Schwertmann (1982) reported that goethites formed by absolute accumulation of Fe contain low Al substitution (<10 mole %). They further concluded from their study of goethites from different environments, that low Al substitution in goethite is characteristic of hydromorphic environments, while substitution above 15 mole % is typically of highly-weathered, non-hydromorphic environments. These results suggest that goethites in Fe-rich duricrusts are formed by absolute accumulation of Fe. This is discussed in detail in section 7.6.

7.5 Geochemistry

The chemical composition of bulk samples of Fe-rich duricrust is given in Table 11. These are characterized by high concentrations of Fe_2O_3 and low concentrations of SiO_2 and Al_2O_3. Electron microprobe analysis of nodules and matrix shows that both are Fe-rich and that the composition of internodular matrix is not significantly different from that of the nodules (Table 12). Small concentrations of Al, both in the matrix and nodules of iron-rich duricrusts, further confirm the low degree of Al substitution in Fe oxides. Similar results were obtained from XRD data.

Analysis of a weathered ilmenite grain within a nodule shows the presence of Ti-rich minerals. One spot analysis of a mixture of hematite and goethite shows high values of Ti which probably occurs as coatings or substitutes for Fe^{3+} in Fe oxides.

Fe-rich duricrusts show large ranges in values of Mn, Cr, V, Zn, Ni, Co, As, Sb, and Ga. This distribution may be controlled by the nature of bedrock; however, as mentioned above, bedrock control is presently inadequate for this purpose. High values of Cr are accompanied by moderate values of Ni and Co suggesting an ultramafic origin for some samples. Arsenic and Sb values reach 340 and 72 ppm

Table 9 Semi-quantitative mineralogy (wt.%) of Fe-rich duricrusts

Sample No.	Type	Hematite	Goethite	Maghemite	Kaolinite	Quartz	Rutile	Anatase	Talc	Gibbsite	Hm/Hm+Gt
07-0825	Nodular LT 224	53	21	10	Tr	1	7	2	0	Tr	0.72
07-0828	Nodular LT 224	32	38	12	Tr	5	0	0	0	Tr	0.46
07-0921	Nodular LT 224	35	30	12	Tr	2	4	2	0	Tr	0.54
07-0922	Nodular LT 224	70	13	Tr	Tr	3	6	4	0	Tr	0.84
07-1314	Nodular LT 224	44	20	18	0	4	1	2	0	3	0.69
07-1344	Nodular LT 224	56	22	8	0	5	2	4	0	0	0.72
07-1378	Nodular LT 224	52	20	17	0	2	1	5	<1	0	0.72
07-1390	Oolitic LT 221	24	45	15	0	5	0	1	<2	0	0.35

0 = below detection limit
Tr = traces
Hm = hematite
Gt = goethite

Table 10. Al substitution in goethite, hematite, and maghemite of some Fe-rich lateritic duricrusts

Sample No.	Type	Goethite (mole % Al)	Hematite (mole % Al)	Maghemite (mole % Al)
07-0825	Nodular LT 224	4	4	2
07-0828	Nodular LT 224	3	4	3
07-0921	Nodular LT 224	9	6	4
07-0922	Nodular LT 224	10	5	3
07-1314	Nodular LT 224	9	6	4
07-1344	Nodular LT 224	6	5	4
07-1378	Nodular LT 224	9	6	0
07-1390	Oolitic LT 221	4	0	0

TABLE 11. Chemical analyses of some Fe-rich duricrusts.

Sample	07-0825	07-0828	07-0921	07-0922	07-1314	07-1344	07-1378	07-1390
Type	Nodular	Nodular	Nodular	Nodular	Nodular	Nodular	Nodular	Oolitic
Element/ Oxide								
Wt %								
SiO_2	5.7	7.2	7.8	4.7	4.5	6.5	2.0	5.7
Al_2O_3	3.99	6.03	9.11	4.21	7.10	4.91	4.97	4.67
Fe_2O_3	78.90	75.90	69.40	78.10	76.20	76.92	82.42	79.03
MgO	0.064	0.142	0.135	0.080	0.056	0.042	0.029	0.056
CaO	0.030	0.036	0.047	0.122	0.032	0.088	0.046	0.040
Na_2O	<0.007	<0.007	0.013	0.017	0.013	0.013	0.013	0.014
K_2O	<0.06	<0.06	<0.06	<0.06	<0.06	<0.06	<0.06	<0.06
TiO_2	8.040	1.012	5.621	9.541	2.519	5.688	4.421	1.020
ppm								
Mn	218	1265	253	326	1432	255	493	479
Cr	1031	16700	7701	3550	12600	917	10100	2849
V	3884	410	1823	3498	1486	2326	1758	760
Cu	13	14	22	26	17	25	15	11
Pb	9	18	6	16	10	<2	<2	11
Zn	15	50	5	3	55	44	60	20
Ni	<4	1820	94	44	330	42	190	590
Co	10	135	24	14	78	20	50	210
As	66	74	340	340	68	16	<2	11
Sb	11	<2	64	72	2	<2	<2	<2
Bi	<2	<2	4	<2	>2	3	2	>2
Mo	9	7	7	9	3	9	5	3
Ag	<0.1	0.6	<0.1	0.5	0.3	<0.1	<0.1	<0.1
Sn	6	<2	3	6	<2	6	7	4
Ge	<4	<4	4	<4	<2	<2	<2	<2
Ga	155	30	96	100	90	135	100	18
W	54	6	22	10	<4	14	<4	4
Ba	837	272	1277	71	142	766	56	672
Zr	108	38	97	73	68	68	26	21
Nb	34	11	26	34	9	19	18	<2
Au	0.009	0.004	0.013	0.130	<0.001	<0.001	<0.001	<0.001

Table 12. Electron-microprobe analysis of components within some selected Fe-rich duricrusts

Sample No.	Components	wt %						
		SiO_2	Al_2O_3	Fe_2O_3	TiO_2	MgO	CaO	TOTAL
07-1314	reddish-	2.05	1.64	88.26	0.15	0.03	0.01	92.14
	black core	2.09	1.60	88.86	0.37	0.06	0.01	92.99
	weak red	1.00	2.97	83.04	1.35	0.01	0.02	88.39
	matrix	1.41	2.43	80.95	1.08	0.03	0.01	85.91
		1.05	1.85	80.16	6.89	0.05	0.01	90.01
07-921	reddish-	1.76	1.23	87.89	1.41	0.03	0.01	92.33
	black core	1.35	1.11	89.34	1.63	0.05	0.01	93.49
	weak red	2.10	1.61	82.56	1.21	0.03	0.01	87.52
	matrix	2.08	1.50	84.36	0.89	0.06	0.03	88.92

respectively. Gold values, however, are low, in the ppb range. Copper, Pb, Bi, Sn, and Ge occur in small amounts.

7.6 Genesis

Genesis of Fe-rich duricrust in the Lawlers district may be explained by two alternate scenarios. Lateritic processes have produced the Fe-rich duricrust by the *in situ* deep weathering of mafic and ultramafic rocks, resulting in a relative accumulation of Fe. Alternatively, the Fe-rich duricrusts may have been produced by the absolute accumulation of Fe in ancient valley floors, in this manner receiving a considerable contribution of Fe in solution from upland areas of that time. The occurrence of Fe-rich duricrust on present topographically high areas may be explained by the process of relief inversion. These two hypotheses are now discussed.

Hypothesis 1:
If the Fe-rich duricrust is residuum, it might be expected that part of its gross chemistry would relate to that of the parent rock. Experience has shown that concentrations of Cr, Co, and Ni can sometimes be used to discriminate the duricrusts derived from mafic and ultramafic rocks. Our data suggest that these Fe-rich duricrusts do have a geochemical affinity with mafic and ultramafic Fe-rich bedrocks. Those rich in Cr, Ni, and Co are likely to be derived from the weathering of ultramafic rocks whereas those containing relatively-low levels of these elements are likely to have a mafic origin. Ilmenite and weathered ilmenite grains in the nodules are probably inherited from Ti-rich parent materials which further suggest their origin from Ti-rich bedrock such as gabbros. However, Ti appears to be fairly mobile as indicated by the presence of Ti coatings around nodules and Ti-rich ooliths in the matrix which may indicate its introduction from external sources.

Hypothesis 2:
The fabric and Al substitution of goethite in Fe-rich duricrust does not fully support its origin as a residuum. The goethites show little Al substitution, so that they must have grown in an environment almost free of accessible Al. This is supported by the observation that neither kaolinite nor gibbsite were detected in appreciable amounts. By contrast, the goethites from loose pisoliths and from nodular duricrust (low in Fe) from the North Pit area, Agnew gravel pit, and the Meatoa areas have higher Al substitution (17-26 mole%) (Anand *et al.*, 1989; and this report). Fitzpatrick (1988) interpreted from his study that the degree of Al substitution in goethite structure can be used to differentiate between the older "iron segregations" formed by the relative accumulation of Fe (>15 mole% Al OOH in goethite) and relatively younger "iron segregations" formed primarily by absolute accumulation of Fe (< 10 mole% Al OOH in goethite). This suggests that Fe-rich duricrusts in the Lawlers district are formed by absolute accumulation of Fe. Iron segregations formed by absolute accumulation of Fe in ancient lowland positions were reported from South Australia by Maud (1972) and Milnes *et al.* (1985) and contain goethite of low Al substitution (<10 mole%). Fe-rich duricrusts in the Lawlers district occur on ridge crests so that their formation is a paradox and may be explained by the following. Ridge crest duricrusts are remnants of what was once an ancient valley or depression, into which sediments accumulated. The valleys became favoured sites for the precipitation of Fe oxides from groundwater. In this regard, ridge crests and their Fe-rich duricrusts could be an expression of a complex series of erosional, aggradational and weathering events. Relief inversion in the Lawlers district may have occurred and duricrust-covered valleys may have become ridges (Fig. 35). Many examples of relief inversion have been provided in the literature, some including laterites which occur as long sinuous ridges and may have formed as valley laterites (Maignien, 1966, Goudie, 1973, Ollier *et al.*, 1988). Iron may have been derived by weathering processes from ancient upland positions and transported laterally to valley floors. The dissolved ferrous iron is subsequently precipitated and oxidized or oxidized and precipitated. In general, goethite and hematite form where oxidation precedes hydrolysis, when hydrolysis and precipitation occur before oxidation lepidocrocite and maghemite may occur (Taylor *et al.*, 1974a). This process results in the formation of hard Fe-rich duricrust. The valley floors capped with Fe-rich duricrust are the most

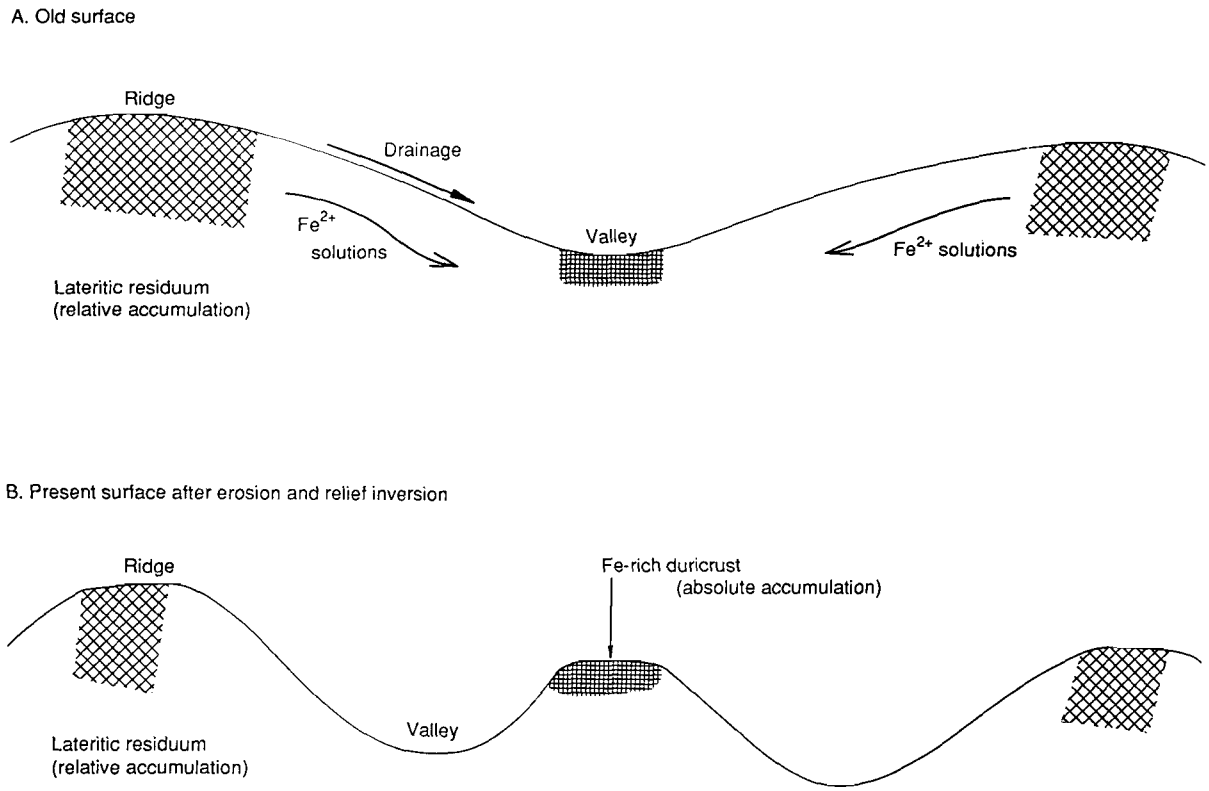

Fig. 35. The development of Fe-rich duricrust by absolute accumulation of Fe and relief inversion.

indurated, and as they are then resistant to erosion, rivers tend to erode the softer material, leaving the former valleys as the ridges.

On the available evidence, either of the two mechanisms described above could have been responsible for the formation of Fe-rich duricrusts. The lack of knowledge on bedrock underneath the duricrusts does not allow us to make conclusions about its influence on the genesis of Fe-rich duricrusts. The geochemistry of duricrusts suggests that their component materials were derived from both the mafic and ultramafic rocks. However, it is the factors which affect the Al substitution in pedogenic environments which provided a basis for the interpretation of conditions under which Fe-rich duricrusts are formed. Low Al substitution in goethites suggests that Fe-rich duricrusts are formed by absolute accumulation of Fe. Iron impregnated the soils/sediments in ancient valleys or drainage depressions which now occur as crests in the present landscape because of inversion of relief.

8.0 PRELIMINARY INVESTIGATIONS OF THE SITING AND BONDING OF ELEMENTS AND DISPERSION PROCESSES

8.1 Introduction

The objectives of this section of the research are to establish (a) the morphology of Au; (b) the siting and bonding of Au and the ore associated elements within selected samples from within laterite geochemical anomalies in order to establish any relationships of these elements to iron oxides, clay minerals or carbonates; and (c) to complement petrographic studies on the types of nodules in lateritic environments. This research should lead to an improvement of geochemical exploration sampling methods, a better understanding of the mobility and behaviour of Au and chalcophile elements in weathering profiles, provide information on whether anomalies may exist from which Au is leached, but chalcophile elements remain; and aid the understanding of the genesis of nodules and the accompanying dispersion processes.

Preliminary investigations on the above topics were made on geochemically anomalous laterite samples collected from the North Pit and Turret areas.

8.2 North Pit Area

Gold-rich lateritic material was examined from drill hole 783 which occurs on line 9900N (local grid). The local regolith setting together with cross-sections through the regolith units is given in Anand et al. (April, 1989). The lateritic weathering profile at this location is about 40 m thick and distinct horizons from drill spoil have been recognized. At the base of the profile, the mafic lithologies are altered to kaolinite, smectite, and goethite to produce the saprolite. The saprolite grades into ferruginized saprolite/mottled saprolite comprising goethite, kaolinite, and quartz. The residual laterite horizon is about 6 m thick and consists of loose nodules and nodular duricrust, overlying ferruginized saprolite. The duricrust comprises of kaolinite, hematite, goethite, gibbsite, maghemite, and quartz. The residual laterite profile is overlain by a thin layer of transported loose lateritic nodules (2 m thick) and hardpanized colluvium of variable mineralogy.

8.2.1 Morphology and Composition of Gold

The lateritic nodules examined are 10-20 mm in size, subrounded and consist of multicoloured cores ranging from yellowish brown to reddish brown. These nodules have thin greenish-yellow goethite-rich cutans. Kaolinite, hematite, and goethite are the main minerals; gibbsite, maghemite, and quartz are less abundant. Cores of the nodules have compositions of 56.0-82.4% Fe_2O_3, 2.5-26.0% SiO_2, and 3.1-26.2% Al_2O_3. Iron is mainly present as goethite and hematite, whereas Al and Si are present as kaolinite. The bulk sample from which these nodules were taken contains 17 ppm Au.

The Au observed in the nodules occurs as irregular subhedral to anhedral crystals, and as delicate wire forms in voids or cracks, which are either filled with kaolinite and goethite or are empty. Gold crystals also commonly occur on the surfaces of residual or colloform goethite and range in size from 15 to 80 μm (Fig. 36). Under higher magnification some of these Au crystals show dissolution features and surface pitting. Both small (5-10 μm) and large voids (50-100 μm) are observed in the cores of nodules and in the gold crystals. Occasionally, these voids may be connected to each other, creating bigger voids which are filled with Au or highly crystalline kaolinite and goethite. Energy dispersive microprobe analysis shows that Ag in the Au grains is below the detection limit of the technique (~1%). Such a low Ag content is compatible with other observations on secondary Au and leached primary Au (Freyssinet and Butt, 1988a, b).

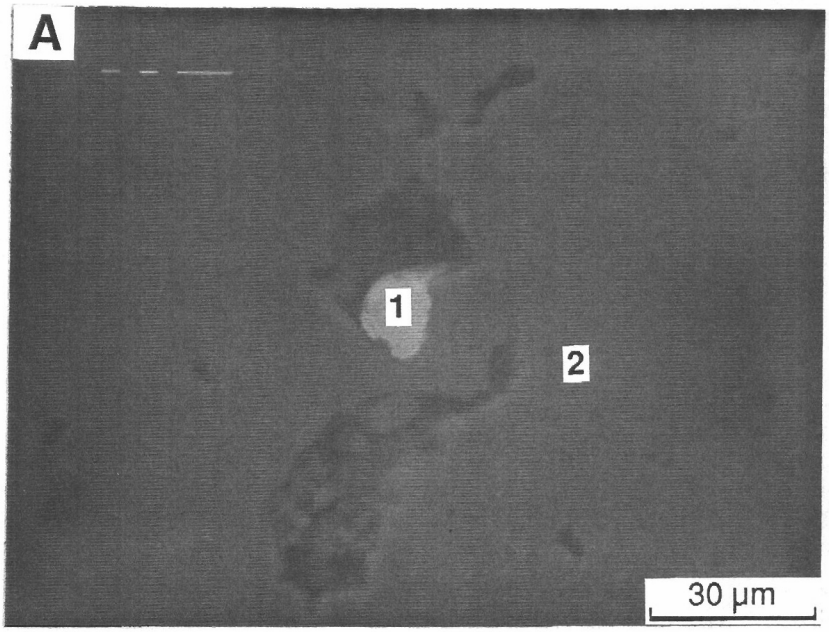

Fig. 36A. Scanning electron photomicrograph of part of a lateritic nodule showing a subhedral crystal of Au (1) in a void. Matrix of the nodule is Fe-rich which is a mixture of hematite and goethite (2). Location 9899N, 5296E N pit (Sample 07-0878).

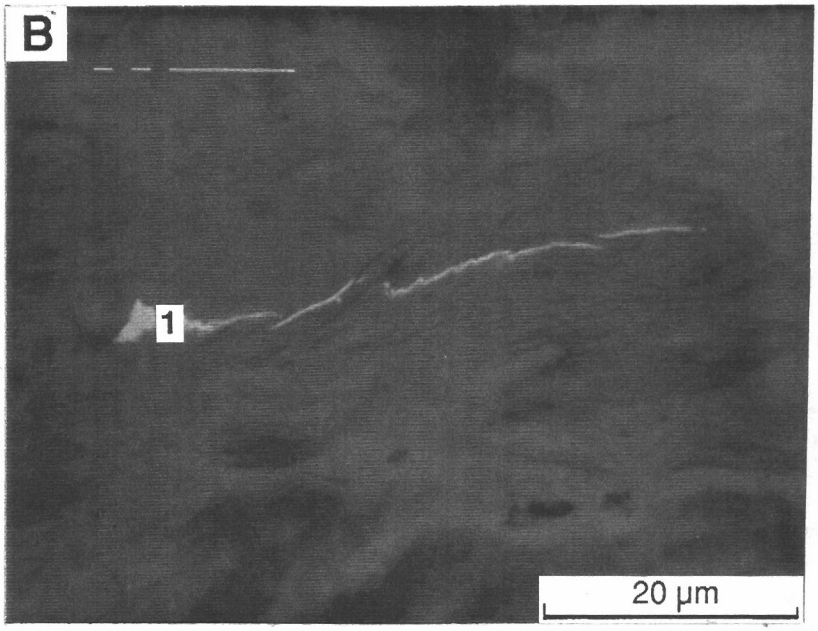

Fig. 36B. Scanning electron photomicrograph of part of a lateritic nodule showing wire shaped crystals of Au (1) attached to the goethite-rich surface, location 9899N, 5296E North Pit. Sample 07-0878.

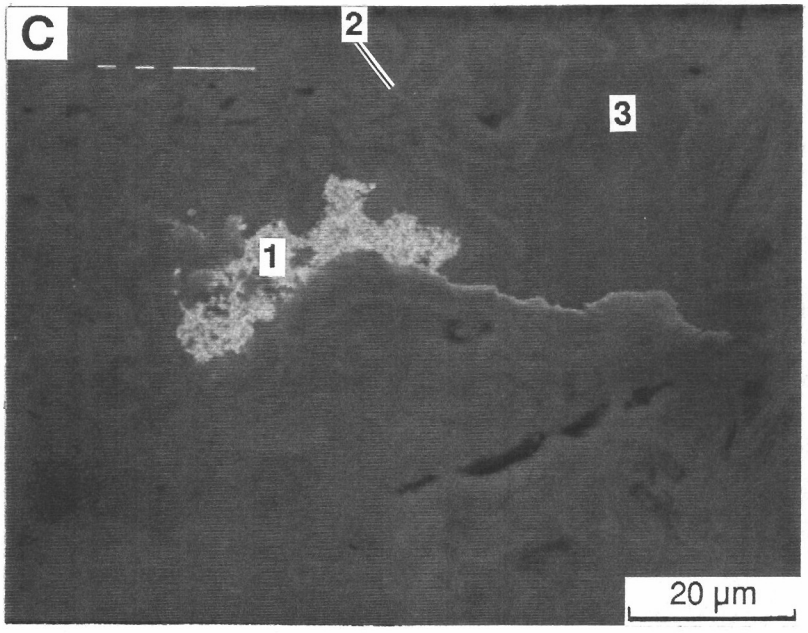

Fig. 36C. Scanning electron photomicrograph of part of a nodule showing dendritic form of Au (1) attached to the goethite-rich surface. The Au crystal shows dissolution features. Light areas of matrix are Fe-rich (2), dark areas are Al-Si rich (3), location 9899N 5296E N pit. Sample 07-0878.

The close association of Au and Fe-oxides, morphology, and geochemistry (low Ag) of Au indicates that the Au analysed is dominantly secondary, having been remobilized and precipitated (Mann, 1984). During weathering, both the crystal morphology and composition will change as primary Au is dissolved and reprecipitated as secondary crystals. The physico-chemical conditions required for the dissolution of Au have been studied intensively (Boyle, 1979). The most common ionic species are Au^{+} and Au^{3+}. Ions in these oxidation states are unstable in solution. To remain in solution, the ions need appropriate ligands as well as suitable pH and Eh conditions. Possible ligand donor ions are OH^{-}, I^{-}, Br^{-}, Cl^{-}, SO_3^{2-}, $S_2O_3^{2-}$ and SO_4^{2-} (Boyle, 1979), but few of these anions occur in percolating solutions under semi-arid conditions. In the semi-arid environment of Western Australia, Au is thought to have been remobilized and precipitated during saline groundwaters conditions and reprecipitated by supergene processes (Mann, 1984; Gray, 1988). Processes operating during the formation of the lateritic nodules could also have contributed to dissolution of Au particles. For example, the epigenetic replacement of kaolinite by hematite in the ferruginous zone involves the dissolution of kaolinite and the release of protons which may contribute to the dissolution of Au particles (Colin *et al.* 1989).

8.2.2 Other Elements

Arsenic was found to range from 900 to 4400 ppm and was strongly associated with goethite/hematite. Kaolinite-rich areas of nodules generally contained small amounts of As. The distribution of Cu (100 to 1500 ppm) within nodules was erratic and tends to dominate the kaolinite-rich areas. The surface adsorption of Cu by kaolinites has also been noted by Farrah and Pickering (1976) and McBride (1978). However, McLaren and Crawford (1973) give 120 ppm for kaolinite as the maximum Cu adsorption calculated with Langmuir equations at pH 5.5. The much higher values found here permit us to assume that Cu is mainly in the lattice and not adsorbed on the surface of kaolinite. This means that the metal is not likely to be released by partial or weak extraction techniques. Bismuth and Sb were below the detection limit (~40 ppm) of the microprobe techniques used.

8.3 Turret Area

The morphology of Au and siting and bonding of elements were also investigated on laterite samples from Turret area. A total of 28 samples of lateritic residuum and saprolite from three holes (T271A, T274, T327) were collected. In these holes, lateritic residuum up to 7 m thick is overlain by a 1-3 m layer gravelly colluvium. The residual laterite generally passes downwards into saprolite/collapsed saprolite which is often ferruginized. The pisoliths/nodules are dark reddish brown/black to red, rounded to subrounded, with a size range of 3-15 mm. The cutans are greenish and are less than 1 mm thick. The saprolite and lateritic residuum are dominated by goethite and talc. Kaolinite and hematite are either absent or present in very small amounts. These samples contain high concentrations of Cr (to 1.4%), Ni (to 6900 ppm) and Mg (to 10%). The mineralogy and geochemistry indicate that these three weathering profiles are ultramafic in origin.

8.3.1 Morphology and Composition of Gold

Gold ranges in values from 0.005 to 8.0 ppm for whole samples studied, however, visible Au was not detected under SEM and optical microscopy. Research on this topic is continuing.

8.3.2 Other Elements

Preliminary results on lateritic pisoliths show Ba occurring as laths of barite in their cutans (Fig. 37A). The dark areas of cutans shown in Fig. 37A are Al- and Si-rich, whereas the light areas are Fe-rich. The cores of pisoliths are Fe-rich with some Cr and Mn. One possible explanation is that Ba occurs as secondary barite formed by the precipitation of evaporite-derived sulphate in groundwaters.

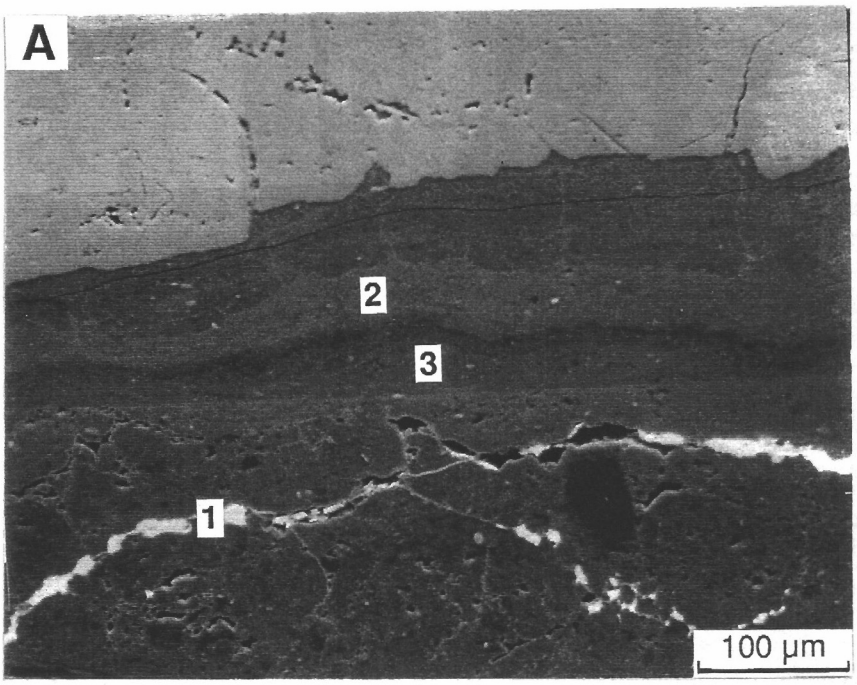

Fig. 37A. Scanning electron photomicrograph of part of a lateritic pisolith showing barite grains (1) in cracks of cutans. Alternative light (2) and dark areas (3) in cutans are caused by variation in Fe, Al/Si contents. Light areas are Fe-rich, dark areas are Al-Si rich. Location Turret area, hole No. T271A. Sample 07-1295.

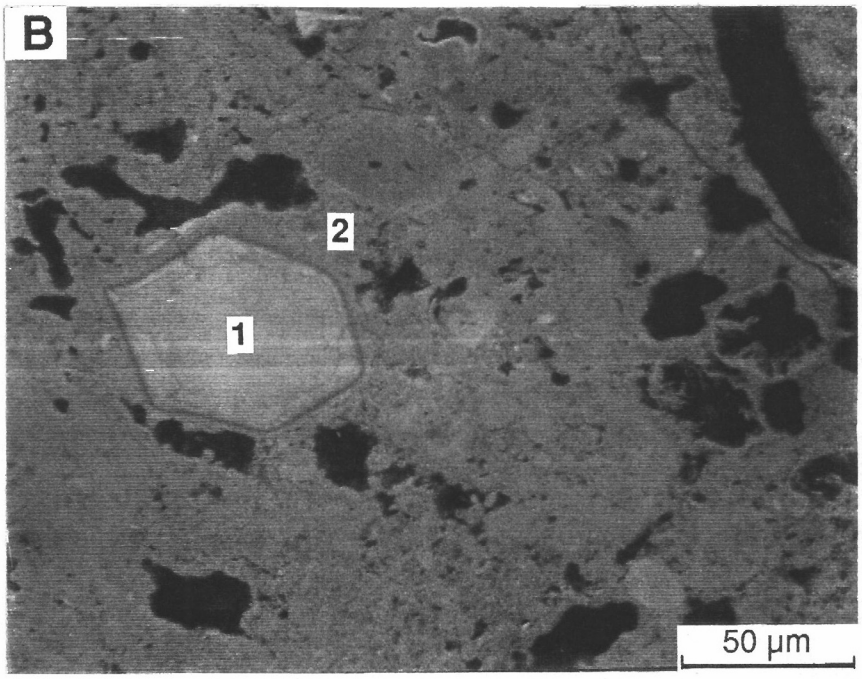

Fig. 37B. Scanning electron photomicrograph of part of a lateritic pisolith showing a hexagonal chromite grain (1) in an Fe-rich core (2). Black areas are voids, location Turret area, hole No. T271A. Sample 07-1295.

Investigation of a barite-containing pisolith shows that Cr mainly occurs as chromite in the Fe-rich core (Fig. 37B). The core of this pisolith apparently formed from saprolite preserving a primary chromite grain which provides an indication of ultramafic lithology underneath. Arsenic, V, and Mn appear to be strongly associated with goethite and do not occur as discrete mineral species.

9.0 CONCLUSIONS

- The regolith and landforms of the Meatoa, Brilliant, and Agnew-McCaffery areas are related to the complex geomorphic history, including deep lateritic weathering and subsequent erosion and deposition.

- At Meatoa, dismantling of the lateritic residuum from the areas of low hilly terrain has resulted in the burial of partly-truncated and/or complete laterite profiles in the adjacent lower slope areas.

- The nature and origin of lag gravels and soils are related to regolith substrate and processes of erosion and deposition. Morphological, mineralogical, and geochemical characteristics of lag gravels allow differentiation between the various lag types.

- The morphology, mineralogy, and geochemistry of the lag gravels at Meatoa can be understood in terms of their origin. Anomalous levels of As, Pb, and to a lesser degree W, in the lag of lateritic lithic fragments and lateritic lag are not supported by high values of Au.

- Existing evidence suggests that the Fe-rich duricrusts from various locations in the Lawlers district are probably formed by absolute accumulation of Fe originally impregnating the soils/sediments in previously low lying areas. Their present high landscape position could result from inversion of relief.

- The degree of Al substitution in goethite can be used to predict the weathering status of regolith materials and the environments in which they have formed.

- Idealized regolith/landform models for the Brilliant, Agnew-McCaffery, and Meatoa areas have been established to predict regolith relationships in comparable areas elsewhere.

- Hardpan has developed in both *in situ* regolith and detritus, resulting from the erosional modification of the old surface.

- The understanding of regolith relationships has provided the framework for geochemical sampling at Lawlers and in other districts of similar terrain type.

- The distribution of clay minerals in the landscape suggests that the present climate does not favour the transformation of smectite to kaolinite and the preservation of smectite under present environmental conditions may be evidence for paleoclimatic changes from warm humid to arid claimate in Yilgarn Block.

- Preliminary investigation on morphology of Au suggests that Au from anomalous laterite samples in the North Pit area is mainly secondary, having been remobilized and precipitated during weathering. Arsenic appears to be strongly associated with goethite and Cu with kaolinite.

10.0 OUTLOOK

- Regolith/landform relationships at the Meatoa, Brilliant, and Agnew-McCaffery areas are now adequately understood. These relationships will be extrapolated over the Lawlers district.

- Further work on the origin of the Fe-rich duricrusts will focus on the alternative hypotheses of bedrock control versus paleoenvironment.

- Research into the siting and bonding of Au and ore-associated elements will continue in order to investigate the dispersion processes.

- Some trial applications of multivariate data interpretational procedures, in collaboration with GEOCHEMEX, will be undertaken on the Lawlers laterite exploration data.

- Relationships between bedrock composition and overlying laterite will be investigated, provided an area can be chosen for which a suitably-controlled solid bedrock geological map is available.

11.0 ACKNOWLEDGEMENTS

We wish to thank the Management and Staff of Forsayth (Lawlers) and Geochemex Australia for their co-operation and collaboration, as well as the hospitality provided by Forsayth in the field. This research has been carried out under the Lawlers collaborative research agreement between CSIRO and Geochemex, sponsored by Forsayth NL as an adjunct to research activities of the CSIRO/AMIRA Laterite Geochemistry Project P240.

Sample preparation was carried out by Ms Angela Janes under supervision by Mr John Crabb. The XRD analyses were performed by Mr M.K.W. Hart. Polished sections were prepared by Mr A.G. Bowyer. Assistance on the SEM and Cameca microprobe was given by Mr B.W. Robinson and G. Burkhalter.

Mr John Perdrix maintained the geochemical database and assisted with checking the final document. Typing to the tight deadline was admirably carried out by Ms Jenny Porter. Diagrams were drafted by Mr Colin Steel.

12.0 REFERENCES

Ambrosi, J.P., Nahon, D. and Herbillon, A.J., 1986. A study of the epigenetic replacement of kaolinite by hematite in laterite - petrographical evidences and a discussion on the mechanism involved. *Geoderma*, **37**, 283-294.

Anand, R.R. and Gilkes, R.J., 1987. Variations in the properties of iron oxides within individual specimens of lateritic duricrust. *Aust. J. Soil. Res.*, **25**, 287-302.

Anand, R.R., Innes, J. and Smith, R.E., April 1989. Research into laterite geochemistry Lawlers District, Western Australia. Progress report to Geochemex Australia and Forsayth Mining Ltd. CSIRO Division of Exploration Geoscience, Restricted Report 22R, 42 pp.

Anand, R.R., Smith, R.E., Innes, J., Churchward, H.M., Perdrix, J.L. and Grunsky, E.C., August 1989. Laterite types and associated ferruginous materials, Yilgarn Block, WA. *Terminology, Classification and Atlas*. CSIRO Division of Exploration Geoscience, Restricted Report 60R (unpaginated).

Boyle, R.W., 1979. The geochemistry of gold and its deposits. *Geol. Surv. Can. Bull.*, **280**, 584 pp.

Butler, I.K., Ewers, A., Birrell, R. and Smith, R.E., 1989. *Results of a landform survey and geochemical exploration programme, Lawlers Area, Western Australia*. Progress report of Geochemex Australia to Forsayth Mining Ltd, February 1989, 66 pp.

Carver, R.N., Chenworth, L.M., Mazzucchelli, R.M., Oates, C.J. and Robins, T.W., 1987. Lag - A geochemical sampling medium for arid regions. *J. Geochem. Explor.*, **28**, 183-189.

Colin, R., Lecomte, P. and Boulange, B., 1989. Dissolution features of gold particles in a lateritic profile at Dondo Mobi, Gabon. *Geoderma*, **45**, 241-250.

Davy, R., 1979. A study of laterite profiles in relation to bed rock in the Darling Range near Perth, W.A. Geological Survey of Western Australia, Report 8, 87p.

Dixon, J.B., 1977. Kaolinite and serpentine group minerals. In: Dixon, J.B. and Weed, S.B. (eds), *Minerals in Soil Environments*, Soil Sci. Soc. Am., Madison, Wisc., 2nd Ed., pp.357-402.

Fankel, J.J. and Bayliss, P., 1966. Ferruginized surface deposits from Natal and Zumland, South Africa. *J. Sediment. Petrol.*, **36**, 193-201.

Farrah, H. and Pickering, W.F., 1976. The sorption of copper by clays. 1. Kaolinite. *Aust. J. Chem.*, **29**, 1167-1176.

Fitzpatrick, R.W., 1988. Iron compounds as indicators of pedogenic processes: examples from the Southern Hemisphere. In: Stucki, J.W., Goodman, B.A. and Schwertmann, V. (eds.), *Iron in Soils and Clay Minerals*, D. Reidel Publishing Company, Tokyo, pp.351-396.

Fitzpatrick, R.W. and Schwertmann, U., 1982. Al-substituted goethite - an indicator of pedogenic and other weathering environments in South Africa. *Geoderma*, **27**, 335-347.

Freyssinet, Ph. and Butt, C.R.M., 1988a. *Morphology and geochemistry of gold in a lateritic profile Beasley Creek, Laverton, Western Australia*. Report to Western Mining Corporation. CSIRO Division of Exploration Geoscience Report MG 60R.

Freyssinet, Ph. and Butt, C.R.M., 1988b. *Morphology and geochemistry of gold in a lateritic profile Bardoc Mine, Western Australia*. Report to Aberfoyle Resources Ltd. CSIRO Division of Exploration Geoscience Report MG 59R.

Goudie, A., 1973. *Duricrusts in Tropical and Sub-Tropical Landscapes. Oxford Research Studies in Geography*, Oxford University Press, London, 174 pp.

Gray, D.G., 1988. *The aqueous chemistry of gold in the weathering environment*. CSIRO Division of Exploration Geoscience Restricted Report EG4R, 65 pp.

Mabbutt, J.A., 1963. Wanderrie Bank: micro-relief patterns in semi-arid Western Australia. *Geol. Soc. Amer. Bull.* **74**, 529-540.

Mabbutt, J.A., 1977. *Desert Landforms, Vol.2*, Australian Nat. Univ. Press, Canberra, 340 pp.

McBride, M.B., 1978. Copper (II) interaction with kaolinite: factors controlling adsorption. *Clays Clay Miner.*, **26**, 101-106.

McLaren, R.B. and Crawford, D.W., 1973. Studies on soil copper. II. The specific adsorption of copper by soils, *J. Soil. Sci.*, 24, 352-443.

Maignien, R., 1966. *Review of Research on Laterites*, Unesco, Natural Resources Research Sc., IV., Paris, 148 pp.

Mann, A.W., 1984. Mobility of gold and silver in lateritic weathering profiles: Some observations from Western Australia. *Econ. Geol.*, **79**, 38-49.

Maud, R.R., 1972. *Geology, Geomorphology and Soils of Central County Hindmarsh (Mount Compass-Milang) South Australia*. Soil publication No.29, CSIRO, Melbourne, Australia, 85 pp.

Milnes, A.R., Bourman, R.P. and Northcote, K.M., 1985. Field relationships of ferricretes and weathered zones in southern South Australia: A contribution to "laterite" studies in Australia. *Aust. J. Soil Res.*, **23**, 441-465.

Muller, J.P. and Bocquier, G., 1986. Dissolution of kaolinites and accumulations of iron oxides in lateritic-ferruginous nodules: mineralogical and microstructural transformations. *Geoderma*, **37**, 113-136.

Nahon, D.B., Colin, R., 1982. Chemical weathering of orthopyroxenes under a lateritic condition. *Amer. J. Sc.*, **282**, 1232-1243.

Ollier, C.D., Chan, R.A., Craig, M.A. and Gibson, D.L., 1988. Aspects of landscape history and regolith in the Kalgoorlie region, Western Australia. *BMR J. Aust. Geol. and Geophys.*, **10**, 309-321.

Schulze, D.G., 1984. The influence of aluminium on iron oxides. VIII. Unit cell dimensions of Al-substituted goethites and estimation of Al from them. *Clays Clay Miner.*, **32**, 36-44.

Schwertman, U., 1985. The effect of pedogenic environments on iron oxide minerals. In: B.A. Stewart (Ed.), *Advances in Soil Science*, Vol. 1, Springer-Verlag, New York, NY, pp.172-196.

Schwertmann, U. and Fechter, H., 1984. The influence of aluminium on iron oxides. XI Aluminium-substituted maghemite in soils and its formation. *Soil Sci. Soc. Am. J.*, **48**, 1462-1463.

Schwertmann, U. and Latham, M., 1986. Properites of iron oxides in some new Caledonian oxisols. *Geoderma*, **39**, 105-123.

Schwertmann, U., Fitzpatrick, R.W. and Roux Le, J., 1977. Al-substitution and differential disorder in soil hematites. *Clays Clay Miner.* **25**, 373-374.

Schwertmann, U., Fitzpatrick, R.W., Taylor, R.M. and Lewis,D.G., 1979. The influence of aluminium on iron oxides. Part II. Preparation and properties of Al-substituted hematites. *Clays Clay Miner.*, **27**, 105-112.

Smith, R.E., 1987. Patterns in laterite geochemistry Mt. Gibson, Western Australia. Progress report of Geochemex Australia to Forsayth NL, December, 37 pp.

Swindale, L.D. and Uehera, G., 1966. Ionic relationships in the pedogenesis of Hawaiian soils. *Soil Sci. Soc. Amer. Proc.* **30**, 726-730.

Taylor, R.M. and Schwertmann, U., 1974. Maghemite in soils and its origins. I. Properties and observations in soil maghemites. *Clay Miner.* **10**, 289-98.

Taylor, R.M. and Schwertmann, U., 1978. The influence of aluminium on iron oxides. I. The influence of Al on Fe oxide formation from the Fe(II) system. *Clays Clay Miner.*, **26**, 373-383.

Tiller, K.G., 1963. Weathering and soil formation in Tasmania with particular reference to several trace elements. *Aust. J. Soil Res.* 1, 74-90.

APPENDICES

Appendix I

Meatoa Lag Samples

Sample	Type	SiO_2	Al_2O_3	Fe_2O_3	MgO	CaO	Na_2O	K_2O	TiO_2
(Laboratory >)		analb	analb	analb	analb	analb	analb	analb	analb
(Method >)		icp	icp	icp	icp	icp	icp	icp	icp
(det. limit >)		(0.2)	(0.04)	(0.03)	(0.004)	(0.007)	(0.007)	(0.06)	(0.003)
07-1310	LG206,203	15.5	3.85	71.77	0.165	0.146	0.014	<0.06	0.615
07-1311	LG203,206	9.4	4.69	76.55	0.063	0.062	0.014	<0.06	1.952
07-1312	LG201,221,103	9.7	7.86	70.76	0.074	0.044	0.013	<0.06	1.206
07-1313	LG221	8.3	12.36	65.54	0.177	0.037	0.013	<0.06	2.202
07-1315	LG100	4.5	7.10	76.20	0.056	0.032	0.013	<0.06	3.003
07-1318	LG221	14.8	16.67	55.92	0.039	0.033	0.012	<0.06	0.829
07-1319	LG201,103,221	15.3	16.17	56.50	0.032	0.036	0.011	<0.06	0.827
07-1320	LG201,103,221	12.0	13.87	64.81	0.034	0.034	0.012	<0.06	0.987
07-1324	LG201,103,221	13.8	13.17	62.15	0.075	0.112	0.084	<0.06	1.512
07-1326	LG201,103,221	12.8	12.49	64.34	0.053	0.040	0.014	<0.06	1.537
07-1328	LG201,103,221	15.2	13.94	61.01	0.046	0.038	0.013	<0.06	1.532
07-1330	LG201,103,221	12.5	12.24	66.90	0.046	0.045	0.014	<0.06	1.559
07-1332	LG201,103,221	13.6	11.89	65.21	0.046	0.045	0.013	<0.06	1.553
07-1335	LG221	14.7	13.98	60.01	0.050	0.038	0.016	<0.06	1.159
07-1336	LG221	13.1	13.36	62.64	0.043	0.040	0.017	<0.06	1.623
07-1342	LG201,103,221	17.1	12.15	63.74	0.051	0.042	0.013	<0.06	1.413
07-1343	LG206,203	8.1	7.12	72.89	0.030	0.035	0.013	<0.06	1.718
07-1345	LG100	6.4	5.67	75.23	0.027	0.049	0.014	<0.06	5.204
07-1353	LG201,103,221	6.1	7.94	75.46	0.035	0.040	0.013	<0.06	3.453
07-1357	LG100	6.4	10.30	69.86	0.045	0.041	0.015	<0.06	4.137
07-1363	LG100	3.2	5.14	77.63	0.037	0.048	0.017	<0.06	8.291
07-1364	LG100	3.6	6.20	77.40	0.117	0.053	0.015	<0.06	4.704
07-1365	LG221	19.7	20.20	46.11	0.042	0.028	0.010	<0.06	0.656

Appendix I continued

Meatoa Lag Samples

Sample	Type	MnO	Cr2O3	V2O5	Mn	Cr	V	Cu	Pb
(Laboratory >)		analb	analb	analb	analb	analb	analb	amdel	amdel
(Method >)		icp	icp	icp	icp	icp	icp	aa-hf	xrf
(det. limit >)		(0.01)	(0.01)	(0.01)	(15)	(20)	(5)	(2)	(2)
07-1310	LG206,203	0.34	0.14	0.07	2640	956	394	180	<2
07-1311	LG203,206	0.34	0.13	0.12	2629	908	668	145	22
07-1312	LG201,221,103	0.17	0.75	0.12	1314	5132	670	195	13
07-1313	LG221	0.07	1.96	0.17	548	13400	950	105	22
07-1315	LG100	0.04	1.83	0.28	316	12500	1569	34	16
07-1318	LG221	0.05	1.56	0.14	369	10700	781	105	13
07-1319	LG201,103,221	0.04	1.46	0.16	337	10000	876	120	12
07-1320	LG201,103,221	0.05	1.62	0.18	390	11100	1001	76	22
07-1324	LG201,103,221	0.07	1.13	0.20	509	7699	1133	130	22
07-1326	LG201,103,221	0.07	0.92	0.21	552	6302	1161	110	30
07-1328	LG201,103,221	0.06	0.94	0.22	443	6446	1227	115	28
07-1330	LG201,103,221	0.05	0.84	0.23	376	5770	1306	84	28
07-1332	LG201,103,221	0.06	0.83	0.21	428	5661	1150	100	16
07-1335	LG221	0.04	0.17	0.25	288	1159	1404	210	12
07-1336	LG221	0.03	0.15	0.28	218	1057	1573	200	17
07-1342	LG201,103,221	0.07	0.57	0.22	549	3903	1244	78	32
07-1343	LG206,203	0.04	0.07	0.18	336	482	1028	65	10
07-1345	LG100	0.05	0.05	0.41	411	342	2272	74	8
07-1353	LG201,103,221	0.08	1.07	0.29	640	7351	1632	50	18
07-1357	LG100	0.03	0.79	0.21	259	5378	1176	32	18
07-1363	LG100	0.04	0.47	0.60	299	3211	3365	17	35
07-1364	LG100	0.05	1.84	0.47	419	12600	2659	22	125
07-1365	LG221	0.04	0.53	0.10	314	3602	564	250	16

Appendix I continued

Meatoa Lag Samples

Sample (Laboratory >) (Method >) (det. limit >)	Type	Zn amdel aa-hf (2)	Ni amdel aa-hf (4)	Co amdel aa-hf (4)	As amdel xrf (2)	Sb amdel xrf (2)	Bi amdel xrf (2)	Mo amdel aa-hf (1)	Ag amdel aa-hf (0.1)
07-1310	LG206,203	500	740	210	13	<2	<2	<1	<0.1
07-1311	LG203,206	500	400	165	7	<2	3	2	<0.1
07-1312	LG201,221,103	300	610	98	48	5	<2	1	<0.1
07-1313	LG221	95	1200	74	220	3	3	4	<0.1
07-1315	LG100	70	820	74	195	5	3	3	<0.1
07-1318	LG221	46	530	34	30	<2	<2	1	<0.1
07-1319	LG201,103,221	54	470	38	34	2	<2	2	0.1
07-1320	LG201,103,221	46	430	48	40	<2	3	3	<0.1
07-1324	LG201,103,221	110	390	58	32	<2	5	2	<0.1
07-1326	LG201,103,221	100	340	44	34	2	3	2	<0.1
07-1328	LG201,103,221	90	330	44	36	3	3	3	<0.1
07-1330	LG201,103,221	85	260	34	45	2	<2	2	0.1
07-1332	LG201,103,221	100	270	38	42	<2	<2	3	<0.1
07-1335	LG221	80	100	38	42	<2	4	<1	<0.1
07-1336	LG221	85	70	24	36	<2	<2	2	<0.1
07-1342	LG201,103,221	90	160	38	34	<2	<2	3	<0.1
07-1343	LG206,203	240	100	54	8	<2	<2	2	<0.1
07-1345	LG100	90	50	28	10	<2	2	3	<0.1
07-1353	LG201,103,221	135	310	54	18	2	<2	3	o.5
07-1357	LG100	55	210	48	18	2	5	6	0.2
07-1363	LG100	40	80	28	35	4	<2	8	0.7
07-1364	LG100	75	240	48	125	6	<2	4	0.2
07-1365	LG221	75	340	78	16	<2	3	<1	<0.1

Appendix I continued

Meatoa Lag Samples

Sample	Type	Sn	Ge	Ga	W	Ba	Zr	Nb	Se
(Laboratory >)		amdel	amdel	amdel	amdel	analb	analb	amdel	amdel
(Method >)		xrf	xrf	xrf	xrf	icp	icp	xrf	xrf
(det. limit >)		(2)	(2)	(4)	(4)	(5)	(5)	(2)	(2)
07-1310	LG206,203	<2	<2	18	6	302	27	3	<2
07-1311	LG203,206	2	<2	36	4	44	49	5	<2
07-1312	LG201,221,103	<2	<2	28	<4	65	68	4	3
07-1313	LG221	5	<2	66	<4	16	106	6	4
07-1315	LG100	2	<2	88	5	11	79	10	2
07-1318	LG221	<2	<2	34	8	18	87	4	8
07-1319	LG201,103,221	<2	<2	28	<4	13	93	2	8
07-1320	LG201,103,221	<2	<2	45	5	19	129	<2	3
07-1324	LG201,103,221	<2	<2	52	10	28	105	4	8
07-1326	LG201,103,221	2	<2	40	<4	42	110	5	<2
07-1328	LG201,103,221	<2	<2	50	16	18	116	5	9
07-1330	LG201,103,221	<2	<2	55	<4	13	126	6	6
07-1332	LG201,103,221	3	<2	50	10	19	110	6	4
07-1335	LG221	5	2	32	6	19	89	2	3
07-1336	LG221	2	<2	45	12	32	129	5	4
07-1342	LG201,103,221	4	<2	52	<4	38	107	6	<2
07-1343	LG206,203,240	3	<2	42	6	13	58	4	<2
07-1345	LG100	2	<2	80	14	34	87	18	5
07-1353	LG201,103,221	4	<2	78	<4	19	68	11	4
07-1357	LG100	6	<2	78	6	31	53	15	<2
07-1363	LG100	12	<2	195	18	18	40	28	5
07-1364	LG100	7	<2	135	<4	30	91	19	<2
07-1365	LG221	<2	2	34	4	15	39	<2	6

Appendix I concluded

Meatoa Lag Samples

Sample	Type	Be	Au
(Laboratory >)		analb	analb
(Method >)		icp	334
(det. limit >)		(1)	(0.001)
07-1310	LG206,203	1	<0.001
07-1311	LG203,206	1	<0.001
07-1312	LG201,221,103	1	0.003
07-1313	LG221	2	0.034
07-1315	LG100	1	<0.001
07-1318	LG221	2	0.008
07-1319	LG201,103,221	2	<0.001
07-1320	LG201,103,221	1	<0.001
07-1324	LG201,103,221	1	<0.001
07-1326	LG201,103,221	1	<0.001
07-1328	LG201,103,221	1	<0.001
07-1330	LG201,103,221	1	<0.001
07-1332	LG201,103,221	2	<0.001
07-1335	LG221	1	0.015
07-1336	LG221	1	0.016
07-1342	LG201,103,221	1	0.003
07-1343	LG206,203,240	1	0.001
07-1345	LG100	1	<0.001
07-1353	LG201,103,221	1	0.001
07-1357	LG100	2	0.002
07-1363	LG100	1	0.003
07-1364	LG100	1	<0.001
07-1365	LG221	2	0.002

Correlation Matrix

Lawlers Lag Samples

Correlation Matrix

	Si	Al	Fe	Mg	Ca	Na	Ti	Ag	Ti	Mn
Si	1.0000	.7576	-.8794	-.1273	.0735	.1031	-.7426	-.4722	-.7426	.0348
Al	.7576	1.0000	-.9575	-.0842	-.3885	.0900	-.5532	-.2796	-.5532	-.4382
Fe	-.8794	-.9575	1.0000	.0771	.2116	-.0977	.6143	.3467	.6143	.2769
Mg	-.1273	-.0842	.0771	1.0000	.1814	-.0017	.0166	-.1206	.0166	.0397
Ca	.0735	-.3885	.2116	.1814	1.0000	.4905	.0424	-.1187	.0424	.5084
Na	.1031	.0900	-.0977	-.0017	.4905	1.0000	-.0479	-.0483	-.0479	-.0425
Ti	-.7426	-.5532	.6143	.0166	.0424	-.0479	1.0000	.6306	1.0000	-.2203
Ag	-.4722	-.2796	.3467	-.1206	-.1187	-.0483	.6306	1.0000	.6306	-.0569
Ti	-.7426	-.5532	.6143	.0166	.0424	-.0479	1.0000	.6306	1.0000	-.2203
Mn	.0348	-.4382	.2769	.0397	.5084	-.0425	-.2203	-.0569	-.2203	1.0000
Cr	-.1943	.2404	-.0627	.3491	-.2515	.0395	-.0378	.0981	-.0378	-.1808
V	-.6044	-.3907	.4763	.0040	-.0435	-.0029	.9004	.5993	.9004	-.3881
Cu	.7662	.5311	-.6880	-.1204	.1084	.0856	-.6092	-.4106	-.6092	.2492
Pb	-.1661	-.0222	.0854	.0379	-.0983	.0389	.2280	.2353	.2280	-.1377
Zn	.1434	-.3764	.1831	.0460	.5235	-.0152	-.2580	-.1715	-.2580	.8817
Ni	.0892	.0938	-.1242	.5332	.1432	-.0061	-.3929	-.2286	-.3929	.3132
Co	-.0204	-.4140	.2681	.1742	.4123	-.0244	-.3370	-.1692	-.3370	.7282
As	-.1770	.0959	-.0232	.7059	-.1104	-.0429	.0466	-.0224	.0466	-.1329
Sb	-.3755	-.1544	.2094	.4748	-.1288	-.1168	.3342	.3653	.3342	-.0667
Bi	.0982	.2436	-.2223	.1505	.1477	.4241	.0212	-.2618	.0212	-.1280
Mo	-.6432	-.4401	.5348	-.0361	.0239	-.0617	.8383	.4542	.8383	-.3061
Sn	-.6086	-.4384	.5019	-.0716	-.0642	-.1109	.7913	.5675	.7913	-.2795
Ga	-.6794	-.4323	.5200	.0938	.0191	-.0139	.9402	.6670	.9402	-.2673
W	.0014	-.0689	-.0007	-.1092	.2129	.1963	.4216	.1517	.4216	-.2250
Ba	-.2241	-.4566	.3807	-.0558	.3671	-.0591	.1170	-.1283	.1170	.1069
Zr	.3992	.5531	-.4510	-.0179	-.2231	.1522	-.2733	-.2455	-.2733	-.3706
Nb	-.7217	-.5474	.6098	.0212	.0662	-.0677	.9810	.5972	.9810	-.1959
Se	.3572	.4725	-.4808	-.1705	.0489	.2627	.0156	-.0180	.0156	-.3749
Au	.0889	.2781	-.2557	.0579	-.2009	-.0626	-.1128	-.1125	-.1128	-.1432

	Cr	V	Cu	Pb	Zn	Ni	Co	As	Sb	Bi
Si	-.1943	-.6044	.7662	-.1661	.1434	.0892	-.0204	-.1770	-.3755	.0982
Al	.2404	-.3907	.5311	-.0222	-.3764	.0938	-.4140	.0959	-.1544	.2436
Fe	-.0627	.4763	-.6880	.0854	.1831	-.1242	.2681	-.0232	.2094	-.2223
Mg	.3491	.0040	-.1204	.0379	.0460	.5332	.1742	.7059	.4748	.1505
Ca	-.2515	-.0435	.1084	-.0983	.5235	.1432	.4123	-.1104	-.1288	.1477
Na	.0395	-.0029	.0856	.0389	-.0152	-.0061	-.0244	-.0429	-.1168	.4241
Ti	-.0378	.9004	-.6092	.2280	-.2580	-.3929	-.3370	.0466	.3342	.0212
Ag	.0981	.5993	-.4106	.2353	-.1715	-.2286	-.1692	-.0224	.3653	-.2618
Ti	-.0378	.9004	-.6092	.2280	-.2580	-.3929	-.3370	.0466	.3342	.0212
Mn	-.1808	-.3881	.2492	-.1377	.8817	.3132	.7282	-.1329	-.0667	-.1280
Cr	1.0000	.0116	-.3431	.3239	-.3920	.4970	-.1896	.6346	.4692	.0186
V	.0116	1.0000	-.5415	.4059	-.4233	-.5168	-.5142	.1071	.3670	-.0967
Cu	-.3431	-.5415	1.0000	-.1930	.4088	.1261	.1318	-.1309	-.2228	.1418
Pb	.3239	.4059	-.1930	1.0000	-.1321	-.0864	-.1672	.3502	.5975	-.1148
Zn	-.3920	-.4233	.4088	-.1321	1.0000	.2297	.6258	-.1824	-.0756	-.0938
Ni	.4970	-.5168	.1261	-.0864	.2297	1.0000	.5098	.6361	.2916	.0501
Co	-.1896	-.5142	.1318	-.1672	.6258	.5098	1.0000	-.0688	-.0885	-.1046
As	.6346	.1071	-.1309	.3502	-.1824	.6361	-.0688	1.0000	.6318	.0948
Sb	.4692	.3670	-.2228	.5975	-.0756	.2916	-.0885	.6318	1.0000	-.1197
Bi	.0186	-.0967	.1418	-.1148	-.0938	.0501	-.1046	.0948	-.1197	1.0000
Mo	.0461	.7077	-.7070	.1078	-.3839	-.2775	-.3129	.0613	.1959	.1165
Sn	-.0702	.7225	-.5015	.2982	-.2706	-.2982	-.2037	.0799	.2522	-.0016
Ga	.1656	.9177	-.6271	.3659	-.3545	-.3288	-.4064	.2060	.4407	-.0267
W	-.4303	.4443	-.0109	-.1423	-.1354	-.3886	-.2706	-.2340	-.1303	.1500
Ba	-.3110	.0320	-.2697	-.2475	-.0156	.0086	.4177	-.2084	-.2290	-.0651
Zr	.2645	.0127	.1694	.2538	-.3094	-.0375	-.5828	.3005	.0569	.0836
Nb	.0209	.8918	-.6151	.2808	-.2472	-.3977	-.3595	.0509	.3632	-.0374
Se	.0165	.0936	.2070	-.1547	-.3199	-.0669	-.4375	-.0765	-.0799	.1330
Au	.1363	-.0841	.2981	-.0393	-.1029	.4003	-.1104	.5341	.0276	.1238

$p = 0.05, r > 0.37$

$p = 0.01, r > 0.48$

Lawlers Lag Samples

	Mo	Sn	Ga	W	Ba	Zr	Nb	Se	Au
Si	-.6432	-.6086	-.6794	.0014	-.2241	.3992	-.7217	.3572	.0889
Al	-.4401	-.4384	-.4323	-.0689	-.4566	.5531	-.5474	.4725	.2781
Fe	.5348	.5019	.5200	-.0007	.3807	-.4510	.6098	-.4808	-.2557
Mg	-.0361	-.0716	.0938	-.1092	-.0558	-.0179	.0212	-.1705	.0579
Ca	.0239	-.0642	.0191	.2129	.3671	-.2231	.0662	.0489	-.2009
Na	-.0617	-.1109	-.0139	.1963	-.0591	.1522	-.0677	.2627	-.0626
Ti	.8383	.7913	.9402	.4216	.1170	-.2733	.9810	.0156	-.1128
Ag	.4542	.5675	.6670	.1517	-.1283	-.2455	.5972	-.0180	-.1125
Ti	.8383	.7913	.9402	.4216	.1170	-.2733	.9810	.0156	-.1128
Mn	-.3061	-.2795	-.2673	-.2250	.1069	-.3706	-.1959	-.3749	-.1432
Cr	.0461	-.0702	.1656	-.4303	-.3110	.2645	.0209	.0165	.1363
V	.7077	.7225	.9177	.4443	.0320	.0127	.8918	.0936	-.0841
Cu	-.7070	-.5015	-.6271	-.0109	-.2697	.1694	-.6151	.2070	.2981
Pb	.1078	.2982	.3659	-.1423	-.2475	.2538	.2808	-.1547	-.0393
Zn	-.3839	-.2706	-.3545	-.1354	-.0156	-.3094	-.2472	-.3199	-.1029
Ni	-.2775	-.2982	-.3288	-.3886	.0086	-.0375	-.3977	-.0669	.4003
Co	-.3129	-.2037	-.4064	-.2706	.4177	-.5828	-.3595	-.4375	-.1104
As	.0613	.0799	.2060	-.2340	-.2084	.3005	.0509	-.0765	.5341
Sb	.1959	.2522	.4407	-.1303	-.2290	.0569	.3632	-.0799	.0276
Bi	.1165	-.0016	-.0267	.1500	-.0651	.0836	-.0374	.1330	.1238
Mo	1.0000	.7482	.8322	.3847	.3681	-.1687	.8070	.0940	-.0638
Sn	.7482	1.0000	.7683	.2194	.1382	-.3434	.7682	-.1977	.1500
Ga	.8322	.7683	1.0000	.3514	.0703	-.1535	.9357	.0564	-.0848
W	.3847	.2194	.3514	1.0000	.1490	.0664	.3664	.5175	-.0460
Ba	.3681	.1382	.0703	.1490	1.0000	-.4002	.0720	.0364	-.1619
Zr	-.1687	-.3434	-.1535	.0664	-.4002	1.0000	-.2543	.3472	.2648
Nb	.8070	.7682	.9357	.3664	.0720	-.2543	1.0000	-.0129	-.1462
Se	.0940	-.1977	.0564	.5175	.0364	.3472	-.0129	1.0000	.0623
Au	-.0638	.1500	-.0848	-.0460	-.1619	.2648	-.1462	.0623	1.0000

Eigenvalues, % Trace,Cumulative Trace

	1	2	3
1	9.3426	32.2157	32.2157
2	4.7707	16.4505	48.6663
3	3.7599	12.9653	61.6316
4	2.1880	7.5448	69.1763
5	1.6736	5.7709	74.9473
6	1.3590	4.6860	79.6333
7	1.1020	3.7999	83.4332
8	.9139	3.1514	86.5846
9	.8632	2.9764	89.5610
10	.7429	2.5618	92.1229
11	.5400	1.8621	93.9849
12	.4255	1.4671	95.4521
13	.3413	1.1770	96.6291
14	.2659	.9168	97.5459
15	.2139	.7377	98.2835
16	.1258	.4338	98.7173
17	.1041	.3591	99.0764
18	.0841	.2901	99.3665
19	.0645	.2225	99.5890
20	.0432	.1489	99.7379
21	.0326	.1125	99.8504
22	.0210	.0723	99.9227
23	.0104	.0360	99.9587
24	.0071	.0244	99.9831
25	.0044	.0153	99.9984
26	.0005	.0016	100.0000
27	.0000	.0000	100.0000
28	.0000	.0000	100.0000
29	.0000	.0000	100.0000

Appendix III

Agnew-McCaffrey Lag Samples

Sample	Type	SiO_2	Al_2O_3	Fe_2O_3	MgO	CaO	Na_2O	K_2O	TiO_2
(Laboratory >)		analb	analb	analb	analb	analb	analb	analb	analb
(Method >)		icp	icp	icp	icp	icp	icp	icp	icp
(det. limit >)		(0.2)	(0.04)	(0.03)	(0.004)	(0.007)	(0.007)	(0.06)	(0.003)
07-1393	LG100	7.8	12.00	72.96	0.029	0.041	0.012	<0.06	3.303
07-1394	LG100	7.2	11.77	74.07	0.027	0.033	0.011	<0.06	1.012
07-1395	LG100	7.9	12.75	72.63	0.030	0.035	0.012	<0.06	1.041
07-1397	LG221	14.8	16.70	54.03	0.034	0.034	0.009	<0.06	0.603
07-1398	LG221	12.5	14.59	60.06	0.039	0.036	0.010	<0.06	0.733
07-1399	LG201,203	7.3	9.26	71.16	0.054	0.041	0.011	<0.06	1.184

Appendix III continued

Agnew-McCaffrey Lag Samples

Sample	Type	MnO	Cr2O3	V2O5	Mn	Cr	V	Cu	Pb
(Laboratory >)		analb	analb	analb	analb	analb	analb	amdel	amdel
(Method >)		icp	icp	icp	icp	icp	icp	aa-hf	xrf
(det. limit >)		(0.01)	(0.01)	(0.01)	(15)	(20)	(5)	(2)	(2)
07-1393	LG100	0.03	2.50	0.17	270	17100	959	28	32
07-1394	LG100	0.05	2.40	0.18	361	16400	984	25	35
07-1395	LG100	0.05	2.53	0.17	378	17300	960	25	26
07-1397	LG221	0.03	1.61	0.10	254	11000	587	180	7
07-1398	LG221	0.03	1.75	0.12	204	12000	658	145	8
07-1399	LG201,203	0.04	1.39	0.14	339	9520	796	125	7

Appendix III continued

Agnew-McCaffrey Lag Samples

Sample	Type	Zn	Ni	Co	As	Sb	Bi	Mo	Ag
(Laboratory >)		amdel	amdel	amdel	amdel	amdel	amdel	amdel	amdel
(Method >)		aa-hf	aa-hf	aa-hf	xrf	xrf	xrf	aa-hf	aa-hf
(det. limit >)		(2)	(4)	(4)	(2)	(2)	(2)	(1)	(0.1)
07-1393	LG100	44	390	30	68	6	7	5	1.2
07-1394	LG100	30	340	26	70	5	5	4	1.0
07-1395	LG100	40	390	34	68	6	3	4	1.2
07-1397	LG221	46	500	44	10	2	<2	<1	<0.1
07-1398	LG221	38	500	44	24	4	2	<1	<0.1
07-1399	LG201,203	60	550	64	22	5	4	1	<0.1

Appendix III continued

Agnew-McCaffrey Lag Samples

Sample	Type	Sn	Ge	Ga	W	Ba	Zr	Nb	Se
(Laboratory >)		amdel	amdel	amdel	amdel	analb	analb	amdel	amdel
(Method >)		xrf	xrf	xrf	xrf	icp	icp	xrf	xrf
(det. limit >)		(2)	(2)	(4)	(4)	(5)	(5)	(2)	(2)
07-1393	LG100	4	<2	54	14	8	136	5	<2
07-1394	LG100	4	<2	56	<4	22	138	4	3
07-1395	LG100	3	<2	50	6	23	141	6	4
07-1397	LG221	<2	<2	24	<4	56	80	<2	4
07-1398	LG221	<2	<2	26	<4	28	76	<2	<2
07-1399	LG201,203	6	<2	32	<4	112	60	5	2

Appendix III concluded

Agnew-McCaffrey Lag Samples

Sample	Type	Be	Au
(Laboratory >)		analb	analb
(Method >)		icp	334
(det. limit >)		(1)	(0.001)
07-1393	LG100	1	<0.001
07-1394	LG100	1	<0.001
07-1395	LG100	1	<0.001
07-1397	LG221	1	<0.001
07-1398	LG221	1	<0.001
07-1399	LG201,203	1	<0.001